Aus dem Adolf-Butenandt-Institut

Lehrstuhl: Stoffwechselbiochemie

Im Biomedizinischen Centrum München, BMC

Vorstand: Prof. Dr. rer. nat. Dr. h. c. Christian Haass

Microglial phagocytosis
of amyloid plaques in an *ex vivo* model
# of Alzheimer's Disease

Dissertation

zum Erwerb des Doktorgrades der Naturwissenschaften (Dr. rer. nat.)

an der Medizinischen Fakultät der Ludwig-Maximilians-Universität zu München

Vorgelegt von

Anna Daria

aus San Candido (BZ), Italien

2018

Mit Genehmigung der Medizinischen Fakultät der Universität München

Betreuer: Prof. Dr. Dr. h. c. Christian Haass

Zweitgutachterin: Prof. Dr. Magdalena Götz

Dekan: Prof. Dr. med. dent. Reinhard Hickel

Tag der mündlichen Prüfung: 01.08.2018

Eidesstattliche Versicherung/Affidavit

Ich erkläre hiermit an Eides statt, dass ich die vorliegende Dissertation mit dem Thema "*Microglial phagocytosis of amyloid plaques in an ex vivo model of Alzheimer's Disease*" selbständig verfasst, mich außer der angegebenen keiner weiteren Hilfsmittel bedient und alle Erkenntnisse, die aus dem Schrifttum ganz oder annähernd übernommen sind, als solche kenntlich gemacht und nach ihrer Herkunft unter Bezeichnung der Fundstelle einzeln nachgewiesen habe.
Ich erkläre des Weiteren, dass die hier vorgelegte Dissertation nicht in gleicher oder in ähnlicher Form bei einer anderen Stelle zur Erlangung eines akademischen Grades eingereicht wurde.

I hereby confirm that the submitted dissertation entitled "*Microglial phagocytosis of amyloid plaques in an ex vivo model of Alzheimer's Disease*" is the result of my own work and that I have only used sources or materials listed and specified in the dissertation. Where the work of others has been quoted or reproduced, the source is always given.
I further declare that the submitted dissertation or parts thereof have not been presented as part of an examination degree to any other university.

Ort, Datum   Santo Stefano di Cadore (BL) – Italy, 03. 09. 2018

Unterschrift   Anna Daria

4

To my family

Summary

Alzheimer's disease (AD) is one of the most severe neurodegenerative disorders defined by deposition of amyloid plaques and neurofibrillary tangles. An important role in AD is also exerted by neuroinflammation and microglial activation is one of the hallmarks of the disease pathology. Although microglia are known to be recruited and to cluster around amyloid plaques in the AD brain, their involvement in amyloid plaque clearance over the course of AD is still controversial. Impaired microglial function resulting in decreased Aβ clearance was reported in sporadic AD cases as well as in mouse models of AD. Moreover, several recently identified genetic risk alleles for AD have been linked to microglial function and phagocytosis. To study the contribution of microglial phagocytosis in amyloid plaque clearance, I established a novel *ex vivo* co-culture model where I combined organotypic brain slices from aged, amyloid plaque-bearing mice (APPPS1) together with slices from young, neonatal wild-type (WT) mice. In the *ex vivo* co-culture model, I observed changes in amyloid plaque morphology over 14 days *in vitro* manifested by clearance of the plaque halo bearing diffuse Aβ and increased number of core-only plaques. Additionally, I found a strong increase in immunoreactivity of CD68, a lysosomal marker of activated microglia/macrophages in the old APPPS1 tissue. Specific recruitment and clustering of CD68 positive cells around amyloid plaques was paralleled by a decrease in plaque size upon co-culturing of old and young brain slices. Pharmacological inhibition of phagocytosis by cytochalasin D prevented clearance of the plaque halo, suggesting that CD68 positive microglial cells detected at amyloid plaques are phagocytosing Aβ. Furthermore, specific removal of either old or young microglial cells by clodronate hindered amyloid plaque clearance, suggesting a synergistic contribution of both microglial populations in plaque phagocytosis. To discriminate between young and old microglial cells, I co-cultured either young slices from $CX_3CR1^{+/GFP}$ reporter mice with old APPPS1 brain slices or old APPPS1/$CX_3CR1^{+/GFP}$ brain slices together with young WT slices. Surprisingly, only the old APPPS1 microglial cells were found in the vicinity of amyloid plaques and thus identified as cells responsible for Aβ uptake in our *ex vivo* co-culture model. Intriguingly, culturing old APPPS1 brain slices in conditioned media collected from young WT brain slices or from cultured young primary microglia was sufficient to increase amyloid plaque clearance, in contrast to media obtained from microglia-depleted young slices. These data suggested that soluble factors released by young microglia promote Aβ uptake by the old APPPS1 microglial cells. Hence, I tested action of several pro- and anti-inflammatory cytokines on amyloid plaque clearance and found enhanced plaque phagocytosis upon direct addition of granulocyte-macrophage colony-stimulating factor (GM-CSF) to old APPPS1 brain slices, mimicking the co-culture condition. Moreover, the GM-CSF treatment increased numbers of CD68 positive cells confirming its mitogenic potential on myeloid cells. Increased numbers of proliferating microglial were also detected upon co-culturing of old and young brain slices. Nevertheless, co-culturing of young slices from GM-CSF$^{-/-}$ mice with old APPPS1 brain slices still resulted in increased numbers of core-only plaques and, accordingly, increased CD68 coverage.

Therefore, GM-CSF is not the sole factor triggering microglial proliferation and Aβ uptake in the *ex vivo* co-culture model. However, proliferation of old microglial cells was necessary for amyloid plaque clearance, as exposure of the old APPPS1 tissue to the young WT conditioned media obtained after treatment with the proliferative inhibitor AraC prevented amyloid plaque clearance. This study suggests that impaired amyloid plaque clearance of aged microglia in AD may be reversed and microglial phagocytic capacity may be restored upon a proper stimulus. The novel *ex vivo* model system can be used as a platform to screen, test and identify factors or compounds directed to therapeutically modulate phagocytic competence of microglia.
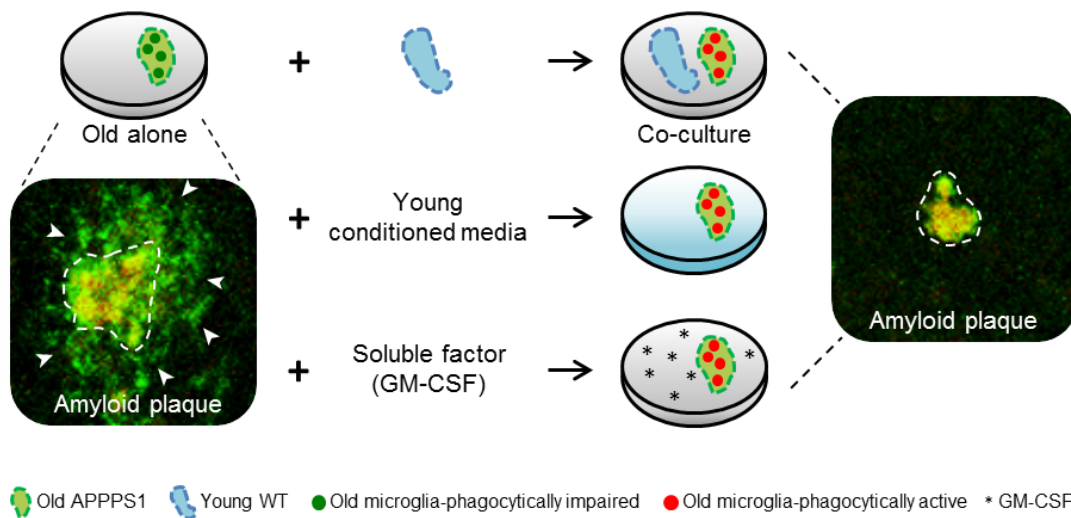
Graphical Abstract.

Zusammenfassung

Die Alzheimer'sche Krankheit (Alzheimer's disease, AD) oder kurz Alzheimer ist eine der schwerwiegendsten neurodegenerativen Erkrankungen und zeichnet sich durch die Ablagerungen von amyloiden Plaques und neurofibrillären Bündeln aus. Eine wichtige Rolle in Alzheimer spielt zudem die Neuroinflammation, die sich pathologisch unter anderem durch die Aktivierung von Mikroglia-Zellen kennzeichnet. Obwohl bereits bekannt ist, dass Mikroglia im Alzheimer-Gehirn rekrutiert werden und sich an den amyloiden Plaques sammeln, bleibt ihre genaue Beteiligung an der Entfernung der Plaques im Zusammenhang mit Alzheimer kontrovers. In Fällen der sporadischen Form von Alzheimer sowie in Mausmodellen konnten mikrogliale Defekte gezeigt werden, die zu einem geringeren Aβ Abbau führen. Darüber hinaus wurden mehrere kürzlich identifizierte genetische Risiko-Allele für Alzheimer mit der mikroglialen Funktion und Phagozytose in Verbindung gebracht.

Um die Beteiligung der mikroglialen Phagozytose an der Beseitigung der amyloiden Plaques zu untersuchen, habe ich ein neues *ex vivo* Ko-Kulturenmodell etabliert, bei dem ich organotypische Gehirnschnitte von gealterten, amyloid Plaque positiven Mäusen (APPPS1) mit Hirnschnitten von jungen, neonatalen Wildtyp-Mäusen (WT) kombiniert habe. In diesem *ex vivo* Ko-Kulturenmodell konnte ich innerhalb von 14 Tagen Veränderungen in der Morphologie der amyloiden Plaques beobachten, nämlich die Höfe diffuser Aβ Plaques wurden zu einem Kern tragendem (core-only) Plaque abgebaut. Weiterhin konnte ich einen starken Anstieg in der Immunreaktivität von CD68, einem lysosomalen Marker aktivierter Mikroglia und Makrophagen, im Gewebe der alten APPPS1 Mäuse beobachten. Die spezifische Rekrutierung und Ansammlung von CD68-positiven Zellen um amyloide Plaques verlief parallel zur Reduktion der Plaque-Größe während der Ko-Kultivierung von alten und jungen Gehirnschnitten. Die pharmakologische Inhibition der Phagozytose mit Cytochalasin D verhinderte den Abbau des Plaque-Hofs und liefert somit den Hinweis, dass CD68-positive Mikroglia, welche an den amyloiden Plaques detektiert wurden, Aβ phagozytieren. Überdies konnte der Abbau von amyloiden Plaques spezifisch durch die Entfernung der alten oder jungen Mikroglia mittels Clodronat verhindert werden, was auf eine synergetische Beteiligung beider Mikroglia-Populationen an der Phagozytose weist.

Um die jungen und alten Mikroglia-Zellen voneinander unterscheiden zu können, wurden entweder junge Schnitte aus $CX_3CR1^{+/GFP}$ –Reportermäusen mit alten APPPS1 Hirnschnitten oder alte $APPPS1/CX_3CR1^{+/GFP}$ –Gehirnschnitte mit jungen Wildtyp-Schnitten kultiviert. Überraschenderweise wurden nur die Mikroglia-Zellen der alten APPPS1-Mäuse in der direkten Umgebung der amyloiden Plaques gefunden und somit als die für die Aβ-Aufnahme verantwortlichen Zellen in unserem *ex vivo* Ko-Kulturenmodell identifiziert. Interessanterweise war die Kultivierung alter APPPS1 Hirnschnitte in Medium, das von jungen WT Hirnschnitten oder von jungen, primären Mikroglia gesammelt wurde, ausreichend, um den Abbau der amyloiden Plaques zu erhöhen. Dies war nicht der Fall für Medium von jungen Hirnschnitten, bei dem die Mikroglia zuvor entfernt wurden. Diese Daten zeigen, dass die jungen Mikroglia lösliche Faktoren abgeben und die Aβ Aufnahme der alten APPPS1 Mikroglia begünstigen. Infolgedessen habe ich verschiedene pro- und anti-inflammatorische Cytokine auf den Abbau der amyloiden Plaques getestet und konnte zeigen, dass die Phagozytose der Plaques nach direkter Zugabe des Granulozyten-Monozyten-Kolonie-stimulierende Faktor (GM-CSF) zu den alten APPPS1

Hirnschnitten erhöht war und so die Bedingungen der Ko-Kultur nachgeahmt werden konnten. Ferner erhöhte die GM-CSF Behandlung die Anzahl CD68-positiver Zellen und bestätigt so sein mitogenes Potential auf myeloide Zellen. Überdies konnte in den Ko-Kulturen alter und junger Hirnschnitte eine ansteigende Anzahl proliferierender Mikroglia detektiert werden. Dennoch resultierte die Ko-Kultivierung junger Hirnschnitte von GM-CSF$^{-/-}$ Mäusen mit alten APPPS1 Hirnschnitten in einer erhöhten Anzahl reiner Kern-Plaques (core-only) und dementsprechend einer höheren Menge von CD68. Folglich ist GM-CSF nicht der einzige Faktor in dem *ex vivo* Ko-Kulturen Modell, der die Mikroglia Proliferation und die Aβ Aufnahme auslöst. Die Proliferation alter Mikroglia-Zellen war für die Entfernung der amyloiden Plaques jedoch nötig, da die Exposition des alten APPPS1 Gewebes mit Medium von jungen WT Schnitten nach Behandlung durch den Proliferations-Inhibitor AraC verhindert wurde.

Diese Studie konnte zeigen, dass der verminderte Abbau von amyloiden Plaques durch gealterte Mikroglia in der Alzheimer Krankheit rückgängig gemacht werden und die mikrogliale Phagozytosekapazität durch einen geeigneten Stimulus wiederhergestellt werden kann. Das neue *ex vivo* Modellsystem kann hierbei als Plattform dienen, Faktoren oder Präparate zu identifizieren, zu selektieren und zu testen, um therapeutisch die Phagozytosekompetenz der Mikroglia zu modulieren.

Table of Contents

List of Figures

List of Abbreviations

Aβ	Amyloid-β peptide
ABCA7	ATP-binding cassette, sub-family A, member 7
ABI3	ABI family member 3
AD	Alzheimer's disease
ADAM10	A disintegrin and metalloproteinase domain 10
AICD	APP intracellular domain
AMPA	α-amino-3-hydroxy-5-methyl-4-isoxazolepropionic acid receptor
APH-1	Anterior pharynx-defective-1
API	Alzheimer's prevention initiative
APOE	Apolipoprotein E
APP	Amyloid precursor protein
APS	Ammonium persulfate
AraC	Cytosine arabinose
BACE-1	β-site amyloid precursor protein cleaving enzyme
BBB	Blood brain barrier
BDNF	Brain-derived neurotrophic factor
BIN1	Bridging integrator 1
BMDM	Bone marrow-derived macrophages
BSA	Bovine serum albumin
CAA	Cerebral Amyloid Angiophaty
CCL-2	C-C motif chemokine ligand 2
CD	Cluster of differentiation
CD33	Sialic acid-binding immunoglobulin (ig)-like lectin
Clo	Clodronate
CLU	Clusterin
CM	Conditioned media
CNS	Central nervous system
CR1	Complement receptor type 1
CR3	Complement receptor type 3
CSF	Cerebrospinal fluid
CSF1R	Colony-stimulating factor 1 receptor
CTF	C-terminal fragment
CX3CL1	CX3C chemokine ligand 1 or fractalkine
CX3CR1	Receptor for CX3C chemokine fractalkine
CytoD	Cytochalasin D
DAPI	4',6-Diamidin-2-phenylindol
DAM	Disease-associated microglia
DAMP	Danger-associated molecular pattern
DIAN	Dominantly inherited Alzheimer network
DIV	Days *in vitro*
DMEM	Dulbecco's modified eagle medium
DMSO	Dimethylsulfoxide
DNA	Desoxyribonucleic acid
dNTP	Deoxynucleotide
ECL	Enhanced chemiluminescence
EDTA	Ethylenediaminetetraacetic acid
EOAD	Early onset Alzheimer's disease
EPHA1	Ephrin receptor A1

FAD	Familial Alzheimer's disease
FERMT2	Fermitin family member 2
GFAP	Glial fibrillary acidic protein
GFP	Green fluorescent protein
GM-CSF	Granulocyte macrophage-colony stimulating factor
GWAS	Genome-wide association study
HBSS	Hank's balanced salt solution
HLA-DRB5/B1	Major histocompatibility complex, class II, DR beta 5/DR beta 1
HRP	Horse radish peroxidase
Iba-1	Ionized calcium binding adapter molecule 1
IDE	Insulin degrading enzyme
IGF-1	Insulin-like growth factor 1
INF-γ	Interferon γ
kDa	Kilodalton
LAMP2	Lysosome-associated membrane protein 2
LOAD	Late onset Alzheimer's disease
LPS	Lipopolysaccharide
LRP1	Receptor-related protein 1
LTP	Long-term potentiation
MCH	Mitochondrial cascade hypothesis
M-CSF	Macrophage-colony stimulating factor
MEM	Minimum essential medium
MG	Microglia
MGnD	Microglial neurodegenerative phenotype
MHC-II	Class II major histocompatibility complex
MRI	Magnetic resonance imaging
MS4A	Membrane-spanning 4-domains, subfamily A
NEP	Neprilysin
NLRP3	NLR family pyrin domain containing 3
NMDA	N-methyl-D-aspartate receptor
NOS	Nitric oxide synthase
NSAID	Nonsteroidal anti-inflammatory drug
NTF	Neurofibrillary tangle
PAMP	Pathogen-associated molecular pattern
PBS	Phosphate-buffered saline
PCR	Polymerase chain reaction
PEN-2	Presenilin enhancer-2
PET	Positron-emission tomography
PICALM	Phosphatidylinositol binding clathrin assembly protein
PFA	Paraformaldehyde
PLCG2	Phospholipase C gamma 2
PS1	Presenilin-1
PS2	Presenilin-2
PTK2B	Protein tyrosine kinase 2 beta
RAGE	Advanced-glycation end-products
ROI	Region of interest
ROS	Reactive oxygen species
RT	Room temperature
SAD	Sporadic Alzheimer's disease
SAD-PAGE	Sodium dodecyl sulfate-polyacrylamide gel electrophoresis
SORL1	Sortilin-related receptor with A-type repeats
TAE	Tris-acetate EDTA

TAU	Tubulin associated unit
TEMED	Tetramethylethylendiamin
TGF-β	Transforming growth factor β
TNF-α	Tumor necrosis factor α
TLR-2	Toll like receptor 2
Tg	Transgenic
TREM2	Triggering receptor expressed on myeloid cells 2
WT	Wild type

1. Introduction

1.1 Alzheimer's Disease

Alzheimer's disease (AD) is the most common form of dementia worldwide (Andrieu et al 2015), estimated to contribute to about 60-80% of all dementia cases (2016 Alz Association report, www.alz.org/facts). The Alzheimer's disease International Consortium reported in 2016 ~47 million people living with dementia, 11% of which over the age of 65 and 81% over the age of 75 (https://www.alz.co.uk/research/world-report-2016). The primary risk factor for AD is old age. Because of the demographic aging, the worldwide prevalence of AD is expected to quadruplicate in the next years with more than 130 million affected persons by 2050 (Brookmeyer et al 2011). Thus, AD represents a major global public health problem with a huge economic impact. The cost AD represents for the individual, family and society also puts great pressure in order to better understand the disease mechanisms and to find an effective cure (Graham et al 2017).

1.1.1 Pathological hallmarks of Alzheimer's Disease

The key neuropathological elements of AD were first described by Alois Alzheimer in 1906 in his original case report of a 51 year old patient, Auguste D., who presented a "peculiar" dementia (Alzheimer 1907). At the macroscopic level, a severe atrophy of the brain could be detected (Fig 1.1). At the microscopic level, the disease manifested by amyloid plaques and neurofibrillary tangles (NFTs) in the medial temporal lobe and cortical areas of the brain (Fig 1.2), together with extensive synaptic degeneration, neuronal loss, and neuroinflammation.

Amyloid plaques are abnormal extracellular accumulations of the amyloid-β (Aβ) peptide, a 37-43 amino acid peptide in the brain parenchyma (Fig 1.2). Aβ is generated by sequential proteolytic cleavage of the amyloid precursor protein (APP) by the enzymes β- and γ-secretases (Haass 2004, Haass & Selkoe 1993, Selkoe 2001). APP processing will be described in more detail in section number 1.1.2. Monomers of Aβ peptide, predominantly with 42 or 40 amino acids (Aβ42 and Aβ40), eventually self-assemble to form intermediate oligomers as well as protofibrils, a heterogeneous class of soluble prefibrillar species with a characteristic secondary β-sheet and supersecondary structure. Protofibrils go on to form fibrils that deposit as plaques and disrupt normal tissue architecture (Ahmed et al 2010, Walsh et al 1999). Aβ can also deposit in the blood vessel walls in the form of cerebral amyloid angiopathy (CAA) (Smith & Greenberg 2009). CAA most often accompanies the pathology of AD and can cause lobar hemorrhage and contribute to ischemic damage of the brain (Biffi & Greenberg 2011).

In addition to the deposition of Aβ in plaques, formation of NFTs occurs in the AD brain (Fig 1.2). NFTs are intracellular inclusions constituted by hyperphosphorylated form of the microtubule binding protein, tau (Tubulin associated unit) (Grundke-Iqbal et al 1986). Tau is synthesized and produced in all neurons (Migheli et al 1988). The normal function of tau is to bind to tubulin and

stabilize microtubules, maintaining neuronal stability and homeostasis (Drechsel et al 1992). However, in AD, tau becomes hyperphosphorylated and this form of tau dissociates from microtubules and self-aggregates into paired helical filaments (PHFs), a major constituent of NFTs, leading to destabilization of microtubules, synaptic defects, plasma-membrane degeneration and neuronal damage (Iqbal et al 2005). Neuropathological studies suggest that the evolution of NFT distribution in the brain correlates with the clinical progression of cognitive deficits in AD (Perrin et al 2009).
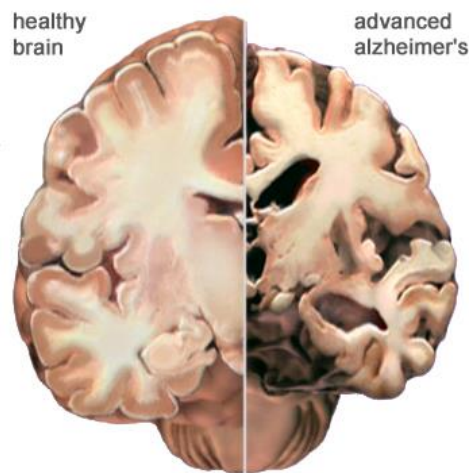
Figure 1.1. Brain atrophy in advanced AD patient.
Compared to a healthy individual, a patient with Alzheimer's disease typically presents with diffuse brain atrophy manifested by cortical thinning and ventricle dilatation. From the Alzheimer's association (www.alz.org).

Furthermore, AD is characterized by the massive loss of neurons, neuropil, and synapsis, which contribute to the gross cortical atrophy of the AD brain (Holtzman et al 2011) (Fig 1.1). Post-mortem samples of AD clearly show substantial loss of cortical grey matter accompanied by ventricular enlargement and severe brain shrinkage (Bird 2008) (Fig 1.1). The neurodegenerative process involves first vulnerable neurons in the entorhinal cortex and hippocampus, then progresses to areas of the temporal, parietal, and frontal neocortex (Holtzman et al 2011). The deterioration process is manifested by early damage to synapses with retrograde degeneration of axons and eventual atrophy of the dendritic tree (Perlson et al 2010). Indeed, the loss of synapses in the limbic system and neocortex is considered to be the best link with the cognitive impairment in patients with AD (DeKosky & Scheff 1990, Scheff et al 2007).
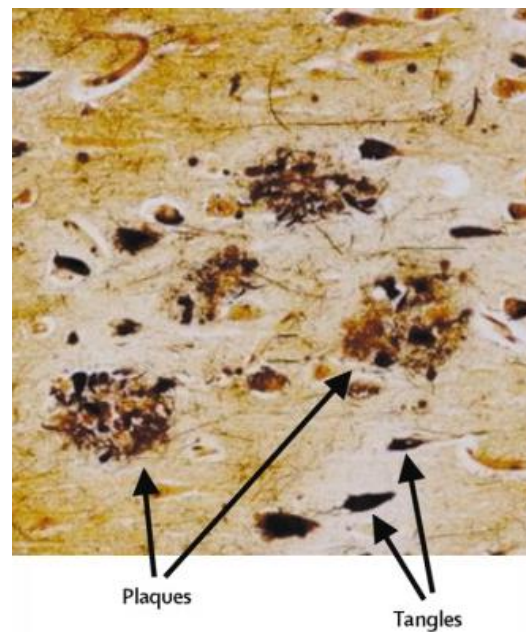
Figure 1.2. Amyloid plaques and neurofibrillary tangles in the cerebral cortex of an AD patient.
Plaques are extracellular deposits of Aβ surrounded by dystrophic neurites. Tangles are intracellular inclusions consisting of hyperphosphorylated tau. From: Blennow et al 2006.

Another major component of AD is the widespread neuroinflammatory process occurring in the brain, which was already recognized and described in the first case report by Alois Alzheimer (Alzheimer 1911) (Fig 1.3). These inflammatory responses include activation of microglia, astrocytes, and perivascular, meningeal and choroid plexus macrophages, resulting in the release of inflammatory mediators in the brain such as cytokines, chemokines, complement system proteins and reactive oxygen species (ROS), which contribute to AD progression (Zhang & Jiang 2015). This topic will be addressed in detail in section number 1.3.
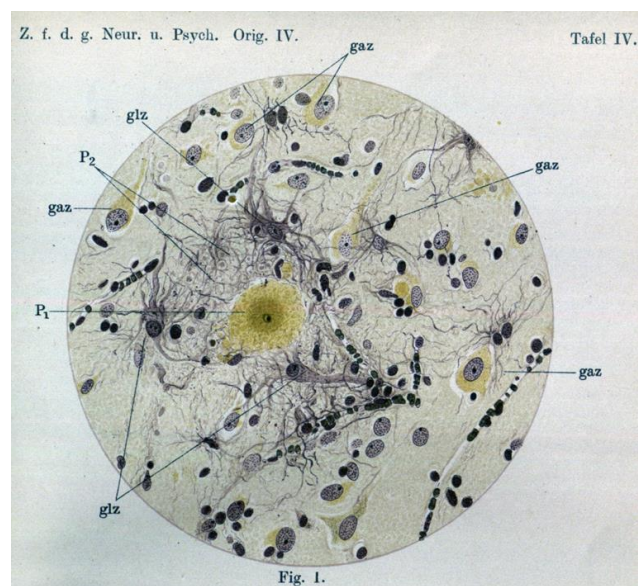
Figure 1.3. Glial cells surrounding amyloid plaques by Alois Alzheimer.
First description of glial cells in relation to amyloid plaques in the brain cortex. The plate (Tafel IV) illustrates a plaque (P_1) consisting of a small dark core and a halo (yellow) surrounded by numerous subtle 'glial fibrils' originating from large glial cells ('fibril-forming glial cells', glz). Neighboring 'nerve cells' (gaz) are also depicted. From: Alzheimer 1911.

21

1.1.2 Origin of Aβ peptide - APP processing

Aβ precursor protein APP is a transmembrane, type-1, integral glycoprotein. There are three main isoforms of APP as a result of alternative splicing. The 695 amino acid form of APP is predominantly expressed in the central nervous system (CNS), particularly by neurons, whereas the 751 and 770 amino acid forms are more broadly expressed (Bayer et al 1999, Tanzi et al 1988). Although the physiological function of APP itself has not been fully determined, it has been associated with neuro- and synaptotrophic properties, and implicated in neuronal development and synaptic plasticity (Dawkins & Small 2014, Muller et al 2017).

The ~4kDa Aβ peptide was first isolated as the principal component of amyloid deposits in the brain and cerebrovasculature of AD and Down's Syndrome patients (Masters et al 1985). Aβ peptides are generated from two consecutive proteolytic cleavages of APP by the proteases BACE1 (protease β-site APP cleaving enzyme), which is the main β-secretase in the brain (Vassar et al 1999), and the tetrameric complex γ-secretase, composed of PS (presenilin), nicastrin, APH-1 (anterior pharynx-defective-1) and PEN-2 (presenilin enhancer-2) (Edbauer et al 2003, Kimberly et al 2003) (Fig 1.4). A third enzyme involved in the APP processing is ADAM10 (a disintegrin and metalloproteinase 10), the major neuronal α-secretase (Kuhn et al 2010), whose activity precludes Aβ generation (Fig 1.4).

APP is cleaved in its extracellular region (at the amino terminus of Aβ domain) by β-secretase, releasing a secreted N-terminal fragment (sAPP-β) and a transmembrane C-terminal fragment C99 (CTF-β) (Fig 1.4). C99 is subsequently cleaved by γ-secretase to generate soluble Aβ peptides of different lengths, including Aβ37, Aβ38, Aβ40, Aβ42, Aβ43 and even longer species like Aβ45, Aβ46, Aβ48, as well as an APP intracellular fragment (AICD) (Takami et al 2009, Vassar et al 2014). This pathway is referred to as amyloidogenic pathway (Fig 1.4). Although numerous Aβ species exist, the most abundant one produced in the brain and found in the cerebrospinal fluid (CSF) is Aβ40 (~80-90%), followed by Aβ42 (~5-10%) (Iwatsubo et al 1994, Selkoe 2001, Shoji et al 1992). The slightly longer forms of Aβ, particularly Aβ42, are more hydrophobic, fibrillogenic, and are the principal species deposited in the brain (Vandersteen et al 2012).

A rather small part of the total cellular APP is processed by β-Secretase and its activity is considered to be the rate-limiting step in the amyloidogenic pathway. The remaining APP is cleaved by α-secretase (within the Aβ sequence) generating a secreted N-terminal fragment (sAPP-α) and a C-terminal fragment C83 (CTF-α) (De Strooper et al 1993, Sisodia 1992) (Fig 1.4). The subsequent γ-secretase cleavage of CTF-α produces a smaller C-terminal fragment of 3 kDa (p3) (Haass et al 1993). In this alternative pathway, generation of Aβ peptides is prevented, thus the pathway also is known as anti-amyloidogenic pathway. γ-Secretase cleavage within the membrane-bound CTF-α also generates an AICD that may have a transcriptional function (Cao & Sudhof 2001) (Fig 1.4). In our lab it was recently discovered that APP processing is even more complex and a novel processing pathway has been identified (Willem et al 2015). η-Secretase processing generates a soluble N-terminal product (sAPP-η) of ~80kDa and membrane bound APP-C-terminal fragments (CTF-η), which were found to accumulate in dystrophic neurites surrounding amyloid plaque cores in both mouse model of AD and human AD patients. CTF-η fragments are further cleaved into longer and shorter soluble Aη peptides by α- or β-secretases (Aη-α, Aη-β respectively) (Fig 1.5). Notably, Aη-α was found to specifically lower neuronal activity and long term-potentiation (LTP) (Willem et al 2015).
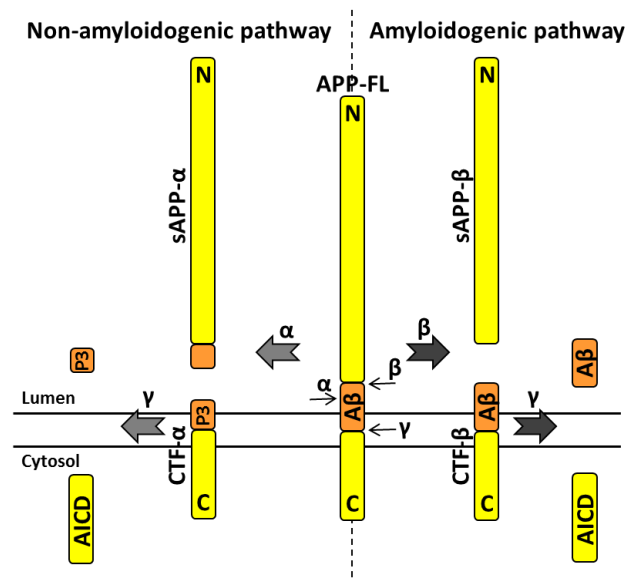
Figure 1.4. APP processing.
Schematic representation of the APP proteolytic processes, illustrating the non-amyloidogenic and the amyloidogenic pathway. Abbreviations: α, α-secretase; β, β-secretase; γ, γ-secretase; sAPP-α and sAPP-β, soluble APP N-terminal fragments derived from α- and β-secretase cleavage, respectively; APP-FL, APP full length; AICD, APP intracellular domain.
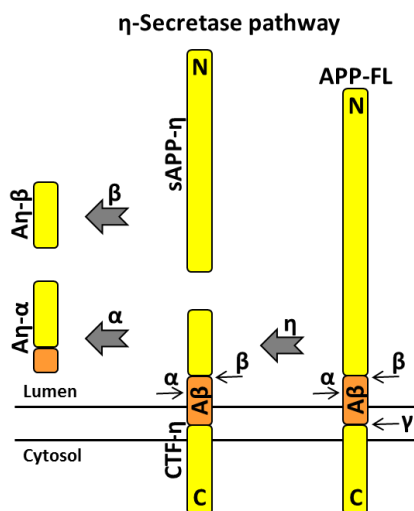
Figure 1.**5. η-Secretase processing.**
Schematic representation of the η-secretase proteolytic process. Abbreviations: α, α-secretase; β, β-secretase; η, η-secretase; γ, γ-secretase; CTF, APP C-terminal fragment; Aη-α and Aη-β, Aη peptides derived from α- and β-secretase cleavage respectively; APP-FL, APP full length. Abbreviations: CTF-η, CTF-β and CTF-α, APP C-terminal fragments derived from η-, β- and α -secretase cleavages, respectively; APP-FL, APP full length.

1.1.3 Genetic and sporadic AD

There are two types of AD: "**f**amilial", also known as **e**arly **o**nset **AD** (FAD or EOAD) or **a**utosomal **d**ominant **AD** (ADAD), and "**s**poradic" also known as **l**ate **o**nset **AD** (SAD or LOAD).

23

FAD is inherited in a Mendelian autosomal dominant fashion and it is relatively rare, accounting for 1-6% of all AD cases with clinical symptom onset between 30 and 65 years of age (Bird 2008). FAD is caused by mutations in genes encoding for APP and presenilin-1 and -2 (PS1 and PS2), which are catalytic subunits of the γ-secretase complex.

Some APP mutations locate at or near the Aβ peptide and affect type or amount of Aβ peptide produced by altering proteolytic activity of β- and γ-secretases, resulting in increased Aβ aggregation and deposition. Examples of APP mutations are the "London" mutation (APP V717I) that increases the Aβ42/Aβ40 ratio by modifying the γ-secretase cleavage of APP (Alison Goate 1991), or the "Swedish" mutation (APP K670N/M671L) enhancing β-secretase cleavage and Aβ production (Mullan Mike 1992). Besides the pathogenic mutations, a rare protective variant, the "Icelandic" variant (APP A673T), was reported to reduce formation of amyloidogenic peptides by decreasing β-secretase processing of APP (Jonsson et al 2012). Triplication of the APP gene located on chromosome 21 as occurring in Down's syndrome (Trisomy 21) (Tokuda et al 1997), or rare familial cases of AD with duplication of the APP gene (Rovelet-Lecrux et al 2006) also lead to AD pathology. Some mutations in PS1 and PS2 genes increase cleavage of APP by γ-secretase, causing elevated Aβ42/Aβ40 ratio (Chavez-Gutierrez et al 2012, Scheuner et al 1996) while others have been described to result in the generation of fewer but longer and more amyloidogenic Aβ peptides, i.e. Aβ43 (Kretner et al 2016, Saito et al 2011).

The vast majority of AD patients are late onset, with risk increasing after 65 years of age. Although LOAD is largely sporadic and considered multifactorial (Van Cauwenberghe et al 2016), there are multiple susceptibility genes that confer risk for developing AD (Naj et al 2017). One of the major genetic risk factors that lowers the age of disease onset is the apolipoprotein E-ε4 allele (*APOE-ε4*). Individuals with one copy of ε4 allele have 3-fold increased risk for AD and carriers of two copies have 12-fold higher risk (Slooter et al 1998). Of note, ApoE4 has been linked to various aspects of Aβ metabolism, such as promoting Aβ aggregation (Castano et al 1995) but also causing a defective Aβ clearance (Verghese et al 2013).

In addition to APOE, genome-wide association studies (GWAS) and next-generation sequencing techniques have allowed identification of more than 20 novel genetic loci associated with AD risk. Interestingly, most of these genes cluster in immune response and inflammation pathway (e.g. *CLU*, *CR1*, *ABCA7*, *CD33*, *TREM2, PLCG2*, *ABI3*), supporting the relevance of immune system for AD etiology (Karch et al 2014, Sims et al 2017, Tosto & Reitz 2016). Additional pathways regulated by AD susceptibility loci are cell migration (e.g. *PTK2B*), APP and tau pathology (e.g. *SORL1* and *FERMT2* respectively), synaptic function, endocytosis (e.g. *BIN1*, *PICALM*), axonal transport and lipid metabolism (e.g. *CLU*, *ABCA7, SORL1*) (Karch et al 2014, Tosto & Reitz 2016). These genes provide insights into the molecular pathways that are altered in AD pathogenesis, and understanding of their mechanism of action will help to elucidate the physiopathology of the disease and to identify novel therapeutic targets.

1.1.4 The amyloid cascade hypothesis

The amyloid cascade hypothesis is the principal hypothesis that combines a sequence of events that are causative for AD (Fig 1.6). According to this hypothesis, an excessive production of Aβ in

the brain leads to its aggregation and deposition into plaques. This initiates a cascade of events that harm synapses and neurons, including aggregation of tau protein in NFTs and widespread neuroinflammation in the brain (described in detail in section number 1.3) ultimately leading to neuronal degeneration and dementia (Haass & Selkoe 2007, Hardy & Higgins 1992, Selkoe & Hardy 2016).

Amyloid cascade hypothesis

Gene mutations (APP, PS1, PS2)
Genetic risk factors (ApoE)
Environmental factors

⬇

Toxic Aβ peptide aggregation
Plaque deposition

⬇

Tau hyperphosphorylation
NFT formation

⬇

Neurodegeneration
Synaptic dysfunction and neuronal loss

⬇

Cognitive impairment
Dementia
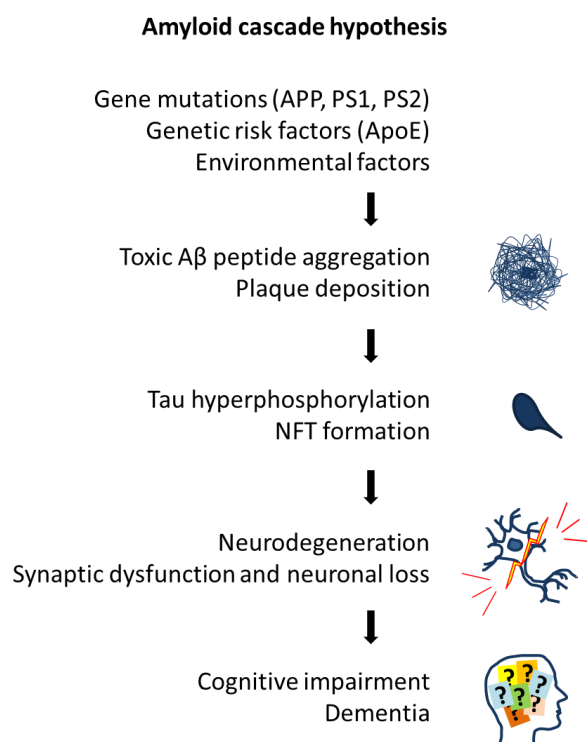
Figure 1.6. Amyloid cascade hypothesis.
Simplified schematic representation of the amyloid cascade hypothesis. Abbreviations: APP, amyloid precursor protein; PS1, presenilin1; PS2, presenilin2; ApoE, apolipoprotein E; NFT, neurofibrillary tangles.

The central role of Aβ in the pathogenesis of AD is strongly supported by evidences from genetic studies where the mutations implicated in familial forms of the disease occur in the genes for the substrate (APP) and the key enzyme (presenilin) for Aβ generation. Moreover, people with Down's syndrome develop AD early in life (Zigman et al 2008), supporting the notion that life-long overproduction of Aβ causes AD. Additional more recent genetic evidence comes from the APP-Icelandic mutation that decreases life-long production and aggregation properties of Aβ and protects against AD (Jonsson et al 2012). Moreover, introduction of human disease-associated mutations into mice recapitulates some aspects of the human disease (Games et al 1995, Radde et al 2006), further supporting the link between aberrant Aβ production and the AD phenotype.

Along these lines, Aβ42 oligomers isolated from cortex of AD patients were found to decrease synapse density and inhibit LTP in rodent hippocampus, and their injection disrupts memory and learning in normal rats (Shankar et al 2008). Further studies showed that isolated human Aβ42 oligomers induce tau hyperphosphorylation and cause neuritic dystrophy in cultured rat neurons, whereas co-treatment with Aβ antibodies mitigates this effect (Jin et al 2011).

Moreover, Aβ oligomers can be found at the halo surrounding amyloid plaques, this correlating with low synaptic density (Koffie et al 2009).

There is also some criticism regarding the amyloid cascade hypothesis. For example, the fact that amyloid plaque load in the brain does not correlate well with severity of dementia, but does correlate with NFT burden (Knopman et al 2003). Furthermore, amyloid plaques were found in post-mortem brains of non-demented aged subjects (Bennett et al 2006), indicating that Aβ and plaques do not necessarily trigger the neurodegeneration cascade but may associate with normal aging. However, these individuals could have as well been in a very early phase of AD where cognitive alterations were not yet manifested or were able to compensate with higher cognitive reserves or possible protective mechanisms.

Criticism of the amyloid cascade hypothesis often refers to the fact that Aβ-targeted therapies so far were not successful in producing a significant functional recovery in patients with AD or slowing the disease's course. For example, a major phase 3 clinical trial of the γ-secretase inhibitor, semagestat, was terminated early due to increased decline in patients treated with the higher dose of semagestat compared to patients treated with placebo (Doody et al 2013). The failure may be explained by the other functions of γ-secretase on different substrates, such as its function in notch processing, (Karran & Hardy 2014) and could have been anticipated from mouse studies. Another large phase 3 trial of the humanized monoclonal anti-Aβ antibody, solanezumab, failed to improve cognition in mild and moderate AD patients (Doody et al 2014). However, the cognitive decline was slower in patients with mild AD (Doody et al 2014), suggesting that the anti-Aβ therapy should have been started earlier. Indeed, in a recent phase 1 clinical study, either prodromal or mild AD patients treated with the human monoclonal anti-Aβ antibody aducanumab showed pronounced reduction in brain Aβ plaques and slower clinical decline compared to patients receiving placebo (Sevigny et al 2016). These results highlight the possibility that starting the treatment at the beginning of AD development might have higher chances to be successfully beneficial than starting at stages where the disease is already consolidated and irreversible neuronal damaged has occurred. Therefore, the early detection of the diseased condition becomes extremely important and, in this respect, great effort is made in developing CSF biomarkers and neuroimaging approaches (e.g. magnetic resonance imaging, MRI and brain positron emission tomography, PET) (Frisoni et al 2017).

Based on these assumptions, the DIAN (Dominantly Inherited Alzheimer Network) (Morris et al 2012) and the API (Alzheimer's Prevention Initiative) Colombia (Reiman et al 2011) studies use anti-Aβ antibody treatments in pre-symptomatic individuals at risk for FAD with the hope of preventing or altering development of AD. Besides anti-Aβ antibodies, DIAN clinical trials are also using β-secretase inhibitors (Yan & Vassar 2014). If these or other amyloid-targeting treatments succeed in producing benefit to AD patients, this would validate the amyloid cascade hypothesis.

It is worthy to mention that alternative hypothesis have been posited for AD process. Among others, the mitochondrial cascade hypothesis (MCH) states that age-associated dysfunction of mitochondria might contribute to the progressive oxidative and free radical damage in the brain, leading to increased Aβ production and AD pathology (Sonnen et al 2008, Swerdlow & Khan 2004). Other alternative models for AD pathogenesis have proposed age-related increased DNA damage in neurons due to aberrant cell-cycling (Chow & Herrup 2015, Kruman et al 2004) or

cerebral glucose hypometabolism due to altered insulin signaling in the brain (Cholerton et al 2013, Ferreira et al 2014, Steen et al 2005) as possible disease-causing drivers. However, these theories lack of human genetic evidence from GWAS studies so far supporting a valid link with the AD process (Karran & De Strooper 2016, Lambert et al 2013).

Thus, the amyloid hypothesis is the dominant model of AD pathogenesis so far that is guiding the development of potential treatments against AD.

1.2 Mouse models of Alzheimer's Disease

There is no efficient naturally occurring animal model for AD. Very old apes, monkeys, and some other mammals such as bears, cats and dogs may exhibit some Aβ accumulations and slight CAA, but without presenting the complete AD pathology (Cummings et al 1996, Heuer et al 2012). Thus, transgenic rodents, especially mice have become important and the most used to model and study AD. Transgenic modeling in mice is relatively cheap, mice have a reasonably short life span, and the techniques for generating transgenic (tg) mouse lines are well developed. Current animal models are mainly based on naturally occurring human AD mutations. Indeed, mouse Aβ$_{1-42}$ sequence differs from human Aβ by 3 amino acids, causing a reduction in both the propensity of mouse Aβ to self-aggregate and its degree of neurotoxicity (Boyd-Kimball et al 2004). A number of different tg mouse models have been generated in the last years, and an overview of them is available at the Alzforum website (http://www.alzforum.org/research-models/alzheimers-disease). Table 1.1 contains selected examples of the more widely studied mouse models.

Numerous tg mouse lines overexpress one or more of the FAD mutations, such as the Indiana (V717F), London (V717I), and Swedish (K670N/M671L) (Chishti et al 2001, Games et al 1995). In general, those mice develop extracellular Aβ deposits rather late during their life (starting at 6-11 months of age), as well as gliosis and dystrophic neurites. Moreover, animals display cognitive and behavioral deficits when compared to wild-type (WT) animals.
Mice overexpressing PS FAD mutations, such as human PS1 (M146L or M146V) or PS2 alone (Elder et al 2010), have also been generated but failed to develop plaque pathology. Only combination of both mutated human APP and PS resulted in an earlier and more extensive plaque formation and cognitive decline (Holcomb et al 1998).
However, above mentioned mouse models recapitulate only amyloid pathology, but completely lack neurofibrillary tangles. Indeed, to reproduce both Aβ plaques and NFT pathology, mice expressing mutated human APP and PS were crossed with a mouse expressing tau with the P301L mutation (Oddo et al 2003). Despite difficulties in reproducing both amyloid and tau pathology, the substantial neuronal loss associated with AD is completely missing in most of tg mouse models (Elder et al 2010). However, an apparent reduction in neurons, limited to cortical layer 5, was induced in the 5X FAD line including three APP and two PS1 FAD mutations that individually are sufficient to cause disease in humans (Oakley et al 2006).

Model	FAD Mutation	Promoter	Amyloid pathology	Reference
PDAPP	APP-Indiana (V717F)	PDGF	Parenchymal plaques at 6-9 months of age	(Games et al 1995)
Tg2576	APP-Swedish (K670N, M671L)	PrP	Parenchymal plaques by 11-13 months of age with some vascular amyloid	(Hsiao et al 1996)
APP23	APP-Swedish (K670N, M671L)	Thy1	Parenchymal plaques by 6-9 months of age and prominent vascular deposition of amyloid	(Calhoun et al 1999)
TgCRND8	APP-Swedish (K670N, M671L) + Indiana (V717F)	PrP	More aggressive parenchymal plaque pathology present by 3 months of age	(Chishti et al 2001)
PSAPP	PS1 (M146V); APP-Swedish	PS1M146V × Tg2576	Earlier and more extensive plaque pathology than Tg2576 alone	(Holcomb et al 1998)
APPPS1	APP-Swedish (K670N, M671L); PS1 (L166P)	Thy1	Parenchymal plaques by 6-8 weeks of age accompanied by gliosis	(Radde et al 2006)
5x FAD	APP-Swedish (K670N, M671L) + Florida (I716V) + London (V717I); PS1(M146L, L286V)	Thy1	Parenchymal plaque pathology by 2 months of age and loss in synapsis and cortical layer 5 neurons by 9 months of age	(Oakley et al 2006)
3x Tg-AD	APP-Swedish (K670N, M671L); PS1 (M146V); tau (P301L)	Thy1.2 (APP, Tau)	Parenchymal plaques by 6 months of age combined with tau pathology by 12 months of age	(Oddo et al 2003)

Table 1.1. Selected examples of AD transgenic mouse models.
Abbreviations: APP, amyloid precursor protein; FAD, familial Alzheimer´s disease; PDAPP, platelet-derived growth factor promoter driving amyloid precursor protein; PDGF, platelet-derived growth factor β; PrP, prion protein; PS1, presenilin 1; PSAPP, presenilin/amyloid precursor protein; Tg, transgenic. Adapted from: Elder et al 2010.

Besides the widely used overexpression models, a knock-in mouse with a humanized Aβ region containing two or three APP mutations (APP NL-F or APP NL-G-F, respectively) have been recently generated (Saito et al 2014). These mice produce APP under endogenous murine promoter leading to the preservation of the endogenous expression levels of APP and its physiological spatiotemporal expression pattern. The combination of NL, F and G mutations results in enhanced APP processing and elevated Aβ levels, and mice develop amyloid plaques and gliosis starting at the age of 2 months and cognitive impairment by 6 months of age. APP knock-in mice thus offer an improved mouse model of FAD.

Overall, although none of the existing mouse models fully reproduces human AD pathology, AD mouse models have been and continue to be valuable tools for investigating individual aspects of AD pathogenesis.

1.2.1 The APPPS1 mouse model

This thesis uses an APPPS1 tg mouse model of cerebral amyloidosis observed in AD patients. The APPPS1 (line 21) mouse model of AD (Radde et al 2006) co-expresses the human transgenes APP bearing the Swedish mutation (K670N/M671L) and PS1 mutation (L166P), both under the control of the neuron-specific Thy1 promoter (Radde et al 2006). The Swedish APP mutation causes a 2 to 3 fold increased production of Aβ (Hsiao et al 1996, Mullan Mike 1992) by facilitating efficiency of β-secretase cleavage, which in contrast to WT cleavage occurs already in Golgi-derived vesicles (Haass et al 1995). The L166P PS1 mutation is a very aggressive mutation that causes onset of AD as early as 24 years of age (Moehlmann et al 2002). This PS mutation lowers Aβ40 levels resulting in increased Aβ42/Aβ40 ratio (Li et al 2016).
APPPS1 mice have been extensively explored as AD models and are pathologically very well characterized (Radde et al 2006). Amyloid deposition occurs relatively early, with the appearance of first plaques in the neocortex at approximately 6-8 weeks of age (Fig 1.7). Deposits in the hippocampus appear later (3-4 months of age) and increase in size and number with aging. By 8 months of age these mice exhibit a substantial plaque load with the majority of plaques consisting of a dense core surrounded by diffuse amyloid, resembling those in the human AD brain (Fig 1.7). Eight months old APPPS1 mice display increased numbers of microglia as well as dystrophic neurites in proximity to amyloid plaques. Moreover they have deficits in spatial learning and memorizing a maze task (Radde et al 2006).

Therefore, the APPPS1 mouse model is a suitable system to study amyloidosis-related pathomechanisms allowing relatively rapid experimental readouts.
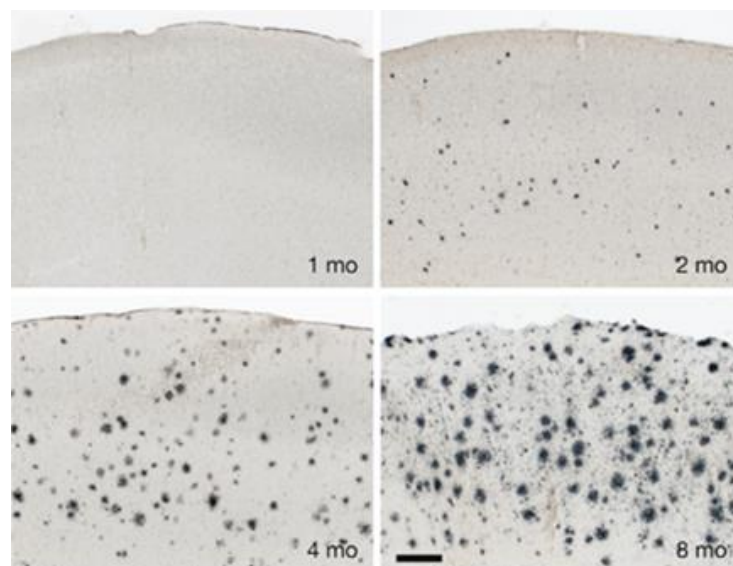
Figure 1.7. Aged-related increase in amyloid plaque load in APPPS1 mice.
Immunostaining of cortical sections from 1-, 2-, 4- and 8-month old APPPS1 mouse brains immunostained with anti-Aβ antibody NT12 to visualize amyloid plaques. Amyloid plaques, not yet detectable at 1 month of age, increase progressively in number and size and reveal substantial plaque pathology at 8-months of age in APPPS1 mice. Scale bar: 200 μm. From: Radde et al 2006.

1.3 Neuroinflammation and AD

Neuroinflammation is defined as activation of the innate immune system in the brain. Its main function is to protect the CNS against infectious insults, injury, or disease, such as AD.
The AD brain pathology is, besides presence of amyloid plaques and neurofibrillary tangles, also characterized by glial cell activation. Indeed, astrocytes and microglia are the major cell types that respond to disease stimuli by innate immune responses involving production and release of inflammatory mediators in the CNS (Zhang & Jiang 2015). In addition, perivascular macrophages and peripheral myeloid cells that can enter the diseased brain may also participate in neuroinflammatory reactions (Zhang & Jiang 2015).

1.3.1 Astrocytes

Astrocytes are the most abundant cells in the CNS, they provide trophic and metabolic support to neurons and are involved in neurotransmission, synaptic formation and plasticity (Kimelberg & Nedergaard 2010). Astrocytes are also active players in the neuroinflammatory response in AD.
It is known that amyloid plaques induce development of reactive astrocytes, which cluster around Aβ deposits (Serrano-Pozo et al 2013) (Fig 1.8). Cytokines and chemokines, such as CCL2 and CXCL10, are involved in the activation of astrocytes, chemotaxis and Aβ phagocytosis (Wyss-Coray et al 2003). Moreover, in response to increased levels of Aβ, astrocytes, like microglia, can contribute to maintain a pro-inflammatory condition by releasing IL-1β, IL-6, TNF, nitric oxide synthase (NOS), CCL2, CXCL10 and TGF-β (Garwood et al 2011, White et al 2005). These molecules can affect neurons either directly or indirectly through microglial activation. As an example, exposure to Aβ activates astrocytic NFκB and production of complement protein C3, which can bind neuronal C3aR and induce neuronal damage (Lian et al 2015). The increased cytokine production by activated astrocytes attracts microglia, which further express pro-inflammatory products and increase neuronal damage. Another astrocytic molecule, the Ca^{2+}-binding protein S100β, has been found to be highly expressed in proximity to Aβ deposits. Overexpression of human S100β in Tg2576 mice resulted in increased amyloidogenic processing of APP in addition to reactive astrogliosis and microgliosis. This was accompanied by increased expression of some pro-inflammatory cytokines, thus exacerbating AD-like pathology (Mori et al 2010).
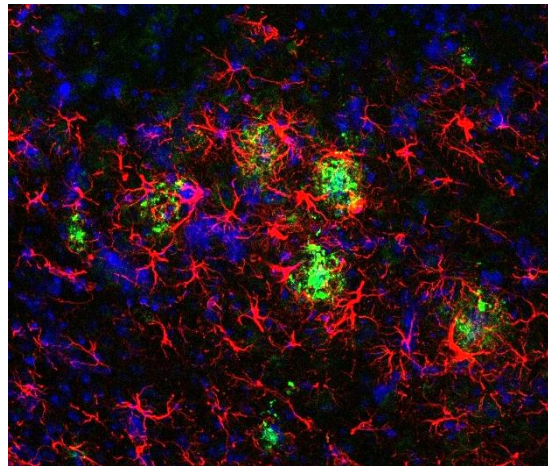
Figure 1.8. Astrocytes encircle amyloid plaques in APPPS1 mouse brain.
Confocal image of a cortical brain section from 5 month old APPPS1 mouse immunostained with anti-GFAP antibody (red) for visualizing astrocytes and anti-Aβ antibody 6E10 (green) for detecting amyloid plaques. Nuclei are counterstained with DAPI (blue). Activated astrocytes surround amyloid plaques and participate to the neuroinflammatory process. Image: courtesy of Laura Sebastian Monasor, German Center for Neurodegenerative Diseases (DZNE) Munich.

Astrocytes have been shown to internalize and phagocytose Aβ in a receptor-mediated fashion, for example through advanced-glycation end-products (RAGE) receptors and Fc receptor (Jones et al 2013, Okun et al 2010). Moreover, astrocytes can uptake Aβ via lipoprotein receptor-related protein 1 (LRP1) in the presence of ApoE, and perivascular astrocytes in AD brains were found to contain both Aβ and ApoE (Utter et al 2008). Astrocytic clearance of Aβ was also assessed in an *ex vivo* system. In this study exogenous astrocytes plated onto unfixed brain sections from AD mice were able to associate with Aβ deposits and induce Aβ removal (Wyss-Coray et al 2003).

1.3.2 Microglia

Microglia are the primary immune cells in the brain. They are considered the resident brain macrophages due to their myeloid origin, ability to migrate within different brain regions and to phagocytose, process and present antigens. Microglia derive from primitive hematopoietic cells in the embryonic yolk sac and invade the brain during fetal development (embryonic day 9.5), expand in numbers after birth, and are self-renewing throughout adult life (Ginhoux et al 2010). They represent around 10% of the CNS population (Lawson et al 1990).

Microglial cells are commonly visualized by cellular markers including ionized calcium binding adapter molecule 1 (Iba-1), which may take part in cell cytoskeletal reorganization (Sasaki et al 2001), CD68, which localizes to the lysosomal membrane and is indicative of phagocytosis, and CD11b, which is part of the type 3 complement receptor (CR3). Other microglial markers are, for example, the class II major histocompatibility complex (MHC II) proteins, such as HLA-DR subgroup, which increase upon inflammatory conditions (Korzhevskii & Kirik 2016) and fractalkine receptor CX3CR1, whose interaction with the neuronal fractalkine ligand CX3CL1 establishes a microglia-neuron communication (Harrison et al 1998).

Both in early and postnatal phases as well as in the adult brain, microglia secrete soluble factors, like insulin-like growth factor 1 (IGF-1) and brain-derived neurotrophic factor (BDNF), which regulate neurogenesis, neuronal migration and survival (Parkhurst et al 2013, Ueno et al 2013). Under physiological conditions, "resting" microglia act as sentinels and play a crucial role in the immune surveillance of the brain (Nimmerjahn et al 2005). Such microglia are highly ramified and that enables continuous scanning of their microenvironment for detection of any endogenous danger- or exogenous pathogen-associated molecular patterns (respectively, DAMPs and PAMPs) (Kettenmann et al 2011). It is estimated that microglial cells survey the entire brain parenchyma every few hours (Nimmerjahn et al 2005). Moreover, microglia fulfill other very important physiological functions. They participate in the removal of debris resulting from apoptotic cells or myelin (Mosley & Cuzner 1996, Sierra et al 2010). In addition, microglia monitor and remodel impaired synapses and thus can module circuit function, which is crucial for maintaining brain homeostasis and tissue integrity (Schafer & Stevens 2015, Wake et al 2009).

Microglia secrete anti- or pro-inflammatory mediators that act as paracrine modulators of neuronal plasticity and survival but that may also stimulate the autocrine polarization into diverse states of microglial activation in response to a danger (Cameron & Landreth 2010, Kettenmann et al 2011). For example, production of the growth factor M-CSF (macrophage-colony stimulating factor) itself can induce microglial chemotaxis, proliferation, increased macrophage scavenger receptor expression, and enhanced cell survival (Lue et al 2001). Similarly, the pro-inflammatory cytokine GM-CSF (granulocyte macrophage-CSF) is involved in the regulation of cell survival, differentiation, proliferation, inflammation and functional activities of microglia (Francisco-Cruz et al 2013).

The classical activation cytokines, including INF-γ, IL-1β, IL-6 and TNF-α, induce the polarization of microglia into a pro-inflammatory phenotype (often referred to as M1 phenotype). Conversely, the alternative activation pathway, induced by increased levels of anti-inflammatory cytokines, like IL-4, IL-10, IL-13 and TGF-β, promote an anti-inflammatory state of microglia (often referred to as M2 phenotype) (Boche et al 2013, Cameron & Landreth 2010). These microglial phenotypes are highly dynamic, dependent on the brain environment and may vary according to the type of stimulation, the progression of the inflammatory response and also with aging (Boche et al 2013, Lucin & Wyss-Coray 2009). It has been proposed that microglia adopt an activated phenotype, which is part of a "continuum" of heterogeneous phenotypes in constant evolution and highly dependent on their spatiotemporal context (Weitz & Town 2012). Thus, there is a common consensus of considering the M1/M2 classification not appropriate for defining microglial phenotypes. In such regard, attempts on improving microglial classification have started. For example, in order to identify microglial phenotypes following a specific stimulus, inflammatory markers and transcriptomic profile of microglia were defined and referred to as M_{LPS} or M_{IL-4} according to the lipopolysaccharide (LPS) or IL-4 stimulation, respectively (Beins et al 2016).

Recently, transcriptomic studies revealed the existence of distinctive gene expression profiles of microglia compared to peripheral immune cells (Sousa et al 2017). Those microglial genes encode integrins, purinergic receptors, clusters of differentiation (CD) markers, and some secreted proteins and include *CSF1R*, *CX3CR1*, *OLFML3*, *P2RY12*, *CD33*, *SIGLECH*, *TMEM119*,

TREM2 (Butovsky et al 2014, Hickman et al 2013, Zhang et al 2014). Transcriptomic studies are helpful in elucidating gene signatures of microglia as well as their transcriptional changes occurring in disease conditions, such as AD (Crotti & Ransohoff 2016, Wes et al 2016).

1.3.2.1 Microglia in the aging brain

Healthy aging is accompanied by enhanced glial activation, high levels of complement proteins and inflammatory factors, as well as atrophy of the brain (Lu et al 2004, Streit et al 2008). Microarray analyses of brains from aged individuals and mice revealed upregulation of genes linked to cell stress and inflammation, whereas genes linked to synaptic function, trophic support and growth factors are downregulated (Lu et al 2004). Although it is not clear yet, these studies propose that DNA damage induced by ROS may be involved in causing aging-related increase in inflammation (Lu et al 2004). It has been proposed that microglia may become dysfunctional and enter a senescent state with aging. These "dystrophic" (or "senescent") microglia are characterized by structural deterioration, including shortening and twisting of processes, cytoplasmic fragmentation and spheroid swellings' formation, as well as reduced migration and increased apoptosis (Streit et al 2008) (Fig 1.9). Such a state may cause reduced secretion of neurotrophic factors as well as downregulation of microglial phagocytic function. This loss of microglial neuroprotection and phagocytic efficiency, accompanied by increased secretion of inflammatory mediators, may lead to chronic neuroinflammation and contribute to progress of neurodegenerative diseases (Lu et al 2004, Streit et al 2008) (Fig 1.9). Furthermore, supporting these evidences, recent RNA-sequencing studies indicate that microglia express a unique set of transcripts, including a sensing cluster or "sensome" of transcripts that are differentially regulated during aging (Hickman et al 2013). These transcriptomic analyses demonstrated age-dependent differences in the expression of receptors for environmental sensing, where aged microglia enhance expression of genes for sensing microbial ligands, while reducing genes for sensing endogenous ligands compared with young microglia (Hickman et al 2013).
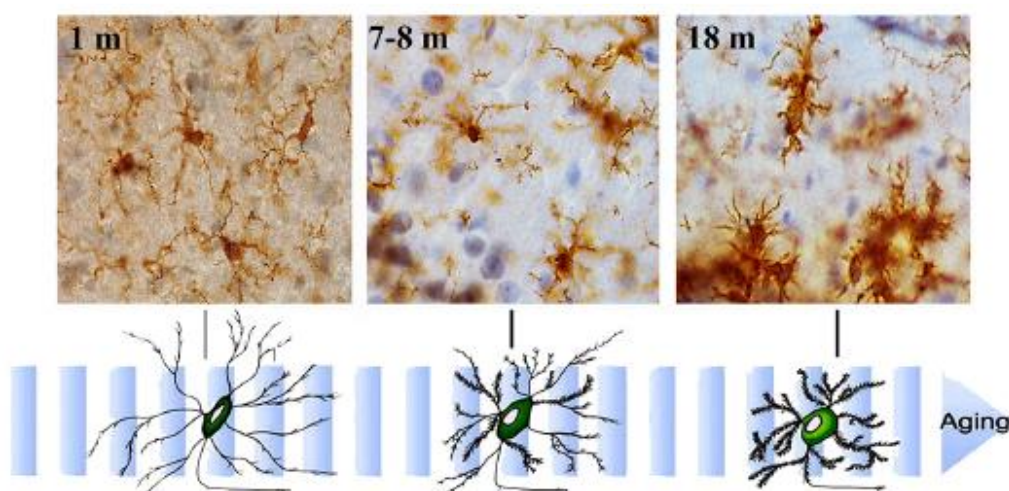
Figure 1.9. Microglial morphology changes with aging.
Immunostaining of hippocampal sections from 1-, 7-8- and 18-month old WT mice immunostained with Iba1 for microglia and hematoxylin for counterstaining. Microglia from young mice display small cell bodies and long, ramified processes. While aging, microglia gradually exhibit larger cell bodies and shorter, thicker processes. From: (Von Bernhardi et al 2015).

1.3.2.2 Microglia in the AD brain

Microglia are tightly associated to Aβ plaques in the brain of both AD patients (Perlmutter et al 1990) and animal models of AD (Frautschy et al 1998) (Fig 1.10). More recently, advanced imaging techniques, such as the two-photon intravital imaging in live AD animals, showed that resident microglia rapidly act in response to Aβ plaque formation by prolonging their processes and subsequently moving towards plaques (Bolmont et al 2008). Moreover, the interaction between microglia and Aβ plaques is regulated in a way that the number and size of microglia augment proportionally to the size of plaques, with the number of microglia surrounding plaques increasing at the pace of circa three cells per plaque per month (Bolmont et al 2008, Meyer-Luehmann et al 2008). Other studies in APPPS1 and 3x Tg-AD mouse models also showed that amyloid plaque formation in AD mouse brains is accompanied by the appearance of microglia that become significantly activated and associated with Aβ plaques (Rodriguez et al 2010, Yan et al 2009). Moreover, some microglial cells displayed amyloid material intracellularly, indicating active phagocytosis (Bolmont et al 2008, Rodriguez et al 2010). Notably, a significant expansion in the population of resting microglial cells has been reported to anticipate plaque formation and large microglial activation (Rodriguez et al 2010).

Despite these and many other studies supporting the involvement of microglia in the AD brain, the precise role of microglia in AD pathogenesis remains to be elucidated and characterized.
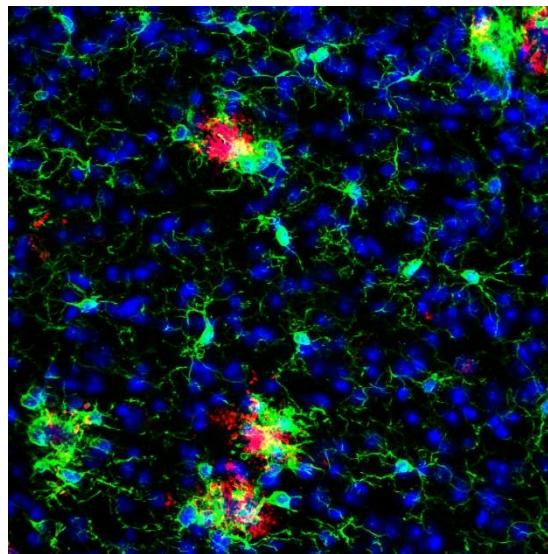
Figure 1.10. Microglial cells clustering around amyloid plaques.
Confocal image of brain section from 5 month old APPPS1 mouse immunostained with anti-Iba1 antibody (green) for visualizing microglia and anti-Aβ antibody 6E10 (red) for detecting amyloid plaques. Nuclei are counterstained with hoechst (blue). Microglial cells are recruited at the plaque sites where they form clusters around the plaques. Image: courtesy of Dr. Alessio Colombo, German Center for Neurodegenerative Diseases (DZNE) Munich.

1.3.2.3 Aβ-induced microglial activation

Microglial cells in the AD brain are constantly exposed to Aβ, which causes activation of their main functions, including phagocytosis and release of inflammatory mediators, both necessary

and potentially beneficial aspects in a diseased context. Additionally, "activated" microglial cells typically change their morphology into a less ramified and more amoeboid phenotype with shorter and thicker processes and enlarged soma (Fig 1.9).

In general, the proposed detrimental role of activated microglia in AD was based on the increased production of neurotoxic pro-inflammatory cytokines, including IL-1β and TNF-α, following Aβ stimulation (Meda et al 1995, Parajuli et al 2013). As an example, it has been described that oligomeric Aβ enhances maturation of pro-IL-1β into IL-1β in microglia via activation of the nucleotide-binding oligomerization domain (nod)-like receptor (NLR) pyrin domain containing-3 (NLRP3) inflammasome (Parajuli et al 2013). Other studies revealed that Aβ can even act synergistically with pro-inflammatory cytokines like INF-γ, driving the production of TNF-α and reactive nitrogen radicals that are neurotoxic (Meda et al 1995).

Microglia emerged as harmful players also in studies focused on CD40, a member of the TNFRs family, whose expression by microglia is enhanced in AD (Togo et al 2000). It has been shown that co-activation of microglia with Aβ and CD40 ligand (CD40L), thus stimulating the interaction CD40-CD40L, potentiates the release of TNF-α and promotes neuronal injury (Tan et al 1999). Moreover, microglia from Tg2576 (APPswe) mice deficient for CD40L showed attenuated activation, suggesting a link between CD40 and microglial activation in AD (Tan et al 1999). In line with that, APPswe/PS1 mice depleted of CD40L display reduced Aβ plaque load as well as microgliosis (Tan et al 2002).

The detrimental effect of microglial activation on neuronal survival has also been linked to the complement receptor 1 (CR1) on microglia. It has been reported that upon LPS or Aβ42 stimulation microglia increase CR1 expression, resulting in neuronal death due to enhanced microglial superoxide production, as well as TNF-α and IL-1β secretion. Moreover, the blockage of microglial CR1 had positive effects on neuronal survival (Crehan et al 2013).

Additional investigations revealed the deleterious consequences of microglial activation reflected by exacerbation of the neuronal injury and associated to Aβ accumulation. Correspondingly, studies on the microglial specific receptor CX3CR1 have shown that CX3CR1 deficiency resulted in a dose-dependent reduction in Aβ deposition in two different AD mouse models (Lee et al 2010). This effect was accompanied by reduced CD68 immunoreactivity as well as reduced numbers of Aβ plaque-associated microglia, decreased expression of TNF-α and chemokine (C-C motif) ligand-2 (CCL-2) and increased expression of IL-1β (Lee et al 2010). Moreover, *in vivo* and *in vitro* analyses demonstrated that CX3CR1-deficient microglia had enhanced capability to phagocytose Aβ, resulting in enhanced Aβ clearance (Lee et al 2010).

A similar approach was performed in another study targeted the NLRP3 inflammasome, whose specific activation by microglia may be implicated in AD pathogenesis. This study found that NLRP3 knockout reduced IL-1β levels and Aβ deposition in APPswe/PS1 mice, and this was associated with enhanced phagocytic capacity of microglia cells (Heneka et al 2013). Indeed, APPswe/PS1-NLRP3 knockout mice showed increased Aβ observed within CD11b-positive microglia, which co-localized with lysosome-associated membrane protein-2 (LAMP2) (Heneka et al 2013).

Above discussed studies suggest that microglial activity needs to be maintained at a level that is not harmful for neurons as inflammatory responses influence the activation state of microglia and may impair microglial capacity to phagocytose Aβ and trigger cascade of events leading to

neuronal degeneration. This continuous activation of microglia turns detrimental and may act as trigger for the progression of AD (Lucin & Wyss-Coray 2009, Wyss-Coray 2006).

1.3.3 AD risk genes cluster in innate immune response pathway

Recent GWASs confirmed the importance of microglia in AD by identifying variants in several microglial genes as risk factors for LOAD. Main LOAD genes implicated in innate immune response are listed in Table 1.2.

Gene	Function	Potential effect on APP	Pathways
TREM2	Immune response, production of inflammatory cytokines	Aβ clearance	Immune response
CLU	Chaperone; impact on microglial activation via complement regulation	Aβ clearance	Immune response and lipid metabolism
ABCA7	Substrate transport across cell membranes; phagocytosis of apoptotic cells and substrates (eg. Aβ)	Aβ clearance	Immune response
CR1	Complement cascade response	Aβ clearance	Immune response
CD33	Sialic acid-dependent binding to cells	Aβ clearance	Immune response
MS4A cluster	Poorly characterized; potential involvement in calcium signaling or regulation of T-cell -microglia interactions	-	Immune response
EPHA1	Neuronal development; angiogenesis, cell proliferation and apoptosis	-	Immune response and neuronal development
HLA-DRB5/B1	Component of MHCII	-	Immune response

Table 1.2. LOAD genes involved in altered microglial function in AD.
Abbreviations: TREM2, triggering receptor expressed on myeloid cells 2 protein; CLU, clusterin; ABCA7, ATP-binding cassette transporter A7; CR1, complement receptor 1; CD33, sialic acid-binding immunoglobulin (Ig)-like lectin; MS4A, membrane-spanning 4A cluster; EPHA1, ephrin receptor A1; HLA-DRB5/B1, Major Histocompatibility Complex, Class II, DR Beta 1/DR Beta 5. "–" indicates that the effect in the context of AD is still unclear. Adapted from: (Karch et al 2014); (Villegas-Llerena et al 2016); http://www.alzforum.org/genetics.

For example, a rare missense mutation in the gene encoding the triggering receptor expressed on myeloid cells 2 (TREM2), which is expressed on microglia, causes increased risk of developing AD (Jonsson et al 2013). It has been shown that TREM2 mutations result in reduced capacity of microglia to migrate to amyloid plaques and reduced clearance of Aβ (Kleinberger et al 2014, Mazaheri et al 2017, Ulrich et al 2014, Xiang et al 2016). Indeed, TREM2 depletion in the 5XFAD mouse model increased cerebral Aβ load due to a dysfunctional response of microglia, which became apoptotic (Wang et al 2015). Furthermore, the TREM2 protein can be measured as a soluble variant (sTREM2) in the CSF and there are recent data demonstrating that CSF sTREM2 levels are enhanced in the early symptomatic phase of AD, possibly correlating with an

early activation state of microglia in response to degenerating neurons (Suarez-Calvet et al 2016a, Suarez-Calvet et al 2016b).

Another example is the transmembrane protein CD33, which expression is increased in AD microglia compared to aged-matched controls. CD33 is involved in innate immunity modulation, with the risk allele inducing higher expression of CD33 in microglia and monocytes (Griciuc et al 2013). The depletion of CD33 in APPswe/PS1 mice decreased levels of insoluble Aβ42 and Aβ plaque deposition, suggesting a role for CD33 in inhibiting microglial uptake of Aβ, thus promoting Aβ accumulation (Griciuc et al 2013).

In addition, the ATP-binding cassette transporter A7 (ABCA7) is also highly expressed in microglia and loss of function variants of ABCA7 can affect AD pathogenesis (Steinberg et al 2015). ABCA7 depletion in PDGF-APPswe/ind mice impaired cerebral Aβ clearance by mainly reducing the capacity of bone marrow-derived macrophages (BMDMs) eliminating oligomeric Aβ, thus causing Aβ accumulation (Kim et al 2013).

These findings further support the link between the immune system/neuroinflammation and AD pathogenesis.

1.3.4 Aβ clearance by microglia

There is a body of evidence suggesting a role for microglia in Aβ clearance. Microglia express numerous surface receptors that promote the clearance and phagocytosis of Aβ, such as receptors for Fc, cytokines and chemokines (e.g. CCR2), scavenger receptors (e.g. CD36 and RAGE), complement receptors (e.g. CR3/CD11b), TLRs and the co-receptor CD14 (Cameron & Landreth 2010). Indeed, microglia in the vicinity of Aβ plaques internalized systemically injected-Aβ binding methoxy-X04 dye, suggesting their engagement in phagocytosis (Bolmont et al 2008).

It has also been shown that TLR4 and TLR2 and the co-receptor CD14 bind to fibrillar forms of Aβ and mediate their internalization and trafficking to the lysosome (Liu et al 2005, Reed-Geaghan et al 2009). This can initiate the activation of intracellular signaling pathways eliciting microglial production and secretion of reactive oxygen and nitrogen species, IL-6, and other neurotoxic factors (Reed-Geaghan et al 2009). Studies in AD mouse models (APPswe/PS1dE9) with mutant TLR2 suggested that deficiency in TLR signaling causes cognitive impairments with concomitant increase in Aβ deposition (Richard et al 2008).

Moreover, studies on complement receptors proposed a synergistic action of CR3/CD11b with the scavenger receptor A (SR-A) in mediating Aβ uptake and showed that murine microglia treated with SR-A ligands were less capable of taking up Aβ (Fu et al 2012).

Additional studies demonstrated that microglia can internalize soluble forms of Aβ through constitutive, fluid-phase micropinocytosis, which involves both actin and microtubules, and the internalized Aβ is then delivered to the late endosomes and lysosomes for degradation (Mandrekar et al 2009).

However, several studies suggest that Aβ clearance seems to be slow and ineffective over the course of disease, thus contributing to Aβ accumulation. For example, it has been reported that the APPswe/PS1dE9 mouse has decreased expression of various Aβ-binding receptors and Aβ-

degrading enzymes at 8 months of age that accompanies an increase in pro-inflammatory gene expression (Hickman et al 2008). Furthermore, microglia isolated from AD mouse (APPswe/PS1dE9) brains showed significant changes in lysosomal genes, such as *CD68*, *Gusb* and *Cts1* (Orre et al 2014). Additionally, *ex vivo* studies, where either acute brain slices or primary microglial cells from APPPS1 and APP23 mice were incubated with bead microspheres, identified impaired microglial phagocytosis compared with age-matched healthy controls (Krabbe et al 2013).

Moreover, it is important to note that AD is a disease of an aging brain and this fact is also relevant for understanding AD pathology. Two-photon studies of AD mouse models revealed that microglia in the aged brain are less motile and possess fewer processes (Meyer-Luehmann et al 2008). In another study, young microglia from AD mice were able to clear exogenously added Aβ in organotypic slice cultures while microglia from adult AD mice displayed a significant loss of their Aβ phagocytic function (Hellwig et al 2015). This supports the concept that aging is accompanied by impaired microglial function (Streit et al 2008).

On the other side, microglial depletion studies do not support a direct role for microglia on Aβ plaque deposition and clearance. In one study, they used the CD11b-thymidine kinase/ganciclovir suicide gene approach to induce selective ablation of microglia in APPswe/PS1 and APP23 mouse models of AD (Grathwohl et al 2009). Surprisingly, the absence of microglia did not change Aβ plaque load as well as morphology, size and cerebral distribution of amyloid deposits (Grathwohl et al 2009). Likewise, a more recent study using a similar approach showed that the conditional ablation of resident microglia did not change Aβ burden in APPswe/PS1 mice (Prokop et al 2015). However, those effects were observed after two to four weeks of microglial ablation and it is feasible that larger periods of ablation are needed to detect significant changes in Aβ dynamics.

1.3.4.1 Other mechanisms of Aβ clearance

In addition to phagocytic clearance of Aβ, microglia can directly secrete proteolytic enzymes that degrade Aβ, such as insulin degrading-enzyme (IDE), neprilysin (NEP), matrix metalloproteinase 9 (MMP9), and plasminogen (Hickman et al 2008). NEP and MMPs can in addition to microglia also be secreted by astrocytes (Eckman et al 2003). For example, deletion of the *NEP* gene increased Aβ levels and amyloid plaque burden in mouse models of AD (Farris et al 2007). Conversely, transgenic mice with NEP overexpression resulted in reduced levels of soluble Aβ and plaque burden (Leissring et al 2003). Similarly, genetic inactivation of *IDE* gene in mice resulted in elevated levels of Aβ in the brain (Farris et al 2003).

Another important clearance mechanism for Aβ is transcytosis across the blood-brain barrier (BBB), which is mediated mainly by the cell surface LRP1 (Shibata et al 2000) and RAGE receptors (Deane et al 2003) expressed on vascular brain endothelial cells. Aβ accumulation causes increased RAGE expression, resulting in cellular dysfunction due to RAGE-Aβ interaction and inflammatory responses in the cerebral endothelium (Deane et al 2003).

Other studies have also suggested that Aβ can be cleared via lymphatic drainage along perivascular channels and deposition of Aβ in the periarterial pathways, along which interstitial

fluid drains from the cerebral cortex, contributes significantly to CAA in AD (Carare et al 2008, Weller et al 1998).

These other mechanisms of Aβ clearance need to be taken into consideration since they may be alternative targets of potential therapeutic approaches aimed to reduce Aβ levels and AD progression.

1.4 *In vitro* and i*n vivo* models of Aβ phagocytosis by microglia

Microglial Aβ phagocytosis is a crucial aspect of the AD research that requires to be investigated. To this end, several approaches have been explored that I will describe here in more detail.

Microglial phagocytosis of Aβ has largely been studied in cultured primary microglial cells obtained from neonatal mice (Floden & Combs 2006) and incubated with recombinant Aβ peptides. For example, in cultured primary microglia incubated with monomeric or oligomeric Aβ42, lysosomal internalization of immuno-labeled Aβ was detected (D'Andrea et al 2004, Mandrekar et al 2009). In addition to primary microglial cells, immortalized microglial cell lines of mouse, rat or human origin are also commonly utilized as *in vitro* models (Malm et al 2012). One of the most used rodent microglial cell line in Aβ phagocytosis studies is the BV-2 (Henn et al 2009).

Of note, it has to be taken into account that the appropriate models for studying microglial phagocytosis in AD would need to consider aging as a crucial parameter. However, although primary microglial cells can be isolated from aged mice (Floden & Combs 2006) or postmortem brains (Walker & Lue 2005), such cells cannot be maintained in culture for prolonged period of time without addition of growth factors (Moussaud & Draheim 2010) that are known to affect microglial homeostasis. Moreover, it has been reported that microglia obtained from aged animals show altered responses to inflammation and decreased Aβ uptake and phagocytosis compared to microglia from young animals (Njie et al 2012). Furthermore, the function of isolated primary microglia could be disturbed by the isolation procedure *per se*. Recent RNA signature analyses demonstrated that changes in microglial gene expression profile occur due to the isolation and culturing conditions (Butovsky et al 2014, Gosselin et al 2017). More specifically, a unique molecular signature of adult microglia has been identified. While freshly isolated newborn and cultured primary microglia revealed to be partially similar to freshly isolated adult microglia, the specific microglia signature was completely missing in microglial cell lines, such as N9 and BV2 lines (Butovsky et al 2014).

In general, the *in vitro* conditions do not reflect the complexity of the microenvironment in which microglia are present *in vivo*, where production of bioactive molecules by other cells as well as direct cell-to-cell interactions may have an impact on microglial phenotypes (Lampron et al 2013). Also, collecting sufficient numbers of microglial cells from either neonatal or adult mouse CNS may be challenging.

Another difficulty in examining Aβ phagocytosis *in vitro* is caused by the propensity of Aβ peptides to self-aggregate. The way Aβ is prepared and solubilized may account for differences in the Aβ species/form that is finally applied onto the cells and the one occurring in disease pathology. Different Aβ forms, which are often poorly characterized in terms of biophysical

properties, may also explain diverse responses to Aβ reported in different cell culture studies (Malm et al 2012). It has been reported that fibrillar Aβ42 (fAβ) but not oligomeric Aβ42 (oAβ) enhanced microglial phagocytic function in a dose-dependent manner (Pan et al 2011). Moreover, pretreatment of microglia with oAβ decreased microglial capacity of phagocytosing fAβ (Pan et al 2011).

Alternatively, brain microglia and their responses to Aβ have been monitored in transgenic mouse models of AD by *in vivo* long-term imaging utilizing 2-photon microscopy (Malm et al 2012). As an example, it has been showed that GFP-labeled microglia migrate towards Aβ plaques and exhibited Aβ-containing lysosomes, suggesting their phagocytosis of Aβ (Bolmont et al 2008).

However, 2-photon microscopy is limited in the depth of tissue that can be imaged and is indeed restricted to superficial cortical areas. Since the imaging is executed in mouse cortical areas in which the skull has been removed or thinned, microglial activation caused by surgical manipulation cannot be circumvented (Nimmerjahn et al 2005). Moreover, for technical/ethical reasons such *in vivo* approach does only allow a certain number of repeated imaging sessions to be performed on the same animal. Furthermore, microglial responses to a specific modulator or drug responses are rather difficult to achieve and monitor *in vivo*.

All the above described tools represent efforts invested so far in the direction of examining microglial phagocytosis in AD. However, there are still limitations and the restricted availability of suitable model systems highlights our needs of developing novel methods for studying Aβ phagocytic functions of microglia. This is important not only for better understanding the AD-related pathological mechanisms but also for gaining knowledge on possible ways to interfere with them as modulating microglial phagocytic function is indeed one of the therapeutically relevant approaches against AD (Sevigny et al 2016).

2. Aim of the study

Neuroinflammation plays an important role in AD progression and microglial activation is one of the hallmarks of the disease pathology. However, a potential microglial function in amyloid plaque clearance is still controversial. Despite microglial recruitment and clustering around amyloid plaques, accumulation of Aβ occurs in AD patients as well as in AD mouse models, suggesting a possible reduction in phagocytic function of microglia over the course of AD. The major aim of my thesis was to investigate microglial amyloid plaques clearance and to understand better the failure of AD microglia to clear amyloid.

Due to the lack of suitable tissue culture system, the first aim was to establish and characterize a model that allows investigating microglial phagocytosis of amyloid plaques. Primary microglial cultures are often used for phagocytic analysis upon incubation with Aβ peptides. However, microglial identity, dynamics, as well as their responses are determined by their cellular context. Consequently, primary microglia isolated from their natural environment and cultured alone display altered microglial homeostasis and reactivity. Therefore, for this study, I cultured organotypic brain slices that resemble a "close-to-*in vivo*"-like situation, where microglia are maintained in their physiological cellular environment, but at the same time easy to manipulate. Moreover, in order to have a system containing amyloid plaques I directly cultured brain slices from a transgenic mouse model for AD pathology.

The second aim was to study microglia-mediated amyloid plaque clearance in the *ex vivo* co-culture model. To this end, I examined microglial cell numbers, morphology and activity as well as their phagocytic capacity. The goal was to identify factors that are able to restore phagocytic activity of aged AD microglia and elucidate molecular mechanism involved in amyloid plaque clearance.

3. Materials and Methods

3.1 Materials

3.1.1 Equipment and tools

3.1.1.1 General equipment and consumables

Product	Company
Analytical balance (0.0001-200g)	Denver Instrument
Balance (0.01-2000g)	Sartorius
Centrifuge (5810R)	Eppendorf
Centrifuge (Heraeus Fresco 17)	Thermo Scientific
Freezer (-20°C)	Liebherr
Freezer (-80°C)	Thermo Scientific
Fridge	Liebherr
Glassware	VWR
Gloves (Nitrile)	Meditrade
Heating and stirring plate	IKA RH
MilliQ plus filtration system	Merck Millipore
N_2 tank	Messer Griesheim
Oven	Memmert
Parafilm "M"	Bemis
pH indicator strips	Millipore
pH meter (Seven easy)	Mettler Toledo
Pipettes	Gilson, Eppendorf
Pipette controller accu-jet pro	BrandTech
Pipette tips (10 µl, 200 µl, 1000 µl)	Sarstedt
Serological pipettes (2 ml, 5 ml, 10 ml, 25 ml)	Sarstedt
Thermomixer compact	Eppendorf
Tubes (1.5 ml, 2 ml)	Sarstedt
Tubes (15 ml, 50 ml)	Sarstedt
Vortexer (Vortex-2 genie)	Scientific industries

3.1.1.2 Microscope and immunofluorescence equipment

Product	Company
Confocal laser scanning microscope (LSM 710)	Zeiss
Dissection microscope (SZ61)	Olympus
Epifluorescence microscope (AxioImager A2)	Zeiss
Gel fluoromont acqueous mounting media	Sigma Aldrich
Immersol 518 F	Zeiss

Microscope cover glasses 24 x 50 mm	Marienfeld
Microscope slides	Thermo Scientific
Objective (Plan Apochromat, 10x/0.45 dry DIC) – LSM 710	Zeiss
Objective (Plan Apochromat, 20x/1 dry DIC) – LSM 710	Zeiss
Objective (Plan Apochromat, 40x/1.4 oil DIC) – LSM 710	Zeiss
Objective (Plan Apochromat, 63x/1.4 oil DIC) – LSM 710	Zeiss
Objective (Plan Apochromat 10x/0.3) – AxioImager A2	Zeiss
Relief Paste Weiss (070)	Marabu
Scalpel	Braun

3.1.1.3 Microsurgical instruments

Name	Company
Dumont #2, laminectomy forceps straight (11223-20)	Fine Science Tolls, FST
Dumont #3, straight forceps (11231-30)	Fine Science Tolls, FST
Dumont #5, straight fine forceps (11252-20)	Fine Science Tolls, FST
Dumont #7, curved forceps (11271-30)	Fine Science Tolls, FST
Hardened fine scissors straight (14090-11)	Fine Science Tolls, FST
Spring scissors-angled to side sharp (15006-09)	Fine Science Tolls, FST
Surgical scissor straight (91400-14)	Fine Science Tolls, FST
Large spatula, double, one round end	Heathrow Scientific
Thin spatula, double, one round end	Heathrow Scientific

3.1.1.4 Cell culture equipment and consumables

Product	Company
Bunsen burner	Fuego
CD11b MicroBeads	Miltenyi Biotec
Cell culture laminar flow hood	Herasafe KS
Cell culture hood	Thermo Scientific
Cell culture dish (3.5 cm, 6 cm, 10 cm) Nunc	Thermo Scientific
Cell culture plate (6 well)	Thermo Scientific
Cell culture flask (75 cm^2)	Thermo Scientific
Cell strainer (40 µm)	NeoLab
Centrifuge tubes corning (15 ml)	Sigma Aldrich
CO_2-incubator	Binder, Thermo Scientific
LS MACS columns	Miltenyi Biotec
Magnetic Activated Cell Sorting-MACS kit	Miltenyi Biotec
Membrane inserts (PICM ORG 050)	Millipore
Neuronal tissue dissociation kit (P)	Miltenyi Biotec
PES sterile membrane filter (0.20 µm, 0.45 µm)	VWR International

quadroMACS separator	Miltenyi Biotec
Stericup and Steritop filter bottles (250 ml, 500 ml)	Millipore
Tissue chopper (TC752)	Mickle Laboratory Engineering Company
Tissue chopper blades	Gilette
Waterbath	GFL

3.1.1.5 Biochemistry equipment and consumables

Product	Company
Developer	Cawo
Glass plates for electrophoresis gels	Bio-Rad
Nitrocellulose membrane, 0.1 μm	GE Healthcare
Power supply	Bio-Rad
Protein electrophoresis gel system	Bio-Rad
PVDF membrane, Immobilon-P	Millipore
Sonifier	Branson/Heinemann
Shaker	Thermo Scientific
Tris-Tricine gels 10-20%	Thermo Scientific
X-ray films	Fuji

3.1.1.6 Molecular biology equipment and consumables

Product	Company
DNA electrophoresis gel system	Bio-Rad
Imager for agarose gels	INTAS Science imaging
Microwave	Sharp
Power supplier	Bio-Rad
PCR tubes	NeoLab
Thermocycler (Analytikjena)	Biometra

3.1.2 Chemicals, reagents, enzymes, antibodies

3.1.2.1 General chemicals

Name	Company
Acetic acid	Merck
Agarose Ultrapure	Life Technologies
Ammonium persulfate (APS)	Sigma Aldrich
Acrylamide/Bis solution 37.5:1	Serva
Bovine serum albumin (BSA)	Sigma Aldrich

Bromophenol blue	Fluka
Dimethylsolfoxide (DMSO)	Roth
ECL	Thermo Scientific
Ethanol	Merck
Ethylenediaminetetraacetic acid (EDTA) TRITLRIPLEX III	Merck
Formic acid	Merck
Glycerol	Merck
Glycine	Biomol
Goat serum	Sigma Aldrich
I-Block	Thermo Scientific
Isopropanol	Roth
KCl	Merck
KH_2PO_4	Merck
NaCl	Roth
Na_2HPO_4	Merck
NaOH	Millipore
NP40	USB
Paraformaldehyde (PFA)	Merck
Sodium deoxycholate	Sigma Aldrich
Sodium dodecyl sulfate (SDS)	Calbiochem
Sucrose	Sigma Aldrich
Tetramethylethylendiamin (TEMED)	Roth
Tricine	Biomol
Tris base	AppliChem
Triton X-100	Merck
Tween 20	Merck
β-Mercaptoethanol	Roth

3.1.2.2 Cell culture reagents

Name	Company
1x Dulbecco's modified eagle medium, DMEM/F12 (1:1) (11320-033)	Gibco
Fetal calf serum (FCS)	Sigma Aldrich
1x Hanks's buffered salt solution, HBSS (14025-050)	Gibco
HEPES	Gibco
Horse serum	Stem Cell Technologies
L-Glutamine	Gibco
1x Minimum essential medium, MEM (32360-026)	Gibco
Penicillin-Streptomycin	Invitrogen

3.1.2.3 Reagents, enzymes, DNA/protein markers and dyes

Name	Company
DAPI	Invitrogen
Deoxyribonucleotides (dNTPs)	Roche
DNA Ladder 1kb Plus	Invitrogen
DNA Polymerase (GoTaq G2)	Promega
GelRed Nucleic Acid Stain	Biotium
GoTaq buffer	Promega
Phalloidin (Alexa Fluor 555-labeled)	Life Technologies
Propidium iodide	Sigma Aldrich
Protease inhibitor cocktail (P8340)	Sigma Aldrich
SeaBlue Protein Ladder Plus 2	Thermo Scientific
Thiazine red	Sigma Aldrich
Tryphan blue	Life Technologies

3.1.2.4 Antibodies

Primary antibodies

Antibody	Clone	Species	Dilution	Company
β3-Tubulin	MM-435-P	mouse	WB: 1:1000	Covance
CD68	MCA1957GA	rat	IF: 1:1000 WB: 1:600	Serotec
GFAP	Z 0334	rabbit	IF: 1:200 WB: 1:1500	Dako Cytomation
GFP	20R-GR011	mouse	IF: 1:200	Fitzgerald
GFP	75-132	rabbit	IF: 1:200	NeuroMab
M3.2	SIG-39155	mouse	IF: 1:500	Covance
NeuN	MAB377	rabbit	IF: 1:200	Millipore
Ki67	12202	rabbit	IF: 1:100	Cell Signaling Technology
6E10 (β-amyloid 1-16)	SIG-39320	mouse	IF: 1:500	Covance
2D8		rat	IF: 0.011 µg/µl WB: 2 µg/ml	(Shirotani et al 2007)

Secondary antibodies

Antigen	Labeled	Species	Dilution	Company
mouse IgG (H+L)	Alexa Fluor 488, 647	goat	IF: 1:200	Life Technologies
rabbit IgG (H+L)	Alexa Fluor 488, 555	goat	IF: 1:200	Life Technologies
rat IgG (H+L)	Alexa Fluor 488, 555, 647	goat	IF: 1:200	Life Technologies

rat IgG (H+L)	Alexa Fluor 555	goat	IF: 1:350	Immunological Sciences
mouse IgG (H+L)	Horse radish peroxidase (HRP)	goat	WB: 1:10000	Promega
rabbit IgG (H+L)	HRP	goat	WB: 1:10000	Promega
rat IgG (H+L)	HRP	goat	WB: 1:10000	Santa Cruz Biotechnology

3.1.3 Drugs and cytokines

Drug	Stock concentration	Solvent	Used concentration	Company
Cytochalasin D (CytoD)	1 mM	DMSO	1 µM	Sigma Aldrich
Clodronate (Clo)	50 mg/ml	H_2O	100 µg/ml	Millipore
Recombinant mouse IL-10	100 µg/ml	PBS	100 ng/ml	R&D systems
Recombinant mouse TGF-β1	50 µg/ml	PBS	100 ng/ml	R&D systems
Recombinant mouse IL-6	100 µg/ml	PBS	100 ng/ml	R&D systems
Recombinant mouse IL-12/p40	100 µg/ml	PBS	100 ng/ml	R&D systems
Recombinant mouse GM-CSF	1 µg/ml	PBS	1 ng/ml	R&D systems
Cytosine arabinose (AraC)	1 mM	H_2O	5 µM	Merck Millipore

3.1.4 Buffers and media

If not differently specified, all buffers were prepared in MilliQ water.

3.1.4.1 Cell culture

Name	Composition
Slice culture dissection media	1% Penicillin-Streptomycin 10 mM Tris pH 7.2 in HEPES buffered-MEM
HBSS buffer	0.6% HEPES in 1x HBSS
MACS buffer	0.5% BSA 0.08 mM EDTA in 1x PBS
Microglia media	10% heat inactivated FCS 1% Penicillin-Streptomycin in DMEM/F12

1x Phosphate-buffered saline (PBS)	137 mM NaCl
	2.7 mM KCl
	2 mM KH_2PO_4
	8.1 mM Na_2HPO_4
Slice culture media	50% HEPES buffered-MEM
	25% heat inactivated horse serum
	25% HBSS
	1 mM L-Glutamine
	pH 7.4

3.1.4.2 Immunofluorescence

Name	Composition
Immunofluorescence blocking solution	0.5% Triton X-100
	5% Goat serum
	in 1x PBS
Permeabilization buffer	0.5% Triton X-100
	in 1x PBS
4% PFA - Fixing solution	4% PFA
	4% Sucrose
	0.15 mM NaOH
	in 1x PBS
	pH 7.4

3.1.4.3 Biochemistry

Name	Composition
I-Block – blocking solution	0.2% I-Block
	0.1% Tween 20
	in 1x PBS
4x Laemmli buffer	125 mM Tris pH 6.8
	8% SDS
	40% Glycerol
	0.025% Bromophenol blue
	10% β-Mercaptoethanol
5x RIPA stock buffer	100 mM Tris pH 7,4
	750 mM NaCl
	5% Igepal (NP40)
	1.25% Triton X-100
	5% Sodium-deoxycholate

1x RIPA lysis buffer (10 ml)	5x RIPA stock buffer (2ml) 0.5 M EDTA (50 µl) 1x Protease inhibitor cocktail 0.1% SDS
4x Separating gel buffer	1.5 M Tris 0.4% (w/v) SDS adjust to pH 8.8
4x Stacking gel buffer	0.5 M Tris 0.4% (w/v) SDS adjust to pH 6.8
1x Transfer buffer	25 mM Tris 80 mM Glycine
1x Tris-Glycine running buffer with SDS	25 mM Tris 80 mM Glycine 0.1% SDS
1x Tris-Tricine running buffer with SDS	100 mM Tris 100 mM Tricine 0.1% SDS

3.1.4.4 Molecular biology

Name	Composition
1% Agarose gel buffer	1% Agarose in 1x TAE buffer
6x DNA loading buffer	30% Glycerol 0.25% Bromophenol blue 0.25% Xylene cyanol FF
Neutralization buffer	1.5 M Tris pH 8.8
1x TAE buffer	40 mM Tris 20 mM Acetic acid 1mM EDTA pH 8.0

3.1.5 DNA oligonucleotides

3.1.5.1 Primers for genotyping

For APPPS1 mouse line

Name	Sequence
APP_forward	GAATTCCGACATGACTCAGG
APP_reverse	GTTCTGCTGCATCTTGGACA
PS1_forward	CAGGTGCTATAAGGTCATCC
PS1_reverse	ATCACAGCCAAGATGAGCCA

For CX$_3$CR1$^{+/GFP}$ mouse line

Name	Sequence (5`→ 3`)
CX3CR1_WT	GTCTTCACGTTCGGTCTGGT
EGFP_mutant	CTCCCCCTGAACCTGAAAC
Upstream primer	CCCAGACACTCGTTGTCCTT

For GM-CSF$^{-/-}$ mouse line

Name	Sequence (5`→ 3`)
Common primer	AGGTCTTCAGGGATTGATGG
Mutant primer	CTCAGCTACCACAGCCATGT
WT primer	CTCCAGACTGCCTTGGGAAAA

3.1.6 Services

Service	Company
Transfers	Eurokurier München
Oligonucleotide synthesis	Sigma Aldrich

3.1.7 Software and online tools

Name	Company
Adobe Illustrator	Adobe Systems
Adobe Photoshop CS5	Adobe Systems
AxioVision	Zeiss
ImageJ/Fiji	National Institute of Health
Imaris x64	Bitplane
MS Office	Microsoft
NCBI (https://www.ncbi.nlm.nih.gov/)	National Institute of Health
ZEN, LSM	Zeiss

3.2 Methods

3.2.1 Animals

The APPPS1 mice (line 21) overexpressing human APP$_{KM670/671NL}$ and PS1$_{L166P}$ under the control of the Thy-1 promoter (Radde et al 2006) and bred in a C57BL/6J background were used. The CX$_3$CR1$^{GFP/GFP}$ reporter line (Jung et al 2000) was purchased from the Jackson Laboratory and bred with C57BL/6J WT and APPPS1 line to obtain CX$_3$CR1$^{+/GFP}$ and CX$_3$CR1$^{+/GFP}$/APPPS1 mice, respectively. The GM-CSF knockout mice (GM-CSF$^{-/-}$) were also purchased from the Jackson Laboratory (Dranoff et al 1994). For all analyses in this study both male and female mice were used. Mice were group housed in specific pathogen-free conditions. Mice had access to standard mouse food and water *ad libitum* and were kept in a 12/12 h light-dark cycle in IVC System Typ

II L-cages (528 cm²) equipped with solid floors and a layer of bedding. All animal experiments were executed in accordance with the German animal welfare law and have been approved by the government of Upper Bavaria.

3.2.2 Genotyping

Genomic DNA was extracted from a small piece of mouse tails or from ear biopsies by alkaline lysis of the tissue. First, the tissue was incubated with 100 µl of 50 mM NaOH and heated at 95°C for approximately 45 min. During the incubation, samples were vortexed every 15 min for about 10 sec at medium intensity to facilitate tissue lysis. Afterwards, samples were put on ice for 1-2 min to cool down and the alkaline reaction was neutralized by addition of 10 µl of neutralization buffer (1.5 M Tris, pH 8.8) and vortexed at medium intensity. Samples were then centrifuged at 4°C at maximum speed in a table top centrifuge for 5 min and stored at 4°C. The extracted DNA was used as template for a polymerase chain reaction (PCR). A typical PCR reaction-mix was prepared as follows (for reaction a volume of 20 µl):

Component	Amount
5x Buffer GoTaq	4 µl
dNTPs (10 mM each)	0.5 µl
Fw-Primer (10 pmol/µl)	1 µl
Rev-Primer (10 pmol/µl)	1 µl
Taq-Polymerase (5 U/µl)	0.2 µl
DNA	1 µl
MilliQ H_2O	12.3 µl

For the APPPS1 line, to test for the presence of the human mutated APP and PS1 genes, two different PCR reaction-mix solutions were prepared (APP_forward + PS1_forward; APP_reverse + PS1_reverse). Also for the CX3CR1[+/GFP] line two different PCR reaction-mix solutions were prepared (upstream primer + CX3CR1_WT primer; upstream primer + EGFP_mutant primer). For the GM-CSF^{-/-} line only one PCR reaction-mix solution was prepared (common + mutant + WT primers). The PCR reaction-mix was placed in a thermocycler and the following PCR cycling programs were applied, respectively:

For APPPS1 mouse line

Step	Temperature	Time	Cycles
Initial denaturation	95°C	10 min	1 x
Denaturation	95°C	30 sec	
Annealing	63°C	30 sec	30 x
Extension	72°C	30 sec	
Final extension	72°C	5 min	1 x
Storage	4°C	hold	

For CX₃CR1⁺ᐟᴳᶠᴾ mouse line

Step	Temperature	Time	Cycles
Initial denaturation	95°C	10 min	1 x
Denaturation	95°C	30 sec	
Annealing	60°C	30 sec	30 x
Extension	72°C	45 sec	
Final extension	72°C	5 min	1 x
Storage	4°C	hold	

For GM-CSF⁻ᐟ⁻ mouse line

Step	Temperature	Time	Note	Cycles
1.	94°C	2 min		1 x
2.	94°C	20 sec		
3.	65°C	15 sec	-0.5°C per cycle decrease	10 x
4.	68°C	10 sec		
5.	94°C	15 sec		
6.	60°C	15 sec		28 x
7.	72°C	10 sec		
8.	72°C	2 min		1 x
9.	4°C	hold		

Separation of the PCR products was performed via gel electrophoresis. Samples (5 or 10 µl each) were loaded on a 1% agarose TAE gel containing 1:20000 intercalating agent gelred and TAE as the running buffer. For the GM-CSF⁻ᐟ⁻ line a 2% agarose TAE gel was used. Voltage was set to 95 V and run for approximately 30 minutes. The gel was then imaged with a UV light source and a picture was taken as documentation. The expected amplification products were as follows. For APPPS1 line: APP band ~250 bp; PS1 band ~250 bp; for CX3CR1⁺ᐟᴳᶠᴾ line: CX3CR1_WT band ~410 bp; EGFP_mutant band ~500 bp; for GM-CSF⁻ᐟ⁻ line: mutant band ~300 bp, WT band ~317 bp.

3.2.3 Organotypic slice cultures

Organotypic slice cultures were prepared according to the membrane interface method described by Stoppini et al with some modifications (Stoppini et al 1991). Brains were isolated from either young neonatal (postnatal day 5 to 7) or old (10- to 20-month of age) mice. Young pups were decapitated and old mice were sacrificed by CO_2 inhalation according to animal handling laws. After opening the skull, the brain was removed and collected in a 6 cm dish containing 3 ml of pre-cooled slice culture dissection media. The two hemispheres were gently separated using a wide spatula and olfactory bulb, cerebellum, and midbrain were cut off under a dissection microscope. Neocortices together with hippocampi were dissected from the neonatal mouse brains and cut to obtain cortico-hippocampal slices, whereas from the old

mouse brains neocortices and hippocampi were dissected and cut separately obtaining hippocampal and cortical slices. Sagittal sections, 350 μm thick, were sliced using a Mcllwain tissue chopper. The sliced tissue was collected using a thin spatula into a 15 ml tube containing 6 ml of pre-cooled slice culture dissection media and transferred to a pre-cooled empty 6 cm dish. Only intact slices were carefully selected under a dissection microscope. Selected slices were moved into a 6 cm dish containing 5 ml of pre-cooled slice culture dissection media using a fire-polished glass pipette with wide tip diameter and incubated for at least 30 min at 4°C. Afterwards, four slices were plated onto 0.4 μm porous polytetrafluoroethylene (PTFE) membrane inserts placed into a previously prepared 3.5 cm dish containing 1 ml of slice culture media. Slice culture samples were kept in a cell-culture incubator at 37°C, 5% CO_2.

Slice culture media were exchanged the day after the preparation and then every 3-4 days. In the co-culture paradigm, two slices of young WT tissue (cortico-hippocampal) were plated together with two slices of old APPPS1 tissue (cortical and hippocampal) in the same culture dish.

3.2.4 Drug and cytokine treatments of slice cultures

Treatments were performed by directly adding drugs to the slice culture media. Slice cultures were usually treated starting from day 1 *in vitro* (DIV) and retreated at every media exchange (each 3-4 days). The drugs/cytokines used for all experiments are listed in the table above.

For the clodronate treatment, either old APPPS1 or young WT tissue was treated till 7 DIV. Afterwards, the treatment was stopped by placing the inserts with the slices in new dishes containing fresh pre-equilibrated slice culture media then and either young WT or old APPPS1 tissue was added to the culture to re-establish the co-culture condition.

3.2.5 Slice culture conditioned media: collection and incubation

Collection of conditioned media (CM) from young WT and old APPPS1 tissue (4 slices/dish) was performed starting from 4-5 DIV and every 3-4 DIV for a total of six times. CM were collected in 1.5 ml tubes, centrifuged at 0.9xg for 5 min at 4°C and supernatants stored at -20°C. CM from different tubes were thawed, pooled and distributed into new 3.5 cm dishes (1 ml/dish) and pre-equilibrated at 37°C, 5% CO_2 for at least 2 hours before incubating the old APPPS1 tissue.

For collection of CM from microglia-depleted young WT tissue, slices (4 slices/dish) were treated with 100 μg/ml of bisphosphonate clodronate (Clo) from 1 DIV until 7 DIV. After stopping the treatment, CM were collected (starting from 10-11 DIV) every 3-4 days for a total of five times. CM were filtered through a 0.2 μm pore size sterile filter (VWR International) and stored at -20°C until usage. As a control, media were collected from vehicle (H_2O)-treated young WT tissue and subjected to the same experimental procedure. Slice cultures were incubated in CM, starting from 1 DIV, and re-incubated every 3-4 days with freshly thawed and pre-equilibrated CM. Samples were fixed at 7, 11 and 14 DIV and immunostained.

For analysis of cell proliferation, old APPPS1 slices were incubated in CM from young WT tissue in combination with 5 μM AraC or H_2O as a vehicle control, starting from 1 DIV and re-incubated every 3-4 days with freshly thawed and pre-equilibrated CM and retreated. Samples were fixed at 14 DIV and immunostained.

3.2.6 Primary microglial cultures, conditioned media: collection and incubation

Isolation of primary microglia was executed from postnatal day 5 WT mouse brains utilizing Magnetic Activated Cell Sorting (MACS) Technology and according to manufacturer's instructions. After decapitation, brains were removed and collected in a 6 cm dish containing 3 ml of HBSS buffer. Cortices were dissected under a dissection microscope, cleaned from meninges and cut in small pieces. Cortical pieces were transferred into a clear 15 ml tube, pieces were left to sink in the tube and the supernatant containing only HBSS buffer was carefully aspirated. Tissue was dissociated by enzymatic digestion using a Neural Tissue Dissociation Kit (P). First, 1950 µl of pre-warmed (37°C) enzyme mix1 (part of the Kit) was added, gently mixed and incubated for 15 minutes at 37°C in the waterbath. Then 30 µl of enzyme mix2 (part of the Kit) were added to the sample, mixed and a mechanical dissociation was carried out using a fire-polished Pasteur pipette with wide diameter and pipetting up and down 10 times followed by incubation for 10 minutes at 37°C. Tissue was mechanically dissociated using two fire-polished Pasteur pipettes in decreasing diameter and again incubated for 10 minutes at 37°C. Cell suspension was applied onto a 40 µm cell strainer placed on a 50 ml tube prior conditioning of the cell strainer with 5 ml of HBSS buffer. Then additional 5 ml of HBSS buffer were added through the cell strainer. Cell suspension was centrifuged at 300xg for 10 minutes at RT, the supernatant was completely aspirated and cells were resuspended in 10 ml of HBSS buffer and counted by diluting 1:2 with tryphan blue using a cell counter chamber. Cell suspension was again centrifuged at 300xg for 10 minutes at RT and cell pellet was resuspended in 90 µl of MACS buffer and 10 µl of CD11b MicroBeads were added per 10^7 cells and incubated for 15 minutes at 4°C with occasional shaking. Cells were washed by addition of 2 ml of MACS buffer and centrifuged at 300xg for 10 minutes. The supernatant was discarded and the pellet plus CD11b-magnetic beads was resuspended in 1 ml of MACS buffer. LS MACS columns were placed in the quadroMACS separator on top of a collecting tube and conditioned with 3 ml of MACS buffer. Then cell suspension was loaded onto the column and subjected to magnetic separation. After three washing steps with 1ml MACS buffer, the column was removed from the separator and placed on a new 15 ml collection tube. 2 ml of MACS buffer was applied onto the column and cells were flushed out by firmly pressing the plunger into the column. Cd11b-positive microglial cells were counted, diluting 1:2 with tryphan blue and centrifuged at 300xg for 2 minutes at RT. The cell pellet was resuspended in 1 ml of pre-warmed microglia media consisting of DMEM/F12 with 10% heat inactivated FCS and 1% penicillin-streptomycin. Microglia were plated onto 6 cm tissue culture dish at density of $1x10^6$cells/dish and cultured for 24 hours in microglia media in a cell-culture incubator at 36.5°C, 5% CO_2. After 24 hours, microglia media were replaced with fresh slice culture media described above.
CM were collected after additional 48 hours and filtered through a 0.45 µm pore size sterile filter and stored at -20°C. Old APPPS1 slices were incubated in CM from young primary microglia or in slice culture media as a control, starting from 1 DIV and re-incubated every 3-4 days with freshly thawed and pre-equilibrated CM. Samples were fixed at 14 DIV and immunostained.

3.2.7 Immunoblotting

For biochemical characterization of slice cultures, samples were prepared as follows. For each sample, 8 brain slices were pooled (from 4 independent slice culture dishes with 2 slices/dish) and this was performed in triplicates and in three independent experiments. Brain slices were collected from the inserts using a thin spatula and transferred into a tube containing ice-cold PBS, centrifuged at 600xg for 5 minutes at 4°C pellets frozen in liquid nitrogen (after removal of the supernatant) and stored at -80°C until usage.

The slices were homogenized with 200 µl 1x RIPA buffer mechanically with a little pestle in 1.5 ml tubes. After centrifugation at 14.000xg for 60 minutes at 4°C RIPA soluble proteins were obtained. The remaining pellet was further homogenized in 100 µl 70% formic acid by sonication for 7 min. The formic acid fraction was neutralized with 20x 1 M Tris-HCl buffer at pH 9.5 and used for Aβ analysis. For Aβ detection, samples were heated at 95°C in 4x Laemmli buffer for 5 minutes and proteins were loaded on precasted Tris-Tricine gels (10-20%). Gels were run at 60 V in Tris Tricine running buffer with SDS for the first 10 min and afterwards at 120 V until the dye front reached the very end of the gel. Proteins were transferred to nitrocellulose membranes at 400 mA for 60 minutes in Tris-Glycine transfer buffer. Membranes were boiled for 5 min in PBS and subsequently incubated with the blocking solution consisting of 0.2% I-Block and 0.1% Tween 20 in PBS for 1 hour, followed by overnight incubation with 2 µg/ml 2D8 antibody diluted in the blocking solution.

RIPA lysates (10 to 20 µg of protein) were separated under denaturing conditions on 8% Tris-Glycine gels (complete composition is described below) in Tris-Glycine running buffer with SDS. Proteins were blotted on isopropanol activated PVDF membranes in Tris-Glycine transfer buffer for the detection of CD68, GFAP and β3-Tubulin. After primary antibody incubation, nitrocellulose membranes were washed in PBS with 0.1% Tween 20 and PVDF membranes in PBS containing 0.2% Triton X-100 three times for 10 minutes. Next, the corresponding anti-horseradish peroxidase (HRP) conjugated secondary antibodies (listed in table above) diluted in blocking solution were added and the membranes were incubated for 1 hour at RT, followed by appropriate washing steps as before. Antibody detection was performed using chemiluminescence detection reagent ECL and films were developed and used for quantifications with ImageJ.

Gel type	Composition of a 8% Tris-Glycine gel
Stacking gel (5 ml)	40% Bisacrylamide (0.5 ml)
	4x stacking gel Tris buffer (1.25 ml)
	TEMED (5 µl)
	10% APS (5 µl)
	H_2O dest (3.2 ml)
Separating gel (20 ml)	40% Bisacrylamide (4.0 ml)
	4x separating gel Tris buffer (5 ml)
	TEMED (20 µl)
	10% APS (20 µl)
	H_2O dest (11.0 ml)

3.2.8 Immunohistochemistry

Slice culture samples were fixed in 4% paraformaldehyde (PFA)/sucrose, pH 7.4 for 15 min at room temperature (RT). 1 ml of PFA/sucrose was pipetted below the insert and 1 ml was directly added onto the slices placed on the insert. Slices were washed three times in PBS and permeabilized for 30 min in permeabilization buffer (0.5% Triton X-100 in PBS). Afterwards, slices were cut from the membrane insert using a scalpel and transferred with a forceps in a wet chamber, where they were incubated for 1 hour in a blocking solution consisting of PBS containing 0.5% Triton X-100 and 5% goat serum. Slices were incubated overnight at RT in blocking solution containing primary antibodies (listed in table above). Slices were washed three times for 10 min with PBS containing 0.5% Triton X-100 and incubated for 3 to 5 hours at RT in blocking solution containing nuclear marker DAPI (1:20000) and appropriate secondary antibodies conjugated to Alexa Fluor (listed in table above). For actin-cytoskeleton staining Phalloidin-Alexa Fluor 555 was used (1:50) in solution together with the secondary antibodies. Subsequently, slices were washed three times for 10 min with PBS containing 0.5% Triton X-100. Fibrillar dense core plaques were stained with the dye Thiazine red (2 µM solution in 1x PBS) for 20 min in the dark at RT followed by three washing steps with PBS, 10 minutes each. Slices were mounted onto glass slides, covered with Gel Mount media and with a glass coverslip. Stained slices were then imaged by confocal and fluorescent microscopy.

3.2.9 Image acquisition, analysis and quantification

Confocal images were taken on a LSM 710 confocal microscope (Zeiss) utilizing ZEN 2011 software package. The acquisition was performed using a Plan-Apochromat 10x/0.45 M27 and 40x/1.4 oil differential interference contrast (DIC) objectives at 0.6 and 1.5-fold magnifications. 3D reconstruction image was done utilizing Imaris x64 software (version 7.6.0). 3D images were analyzed utilizing the "surpass volume" mode. Representative images were taken using the "snapshot" tool. To quantify numbers of amyloid plaques, slice culture samples were immunolabeled with M3.2 or 6E10 anti-Aβ antibodies for visualizing plaques. Stained slices were imaged on a fluorescence microscope (Zeiss AxioImager A2) equipped with AxioCam MRm utilizing AxioVision software package. The objective used was a Plan-Apochromat 10x/0.45. The counting of the total number of amyloid plaques and number of core-only plaques was performed manually from acquired images and normalized to the tissue surface (in square micrometers). The imaged tissue surface was determined utilizing the ZEN lite 2011 software package. Quantified values are expressed as percentages of core-only plaques from the total number of amyloid plaques. All quantification analyses were based on a minimum of 18 images per experiment, from at least 3 independent experiments. As an exception, data showed in Fig 4.20B and Fig 4.27B were based on quantification analyses from 12 images per experiment, from 3 independent experiments. Core-only plaques were categorized as plaques consisting of fibrillar, TR positive amyloid core without detectable halo positive for 6E10 (as illustrated in Fig 4.8 and Fig 4.9). To quantify the number of plaque associated CD68 positive cells and plaque size, slice culture samples were immunolabeled with CD68 and 6E10 antibodies and confocal images were taken using a 40x/1.4 oil DICIII objective at 1.5-fold magnification. The counting of the plaque associated CD68 positive cells was performed manually considering signal of CD68

and nuclear-DAPI staining. Quantified values were expressed as numbers of CD68 positive cells per plaque. The plaque area was calculated by drawing manually its outline and the plaque surface was determined utilizing the ZEN lite 2011 software package and expressed in square micrometers. Quantification analyses were based on a minimum of 50 plaques, from at least 3 independent experiments. To quantify the area occupied by CD68 positive cells (CD68 coverage), slice culture samples were immunolabeled with CD68 antibody and confocal images were taken using a Plan-Apochromat 10x/0.45 objective at 1.5-fold magnification. Images were taken from cortical areas and each image was defined as a region of interest (ROI). A total of 12 ROI per analyzed condition were imaged. Thus, 12 images per experiment, from 3 independent experiments were utilized for the analysis. CD68 coverage was determined from the acquired images by the thresholding technique available on ImageJ software. Measured values were then normalized to CD68 coverage values of the Ctr. To quantify the area occupied by CX_3CR1-GFP positive cells (CX_3CR1-GFP coverage), samples were immunolabeled with GFP antibody and same experimental procedure as described above was performed. To quantify the number of proliferating CD68 positive microglial cells, slice culture samples were immunolabeled with CD68 and Ki67 antibodies and cortical areas imaged using Plan-Apochromat 10x/0.45 objective at 1.5-fold magnification. Both the number of CD68 positive and CD68-Ki67 double positive microglial cells were calculated based on the thresholding technique and the "analyze particle" command available on ImageJ software. The size limit for CD68 positive cells was set to 0.01-Infinity, and for CD68-Ki67 double positive cells was set to 0.0015-Infinity. To define the number of CD68 positive cells, images were subjected to a thresholding step before a "watershed" command was run. Quantification analyses were based on a minimum of 8 images per experiment, from 3 independent experiments for results in Fig 4.25B. Whereas, data showed in Fig 4.25D were based on quantification analyses from 12 images per experiment, from 2 independent experiments. Quantified values are expressed as percentages of Ki67-CD68 double positive cells from the total number of CD68 positive cells.

3.2.10 Cell viability assay

Cell viability was evaluated by incubating brain slices (at 7 and 14 DIV) with 5 μg/ml propidium iodide (PI) directly added to the media for 15 min at 37°C, 5% CO_2. Subsequently, slice culture samples were fixed in 4% PFA/sucrose, pH 7.4 for 15 min at RT, washed three times with PBS and stained with rabbit anti-GFAP, rabbit anti-NeuN antibodies (astrocytic and neuronal markers respectively) and DAPI as described before. Confocal microscopy, using a 20x dry objective, was performed to acquire representative pictures. PI positive cells were quantified and normalized to the total cell number (DAPI positive cells) using an automated counting of single color images available in the ImageJ software (NIH). For the quantification at least 3 pictures per sample from 3 independent experiments were used.

3.2.11 Morphological analysis of microglia

To analyze microglial morphology *ex vivo*, slice cultures from young $CX_3CR1^{+/GFP}$ and old APPPS1/$CX_3CR1^{+/GFP}$ mice were prepared. The microglial specific expression of GFP in these

mice allowed a clear visualization of cell body, processes and ramifications. Only cells not directly in contact with amyloid plaques were considered for the analysis in old APPPS1/CX$_3$CR1$^{+/GFP}$ mice. Brain slices at 0 DIV (young and old) and 10 DIV (young and old cultured alone and in co-culture) were fixed in 4% PFA/sucrose and stained using rabbit anti-GFP, mouse anti-Aβ antibody M3.2 and DAPI as described before. Representative images were acquired with a confocal microscope using a 20x dry objective at 1.7-fold magnification. At least 5 images from each sample, from 3 independent experiments, were used for the analysis. A minimum of 250 cells per condition in each experiment was analyzed. Microglial cells were classified into 2 distinct groups, ramified *versus* amoeboid, according to cell body volume with a cut off of 523 μm^3 (radius = 5 μm). Data are expressed as percentages of amoeboid cells *versus* total number of microglial cells that were analyzed.

3.2.12 Data analysis and statistics

Data were collected and analyzed in Microsoft Excel, which was used to generate all graphics. All data are presented as ± standard error of the mean (± SEM), depicted by the error bars, from at least 3 independent experiments. The statistical significance (P value) of the data was calculated using the unpaired two-tailed Student's *t*-test. P value of <0.05 was considered to be statistically significant (*P < 0.05, **P <0.01 and ***P< 0.001; n.s. = not significant).

# 4. Results

4.1 Development of the *ex vivo* model of AD

4.1.1 Organotypic brain slice culture model (*ex vivo* model)

The thesis uses organotypic slice cultures of mouse brain tissue to investigate microglial phagocytosis of Aβ. This method was chosen as it provides a good compromise between *in vitro* and *in vivo* methods as described in more detail in section 4 of the introduction. The three dimensional tissue architecture is resembling the *in vivo*-like situation (Carson et al 2008) with the well preserved integrity of neurons, microglia and astrocytes (Fig 4.1A, B). Importantly, microglia present *ex vivo* with ramified morphology (Fig 4.2) and can be studied in the vicinity of their CNS counterparts, but in a system where recruitment of immune cells coming from the periphery is excluded (Carson et al 2008). Despite glial activation induced by cutting and preparation procedure, this inflammatory reaction is settling down after one week in culture, a period sometimes referred to as consolidation phase (Humpel 2015a). This is reflected by the ramified morphology of microglia after 7-10 days *in vitro* (DIV) (Fig 4.2). Organotypic brain slices can indeed be maintained in culture over long time periods (in our laboratory up to 6 months) and thus may to a certain extent mimic aging. In addition, they can be relatively easily manipulated and exposed to compounds/drugs, offering the opportunity to monitor and study cell responses over long periods of time (Humpel 2015a). In such respect, the absence of the blood brain barrier makes the system particularly suitable for manipulation.
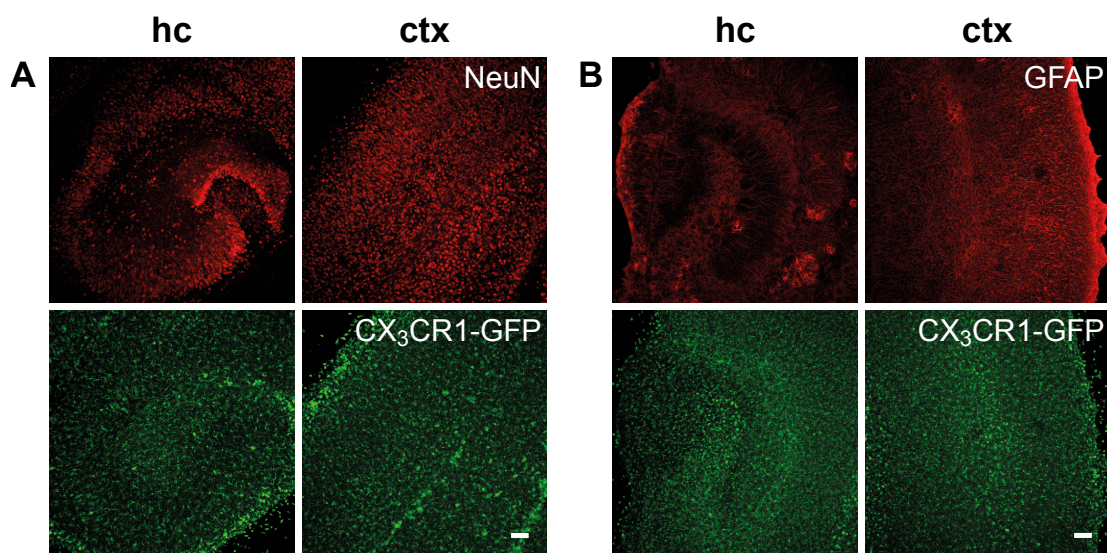
Figure 4.1. Integrity of neurons, microglia and astrocytes in brain organotypic slice cultures.
(A, B) Representative confocal images of brain slices from postnatal day 6-old CX$_3$CR1$^{+/GFP}$ mice, which exhibit GFP-expressing microglia, at 10 days *in vitro* (DIV) immunolabeled with neuronal NeuN **(A)** and astrocytic GFAP **(B)** markers (red). The signal of the GFP-expressing microglial cells was amplified using a GFP-specific antibody (green). Both hippocampal (hc) and cortical (ctx) areas are shown. Scale bar: 100 μm.
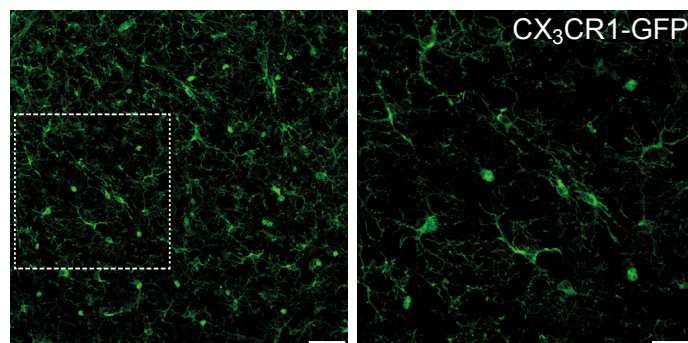
Figure 4.2. Microglial morphology is well preserved in the *ex vivo* model.
Confocal images of microglial cells in brain slices of a young CX$_3$CR1$^{+/GFP}$ reporter mouse at 10 DIV immunostained with GFP (green) to amplify the signal of the GFP-expressing microglial cells. Boxed region in the left panel is shown at higher magnification in the right panel and displays microglial cells homogeneously distributed and mainly resembling their typical ramified morphology. Scale bars: 50 μm (left panel) and 25 μm (right panel).

To investigate the capacity of microglial cells in phagocytosing amyloid plaques, I developed an *ex vivo* co-culture system. Amyloid plaques were provided by culturing organotypic brain slices from 14 up to 20-month-old APPPS1 mice (Radde et al 2006). This mouse model of amyloidosis overexpresses human APP bearing the Swedish mutation (K670N/M671L) and PS1 carrying the L166P mutation under control of Thy1 promoter and shows robust plaque pathology, with Aβ deposition starting already at 6 weeks of age in the cortex (Radde et al 2006). To explore the role of microglia in amyloid plaque clearance, I added to the same culture dish slices from young, neonatal (5-7 days old) WT mice (Fig 4.3A). I used cortico-hippocampal young slices and cortical and hippocampal old slices, since those are the brain regions mainly affected by the amyloid pathology in AD. One example of such co-culture dish is illustrated in Fig 4.3B. Note that the young tissue is transparent compared to the old tissue, which exhibits a more white-yellow color (Fig 4.3B). As healthy slices thin in culture over time, tissue transparency is a good indicator of cell viability (Humpel 2015a).
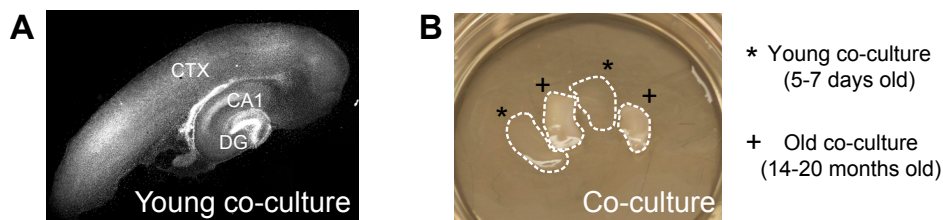
Figure 4.3. The *ex vivo* co-culture model.
(A) Representative image of a characteristic young WT cortico-hippocampal slice (350 μm) from a co-culture sample at 14 DIV. A nuclear staining was performed using DAPI (grey). Tags indicate respectively, dentate gyrus (DG), cornus ammonis 1 (CA1), and cortical (CTX) brain regions. **(B)** Example of a typical co-culture dish consisting of two young WT (*, young co-culture) and two old APPPS1 (+, old co-culture) brain slices.

4.1.2 Characterization of the *ex vivo* co-culture model: cell viability

To characterize cell viability in the *ex vivo* co-culture model, I used propidium iodide (PI), a red-fluorescent intercalating dye which stains nuclei of cells with a compromised plasma membrane. I compared numbers of PI-positive cells from the total number of DAPI-positive cells in young and old brain slices maintained in culture alone, or co-cultured, at 7 and 14 DIV. I observed high cell viability in the young slices either alone or in co-culture with the old at both 7 and 14 DIV. In contrast, the number of PI-positive cells was much higher in the old slices, reflecting approximately 70% reduction in cell viability already at 7 DIV and more than 80% reduced viability at 14 DIV (Fig 4.4A, B). Cell viability was comparable in co-culture and respective tissues cultured alone, indicating that the higher degree of cellular death in the old tissue was not influencing survival of the young tissue, and *vice versa* (Fig 4.4A, B).
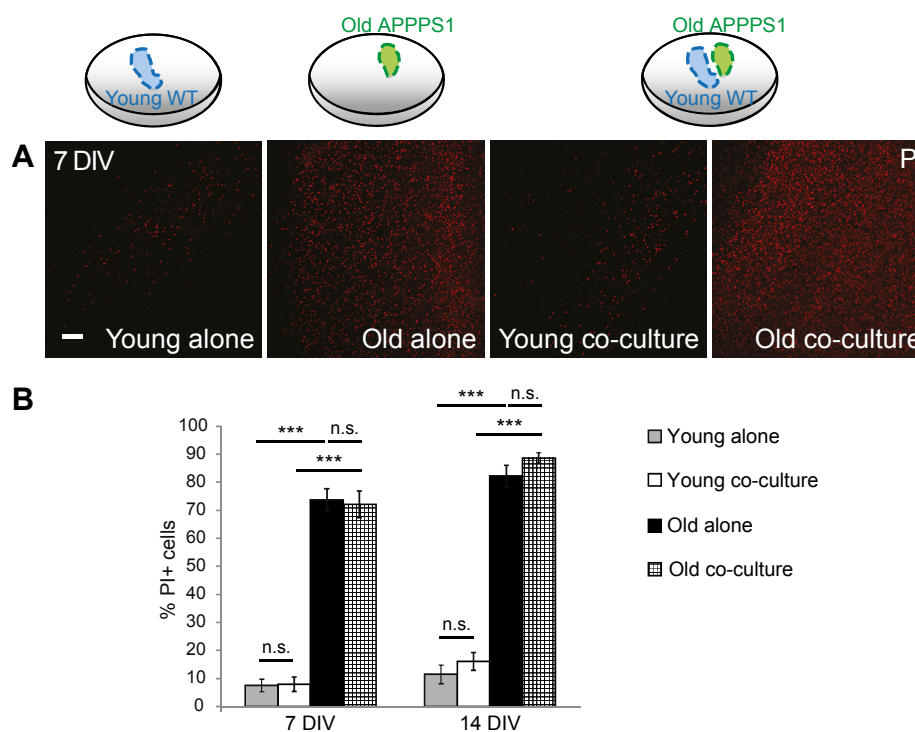
Figure 4.4. Cell viability in the *ex vivo* model at 7 and 14 DIV.
(A) Representative confocal images of young WT and old APPPS1 brain slices alone in culture (young alone, old alone) or in co-culture (young co-culture, old co-culture) at 7 DIV stained with propidium iodide (PI, red). Drawings above the images schematically represent analyzed conditions. The increased PI signal in old brain slices reveals the lower cell viability compared to young brain slices. **(B)** Quantifications of the % of PI-positive cells from the total number of DAPI-positive cells in young WT and old APPPS1 slices alone in culture (grey and black bars, respectively) or in co-culture (white and squared bars, respectively) at 7 and 14 DIV. Data are presented as mean ± SEM from three independent experiments, each experiment including two independent slice culture dishes. *P* values are derived from unpaired two-tailed Student's *t*-test. n.s. = not significant; ***$P < 0.001$. Scale bar: 75 µm.

4.1.3 Characterization of the *ex vivo* co-culture model: cellular markers

To identify different cell populations in the *ex vivo* co-culture model, I performed immunostaining using cellular markers to visualize neurons, astrocytes and microglia in the

young and old slices cultured alone or in co-culture at 7 and 14 DIV. Correspondingly to cell viability data, in the young slices I observed good viability of neurons (positive for NeuN) and astrocytes (positive for GFAP) at both 7 (Fig 4.5A, B) and 14 DIV (Fig 4.5D, E). In the old brain slices, the reduced immunopositivity for NeuN and GFAP already at 7 DIV mirrored the prominent loss of neuronal and astrocytic cells (Fig 4.5A, B and Fig 4.5D, E). To identify microglia, I used the microglial marker CD68, which labels lysosomes of microglial/macrophages and is indicative of phagocytic microglia (Boche et al 2013, Zotova et al 2011). Remarkably, I detected an elevated CD68 signal in the old tissue cultured alone at 7 DIV, which increased further at 14 DIV, indicating that despite the death of neurons and astrocytes microglia were able to survive and got activated. Of note, CD68 immunopositivity was even further elevated upon co-culturing of old and young brain slices (Fig 4.5C, Fig 4.5F). In contrast, I did not observe microglial activation in the young tissue at 7 DIV. Low CD68 signal could only be detected in the young tissue in co-culture with old at 14 DIV.
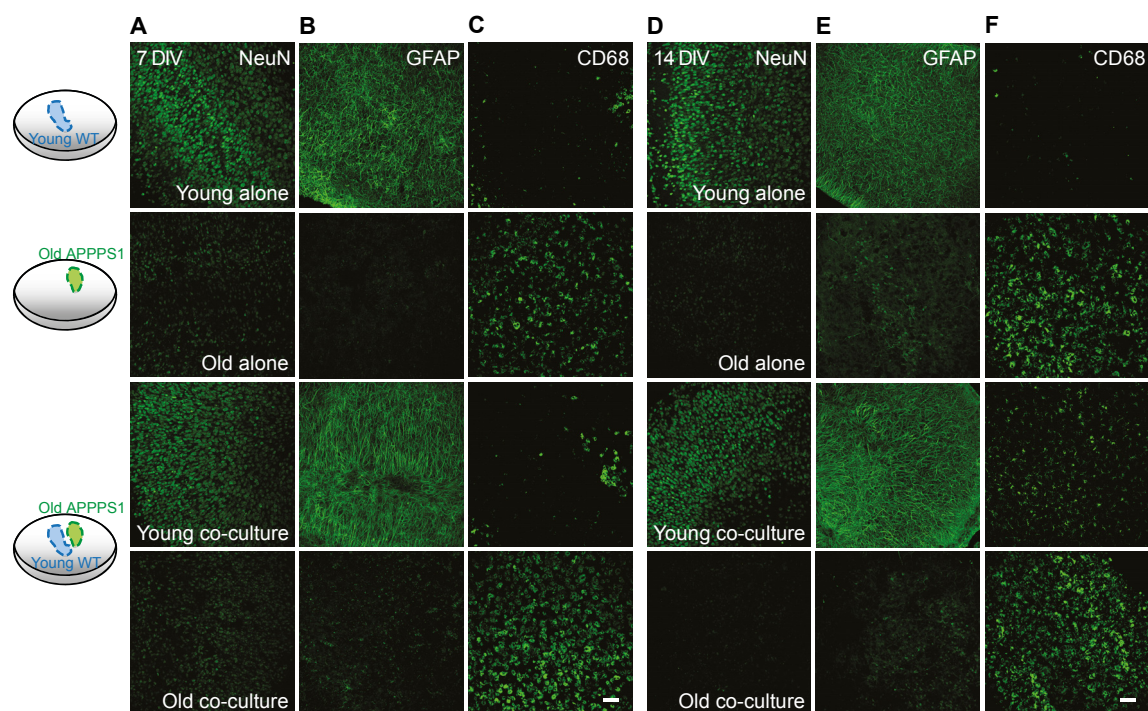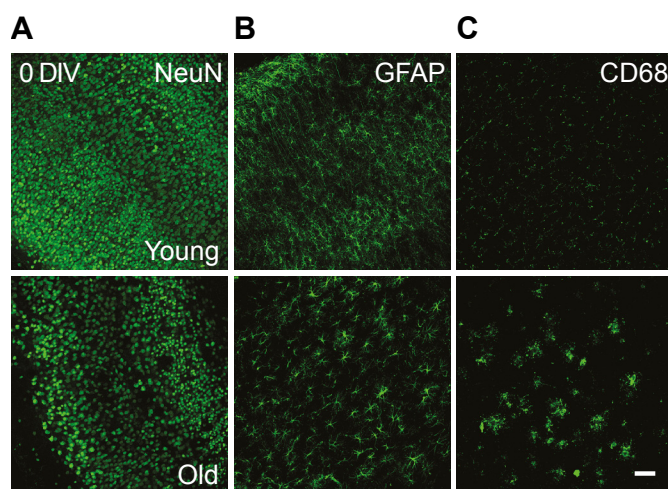

Figure 4.5. Cellular marker characterization of the *ex vivo* model at 7 and 14 DIV.
(A–F) Confocal images of young WT and old APPPS1 brain slices alone in culture or in co-culture at 7 **(A-C)** and 14 **(D-F)** DIV and immunostained for neuronal NeuN, astrocytic GFAP, and microglial CD68 markers (green). Drawings schematically illustrate conditions analyzed. Immunofluorescence analysis shows a robust decrease in NeuN and GFAP immunosignals in old brain slices already at 7 and also at 14 DIV, while CD68 signal increases, compared to young brain slices. Scale bar: 75 μm.

As additional control for tissue preservation after the cut, I fixed both young and old brain slices without culturing them (0 DIV), and performed immunostaining for NeuN, GFAP, and CD68 cellular markers. Immunofluorescence analyses confirmed that integrity of neurons and astrocytes in both young and old tissue was not compromised by the cut (Fig 4.6A-B). As expected, in the old tissue CD68-positive microglial cells were mostly detected at amyloid plaques, while in the young tissue I barely detected CD68 positive microglia (Fig 4.6C).

Figure 4.6. Cellular marker characterization of freshly cut brain slices.
(A-C) Confocal images of young WT and old APPPS1 brain slices immediately after the cut at 0 DIV immunostained for neuronal NeuN, astrocytic GFAP, and microglial CD68 markers (green). Immunofluorescence analysis shows the presence of reactive GFAP and CD68 positive cells in the old APPPS1 slices, which are characteristic signs of gliosis and typically occurring in aged AD brains. Scale bar: 75 µm.

Immunofluorescence data were confirmed by western blot analyses that showed reduced protein levels of neuronal β3-tubulin and astrocytic GFAP and increased protein levels of the microglial marker CD68 in the old tissue at 14 DIV, in contrary to what is observed in the young tissue (Fig 4.7). Importantly, the elevation of CD68 levels in the old tissue co-cultured with the young was clearly evident, suggesting further induction of microglial activation mediated by the young tissue (Fig 4.7).
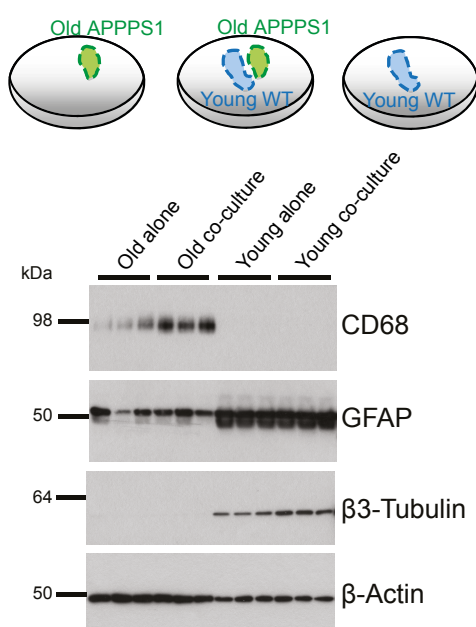
Figure 4.7. Western blot analysis of cellular markers in the *ex vivo* model at 14 DIV.
Immunoblot of microglial CD68, astrocytic GFAP, and neuronal β3-Tubulin protein levels in old APPPS1 and young WT tissue cultured alone or in co-culture at 14 DIV. Drawings schematically illustrate analyzed conditions. For each condition

Results

samples were loaded in triplicates and β-actin was used as a loading control.

Altogether, these observations indicate that viability of neurons and astrocytes in aged brain slices is very poor, as also reported by others (Mewes et al 2012, Staal et al 2011). However it is remarkable that microglia can be maintained in such environment and more importantly can acquire a phagocytically active phenotype.

4.2 Clearance of amyloid plaque halo is enhanced in the *ex vivo* co-culture model

To study microglial phagocytosis of amyloid plaques, I first analyzed amyloid plaque morphology in the *ex vivo* co-culture model. I was still able to detect a typical amyloid plaque morphology in the old APPPS1 tissue until 7 DIV. Amyloid plaques are composed of a fibrillar core visible from co-staining of the human anti-Aβ antibody 6E10 and thiazine red (TR), a dye which labels β-sheet structures of amyloid fibrils, and of a plaque halo of diffuse Aβ detected only by 6E10, surrounding the core (Fig 4.8A). Intriguingly, morphology of amyloid plaques changed over 14 DIV in the co-culture model, resulting in plaques consisting mainly of amyloid cores (Fig 4.8A, B). Upon co-culturing of old APPPS1 with young WT brain slices at 7 DIV, the majority of amyloid plaques still contain 6E10- and TR-positive core surrounded by 6E10-positive halo. In contrast, at 14 DIV, amyloid plaques are mainly 6E10- and TR-positive core-only plaques without 6E10- detectable halo (Fig 4.8B).
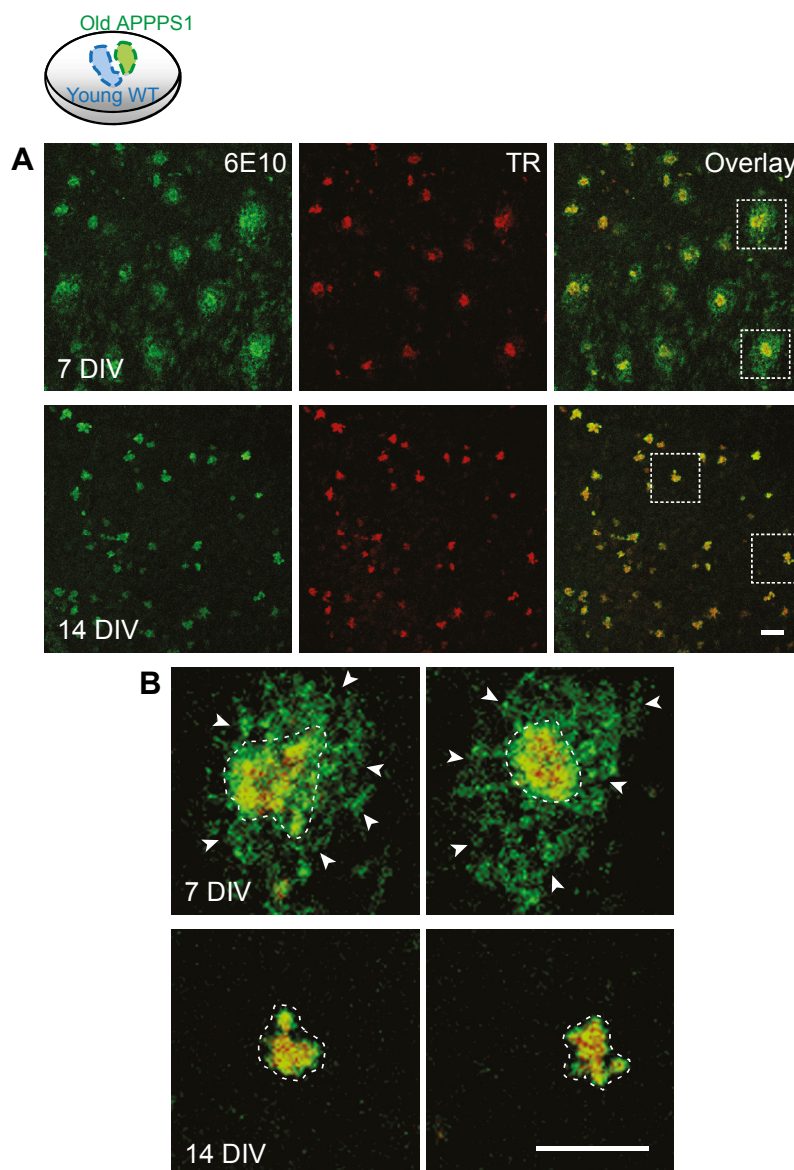
Figure 4.8. Amyloid plaque clearance is increased in the *ex vivo* co-culture model of old and young brain slices.
(A) Confocal images of the old APPPS1 brain slice in co-culture with the young WT immunolabeled with 6E10 antibody for amyloid plaque detection (green) and thiazine red (TR, red) for detection of fibrillar amyloid cores. At 7 DIV, most of the amyloid plaques consist of 6E10- and TR-positive dense core (encircled in B) surrounded by 6E10-positive halo of diffuse Aβ (arrowheads in B). Conversely, at 14 DIV, most of the amyloid plaques are 6E10- and TR-positive core-only plaques without 6E10-positive detectable halo. **(B)** Higher magnification confocal images of boxed regions in (A) showing the different morphology of two representative amyloid plaques at 7DIV (upper panels) and at 14 DIV (lower panels). Scale bars: 50 μm.

In addition, core-only plaques were also positive for the mouse anti-Aβ antibody M3.2. Indeed, as previously described, this is due to the co-aggregation of the endogenously produced mouse Aβ and the human Aβ produced by the transgene (van Groen et al 2006) (Fig 4.9).
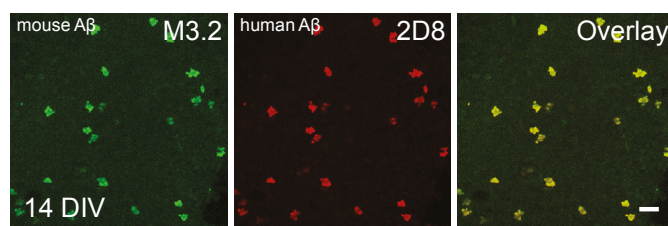
Figure 4.9. Co-deposition of mouse and human Aβ in the *ex vivo* co-culture model.
Confocal images of core-only plaques in the old APPPS1 brain slice in co-culture at 14 DIV immunolabeled with mouse-specific M3.2 (green) and human-specific 2D8 (red) Aβ antibodies. The full co-localization of M3.2 and 2D8 antibodies reveals co-deposition of mouse endogenous and transgenic human Aβ. Scale bar: 50 µm.

Since I observed clearance of the plaque halo in a system where the old APPPS1 tissue is cultured together with the young tissue, I next also examined amyloid plaque morphology in the old slices cultured alone. The analysis revealed that numbers of core-only plaques were significantly higher in the old tissue upon co-culturing with the young already at 7 DIV and further increased at 14 DIV in comparison with the old tissue cultured alone (Fig 4.10A-C). Thus, clearance of the plaque halo is enhanced upon co-culturing of old APPPS1 and young WT slices.
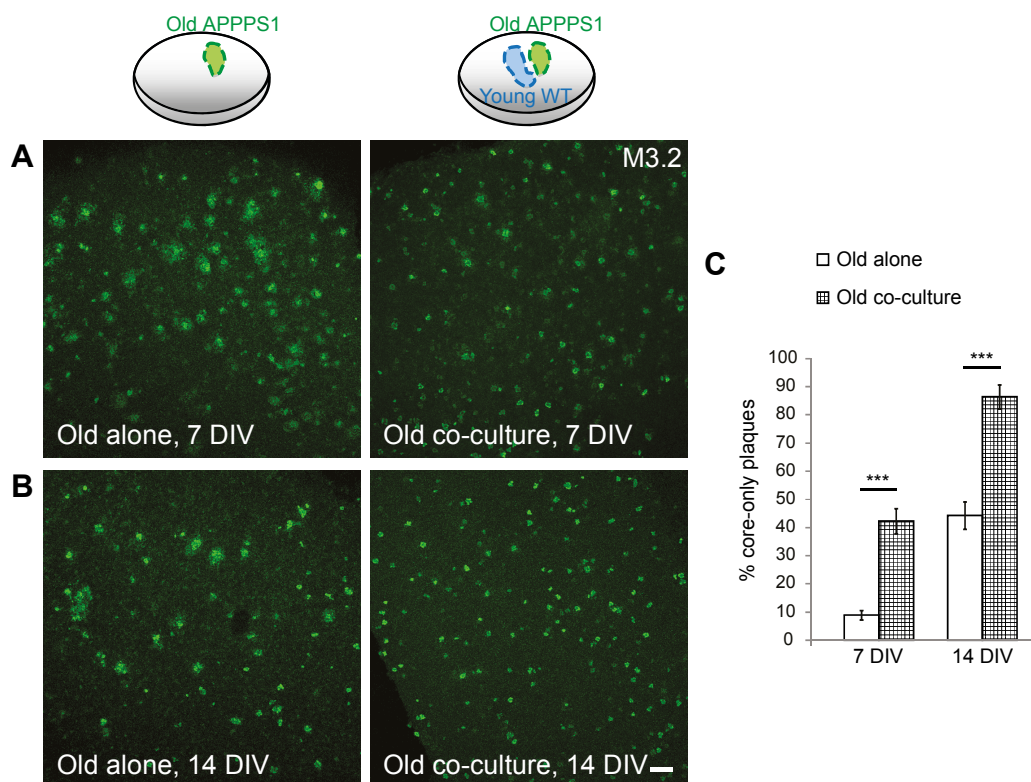
Figure 4.10. Amyloid plaque clearance is increased upon co-culturing of old APPPS1 and young WT brain slices.
(A-B) Confocal images of old APPPS1 slices alone in culture or in co-culture at 7 **(A)** and 14 **(B)** DIV and immunolabeled with M3.2 antibody. Amyloid plaque clearance is enhanced in the old brain slices upon co-culturing with the young slices. Scale bar: 100 µm. **(B)** Quantifications of the % of core-only plaques from the total number of amyloid plaques in old APPPS1 slices alone in culture (white bars) or in co-culture (squared bars) at 7 and 14 DIV. Analysis shows progressive increase in the % of core-only plaques upon co-culturing of old APPPS1 and young WT brain slices together compared to old cultured alone. Data are presented as mean ± SEM from three independent experiments, each experiment including three independent slice culture dishes. *P* values are derived from unpaired two-tailed Student's *t*-test. ***$P < 0.001$.

Furthermore, in line with immunohistochemical analyses of amyloid plaques, also biochemical analyses revealed almost 60% reduced Aβ levels in the old tissue upon co-culturing with the young at 14 DIV compared to old tissue alone (Fig 4.11A, B). Notably, due to our culturing conditions that include frequent media exchange (every 3-4 days), it is not possible to detect accumulation of soluble Aβ (Humpel 2015b). Therefore, soluble Aβ forms in brain slice extracts, protein analyses of brain slices was conducted on the formic acid extractable aggregated Aβ material, whereas the immunofluorescence analyses focused on clearance of the plaque halo of diffuse Aβ. Taken together, co-culturing of old and young brain slices induced, in addition to the clearance of the plaque halo, also removal of fibrillar Aβ.
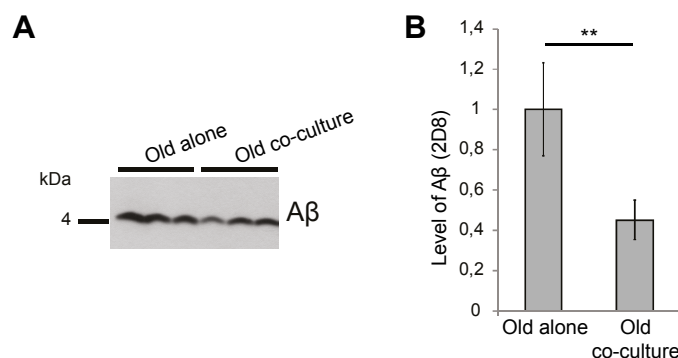
Figure 4.11. Aβ levels are reduced in the co-culture of old APPPS1 and young WT brain slices.
(A) Immunoblot of Aβ levels detected with 2D8 antibody in the old APPPS1 brain slices alone in culture or in co-culture with the young WT at 14 DIV. For both conditions analyzed samples were loaded in triplicates. **(B)** Quantification of immunoblot signals shows reduced Aβ levels when old brain slices are co-cultured together with young slices compared to the old tissue cultured alone. Data are normalized to the Aβ levels in the old tissue cultured alone and are presented as mean ± SEM from two independent experiments, and each experiment was performed in triplicates. *P* values are derived from unpaired two-tailed Student's *t*-test. **$P < 0.01$.

In summary, the old APPPS1 brain tissue exhibits evident amyloid plaque pathology and the presence of the young tissue stimulates clearance of Aβ plaques in the old APPPS1 tissue. The reduction of Aβ levels upon co-culturing of old and young brain slices suggests an increased plaque phagocytosis that goes in parallel with the increased levels of microglial marker CD68.

4.3 Age-dependent reduction of amyloid clearance in old APPPS1 brain slices in the *ex vivo* model

I wondered whether increased amyloid clearance detected in the in the co-culture model was triggered by the different age (young *vs* old) or different genotype (WT *vs* APPPS1) of the co-cultured tissue. Therefore, I extended the amyloid plaque analysis to additional groups, comparing co-cultures of old APPPS1 and young WT brain slices with co-cultures of old APPPS1 and either young APPPS1 or old WT brain slices. Regardless of whether I used young WT or young APPPS1 slices, core-only plaque numbers increased similarly in the APPPS1 old, indicating that the young age of the co-cultured tissue was promoting clearance of Aβ plaque halos independently on its genotype (Fig 4.12). In contrast, presence of old WT brain slices together with old APPPS1 brain slices did not show a profound effect on clearance of Aβ plaque

halos, even though counts of core-only plaques were slightly higher compared to old APPPS1 alone in culture (Fig 4.12).
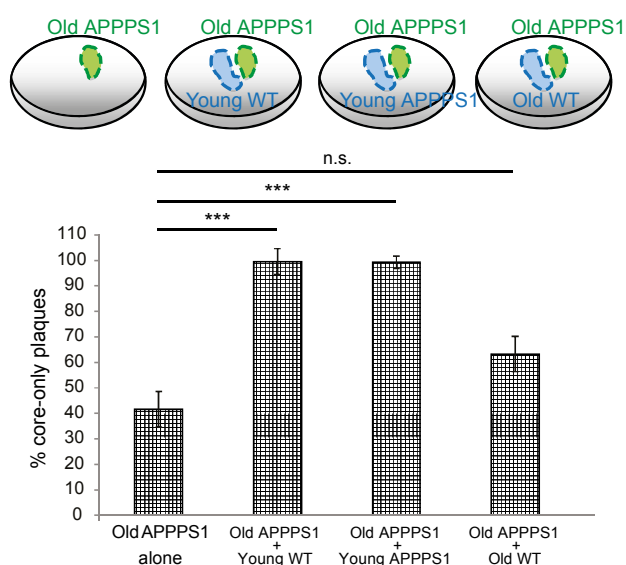
Figure 4.12. Aβ clearance capacity in the *ex vivo* co-culture model is age-dependent.
Quantifications of the % of core-only plaques from the total number of amyloid plaques in old APPPS1 brain slices cultured alone (old APPPS1 alone) or co-cultured with young WT (old APPPS1 + young WT), young APPPS1 (old APPPS1 + young APPPS1), or old WT brain slices (old APPPS1 + old WT) at 14 DIV. Drawings schematically illustrate analyzed conditions. Amyloid plaque clearance increases significantly only upon co-culturing of old APPPS1 brain slices with young slices, both WT and APPPS1, but not upon co-culturing with old slices. Data are presented as mean ± SEM from three independent experiments, each experiment including three independent slice culture dishes. *P* values are derived from unpaired two-tailed Student's *t*-test. n.s. = not significant, ***$P < 0.001$.

Altogether, these results indicate that different effects observed on plaque phagocytosis in the *ex vivo* model depend on the age of the mouse, where the brain slices have been isolated from, rather than its AD-related genotype.

4.4 Microglial recruitment and clustering at amyloid plaques in the co-culture model

The fact that co-culturing of old and young brain slices triggers clearance of the plaque halo suggested involvement of microglial cells in amyloid removal in the *ex vivo* co-culture model. To study microglia in the co-culture model, I used CD68 marker. Immunofluorescence analyses revealed strong upregulation of CD68 in the old APPPS1 brain slices in co-culture with the young WT slices (Fig 4.13A). More closely, I observed that CD68-positive cells were organized in clusters decorating amyloid plaques (Fig 4.13B). I quantified numbers of CD68-positive cells clustering around single amyloid plaques and measured amyloid plaque size at 7 and 14 DIV upon co-culturing. Quantifications showed that numbers of plaque-associated CD68-positive cells had the tendency towards increase between 7 and 14 DIV (Fig 4.13C). This effect was accompanied by a dramatic decrease in plaque size, mostly due to the loss of the plaque halo (Fig 4.13D). Furthermore, I quantified numbers of amyloid plaques, which I defined as clustered

70

plaques when they were surrounded by at least four CD68-positive cells. I observed increase in the number of clustered plaques by two fold from 7 to 14 DIV (Fig 4.13E). This was consistent with the decrease in plaque size.
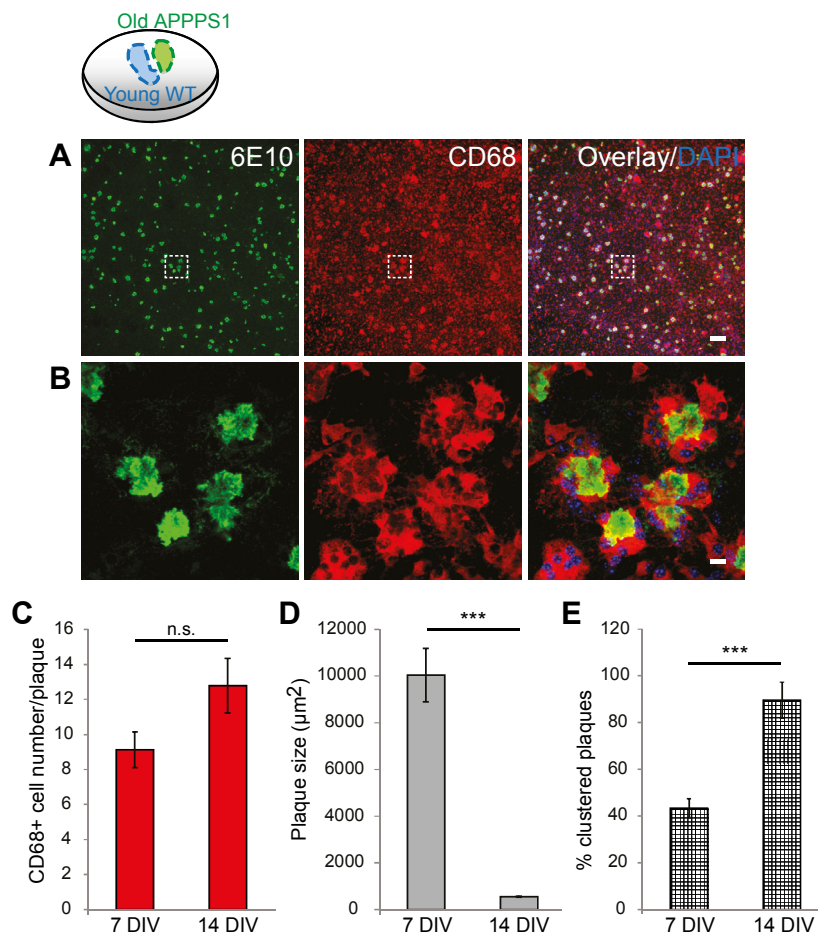
Figure 4.13. Recruitment and clustering of CD68-positive cells around amyloid plaques is accompanied by a reduction in plaque size.
(A, B) Confocal images of the old APPPS1 brain slice in co-culture at 14 DIV and immunostained with 6E10 (green) for amyloid plaques and CD68 (red) for microglial cells. DAPI (blue) was used to counterstain nuclei. Boxed region in (A) is shown at higher magnification in (B) and displays several CD68-positive cells forming clusters around amyloid plaques. Scale bars: 100 μm (A) and 10 μm (B). **(C)** Quantifications of the number of plaque-associated CD68-positive cells in co-culture samples at 7 and 14 DIV show a tendency towards increased number of CD68-positive cells. Data are presented as mean ± SEM from three independent experiments, including total of at least six independent slice culture dishes. *P* values are derived from unpaired two-tailed Student's *t*-test. n.s. = not significant. **(D)** Quantifications of the size of amyloid plaques in co-culture samples at 7 and 14 DIV show a decrease in plaque size. Data are presented as mean ± SEM from at least three independent experiments, including total of at least six replicates. *P* values are derived from unpaired two-tailed Student's *t*-test. ***$P < 0.001$. **(E)** Quantifications of % of plaques encircled by CD68-positive cells (clustered plaques) from the total number of amyloid plaques in co-culture samples at 7 and 14 DIV. Values show increased % of clustered plaques over time. Data are presented as mean ± SEM from three independent experiments, including total of at least six independent slice culture dishes. *P* values are derived from unpaired two-tailed Student's *t*-test. ***$P < 0.001$.

Taken together, presented data suggest that CD68-positive cells may be actively recruited to amyloid plaques in the *ex vivo* co-culture model to initiate phagocytosis. To verify this hypothesis, I used cytochalasin D (CytoD), a drug that binds to cytoskeletal protein actin and

inhibits its polymerization (Schliwa 1982). Interfering with actin cytoskeleton dynamics impaired migration and phagocytosis, abolished microglial clustering at amyloid plaques and caused an almost complete inhibition of the plaque halo clearance (Fig 4.14A, B). Disturbed cytoskeletal disorganization induced by CytoD was confirmed by staining with the actin specific-dye phalloidin. In contrast, ring-like staining pattern was observed upon vehicle- treatment and attributable to actin cytoskeletal structure of CD68-positive cells encircling Aβ plaques (Fig 4.14A). Therefore, CD68-positive microglial cells that cluster around amyloid plaques may be actively engaged in phagocytosing amyloid plaques in the *ex vivo* co-culture model.
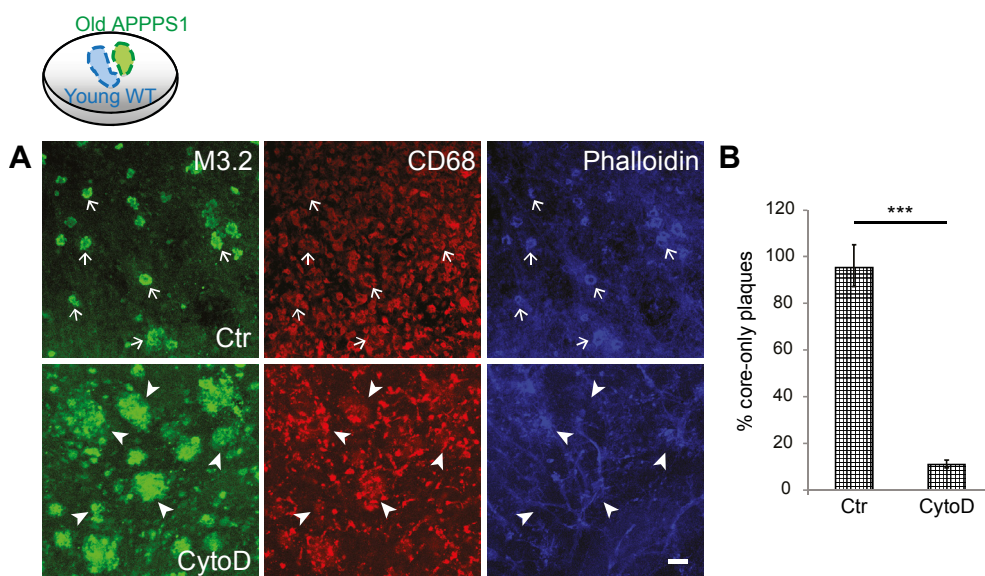
Figure 4.14. CD68-positive microglia actively take up and phagocytose Aβ.
(A) Confocal images of the old APPPS1 brain slice in co-culture at 14 DIV treated with cytochalasin D (CytoD) and vehicle control (Ctr) and immunolabeled with M3.2 (green) and CD68 (red). Phalloidin (blue) was used to stain actin. In the Ctr condition Phalloidin staining shows ring-like structures likely attributable to actin cytoskeleton of microglial cells tightly clustered around amyloid plaques (arrows). In contrast, upon CytoD treatment tissue cytoskeletal organization is clearly disrupted (arrowheads) and microglial clustering is not taking place. Amyloid plaque clearance is also prevented when phagocytosis is inhibited by CytoD. Scale bar: 50 μm. **(B)** Quantifications of the % of core-only plaques from the total number of amyloid plaques in the old APPPS1 brain slice in co-culture at 14 DIV and treated with CytoD and Ctr. Analysis shows very low % of core-only plaques upon CytoD treatment compared to Ctr. Data are presented as mean ± SEM from three independent experiments, including total of six independent slice culture dishes. *P* values are derived from unpaired two-tailed Student's *t*-test. ***$P < 0.001$.

4.5 Young microglia do not infiltrate into the old APPPS1 slice

Since the *ex vivo* co-culture model contains both young and old brain slices, I could not distinguish whether plaque-associated CD68-positive cells derive from young or old brain tissue. To this end, brain slices were prepared from $CX_3CR1^{+/GFP}$ microglia/macrophage mouse reporter line (Jung et al 2000), in which the fraktalkine receptor-encoding gene CX3CR1 that is specifically expressed by microglia/macrophages has been replaced by the GFP-encoding gene, thus these mice exhibit green microglia.
To investigate possible infiltration of young microglial cells into old tissue, I prepared co-cultures of young brain slices from $CX_3CR1^{+/GFP}$ mice with the old APPPS1 brain slices. Immunofluorescence analyses showed young GFP-expressing microglial cells migrating towards

the old tissue at 14 DIV, however only few reached the border of the old slice and almost none were detectable inside of the old tissue (Fig 4.15A, B). This showed that young microglia do not infiltrate the old APPPS1 tissue, at least at the time points when clearance of the plaque halo is evident (14 DIV). Thus, young microglia are not directly participating in amyloid plaque phagocytosis.
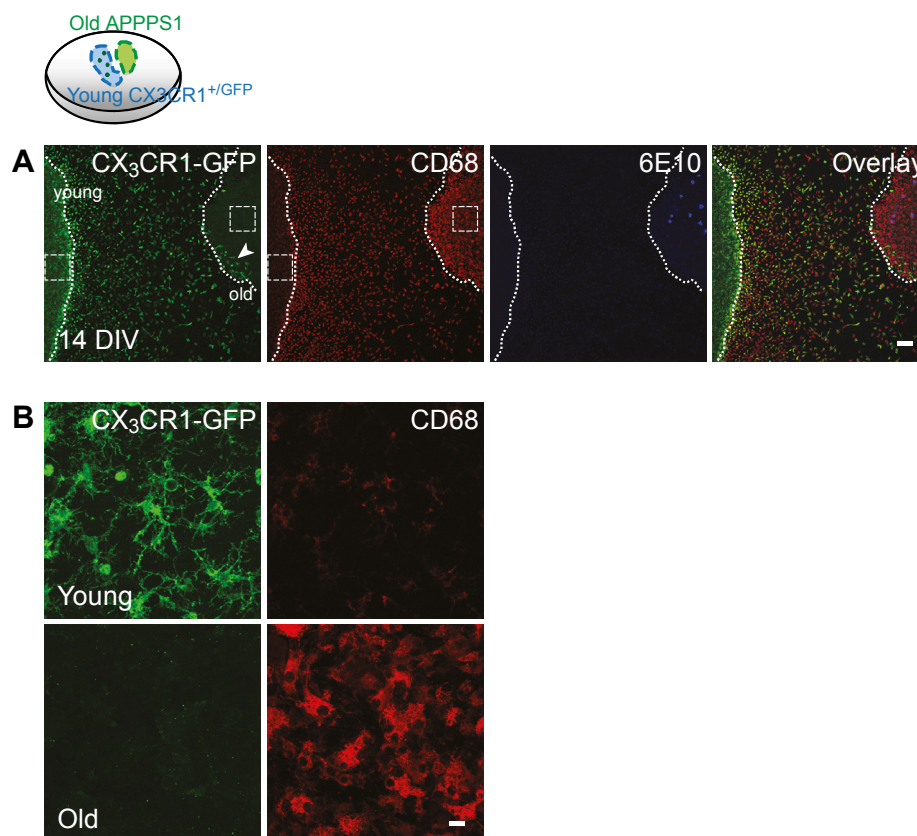
Figure 4.15. Young microglia do not infiltrate into the old APPPS1 brain slice at 14 DIV.
(A, B) Confocal images of young CX$_3$CR1$^{+/GFP}$ co-cultured with old APPPS1 brain slices at 14 DIV and immunostained with GFP (green), CD68 (red), and 6E10 (blue). Drawing schematically illustrates the analyzed condition with GFP-expressing microglia depicted by green dots in the young slice. GFP-positive young microglial cells are moving towards the old tissue, but only few GFP-positive cells are visible within the old slice at 14DIV (arrowhead) and mainly confined to the border of the old tissue. Young and old brain slices are delineated by dotted lines. Boxed regions in (A) are shown at higher magnification in (B) and display that GFP-positive microglial cells are indeed detected in the young slice (upper panels), whereas they are not present in the old slice (lower panels). The signal of the GFP-expressing microglial cells was amplified using a GFP-specific antibody. Scale bars: 100 μm (A) and 10 μm (B).

4.6 Old microglia engulf Aβ

The observation that CD68-positive cells surrounding amyloid plaques were negative for GFP (Fig 4.15A, B) suggested that plaque-associated microglial cells do not derive from the young tissue but rather belong to the old tissue. To verify this hypothesis, I first crossed the CX$_3$CR1$^{+/GFP}$ mouse reporter line with the APPPS1 mouse line and aged those animals to allow development of plaque pathology. Next, I prepared co-cultures of old APPPS1/CX$_3$CR1$^{+/GFP}$ brain slices with young WT brain slices and analyzed localization of microglial cells (Fig 4.16A).

Immunofluorescence analyses revealed that M3.2-labeled amyloid plaques were indeed surrounded by GFP and CD68 double positive microglial cells, confirming their origin from the old tissue (Fig 4.16A).

To further validate involvement of old microglial cells in amyloid plaque phagocytosis, 3-dimensional reconstruction analyses of old GFP-expressing cells were performed in co-cultures of old APPPS1/CX$_3$CR1$^{+/GFP}$ and young WT brain slices using Imaris software. I detected M3.2-positive amyloid material intracellularly within old GFP-positive microglial cells, proving the identity of old AD microglia as Aβ engulfing cells (Fig 4.16B). However, intracellular amyloid material was only occasionally detected, suggesting rapid intracellular degradation of Aβ.

Figure 4.16. Old CD68-positive microglial cells cluster around amyloid plaques, and engulf Aβ.
(A) Confocal images of the old APPPS1/CX$_3$CR1$^{+/GFP}$ brain slice co-cultured with the young WT slice at 14 DIV and immunolabeled with GFP (green), CD68 (red), and M3.2 (blue). Drawing schematically illustrates the analyzed condition with GFP-expressing microglia depicted by green dots in the old slice. GFP-positive old microglial cells co-localize with CD68-positive cells surrounding amyloid plaques (arrows). The signal of the GFP-expressing microglial cells was amplified using a GFP-specific antibody. Scale bar: 10 μm. **(B)** 3D reconstruction of the 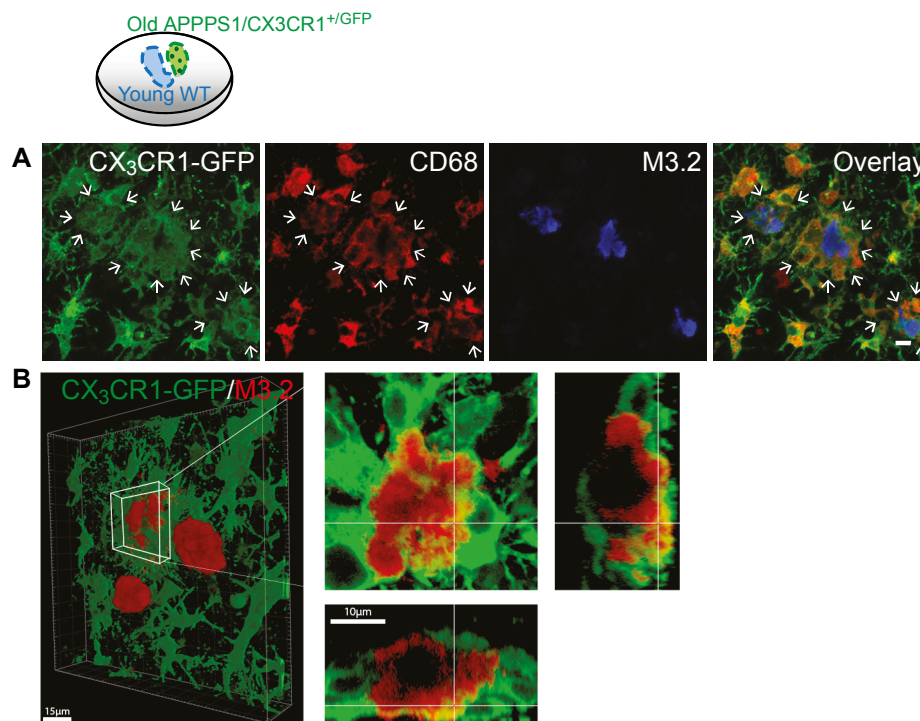old APPPS1/CX$_3$CR1$^{+/GFP}$ brain slice in co-culture with the young WT slice at 10 DIV and immunolabeled with GFP (green) and M3.2 (red). GFP-positive old microglial cells clustering around amyloid plaques display M3.2-positive amyloid material intracellularly suggestive of Aβ uptake. Overview at lower magnification of a representative area is shown in the left panel. Scale bar: 15 μm. A representative amyloid plaque image at higher magnification is shown in the right panels. Scale bar: 10 μm.

4.7 Amyloid plaque clearance depends on both young and old microglia

Clearance of the plaque halo is enhanced in the co-culture model where old microglia are directly involved in phagocytosis of Aβ while young microglia trigger this effect but do not get in direct contact with Aβ plaques. This statement is additionally supported by experimental evidence obtained by pharmacological depletion of young or old microglia using bisphosphonate

clodronate as described below. This toxin is commonly utilized to specifically deplete cells derived from the monocytic cell lineage like osteoclasts, macrophages or microglia and well established protocols are available (Hellwig et al 2015, Ji et al 2013, Kohl et al 2003, Kreutz et al 2009, Vinet et al 2012).

4.7.1 Clodronate efficiently depletes microglial cells

First, I tested the efficiency and specificity of clodronate treatment in young and old brain slices by measuring the tissue area covered by microglial CX_3CR1-GFP positive immunosignal, referred to as microglial coverage and by analyzing other non-target cell types such as astrocytes and neurons. For this examinations, brain slices were prepared from the young $CX_3CR1^{+/GFP}$ microglia/macrophage mouse reporter line (Jung et al 2000) and treated with clodronate or vehicle-control from 1 until 7 DIV, followed by immunofluorescence analysis. Clodronate treatment of young $CX_3CR1^{+/GFP}$ slices resulted in almost complete microglial depletion, as shown by coverage analyses of young GFP-expressing microglial cells (Fig 4.17A-C), without affecting GFAP-positive astrocytic and NeuN-positive neuronal cell numbers (Fig 4.17A, B).
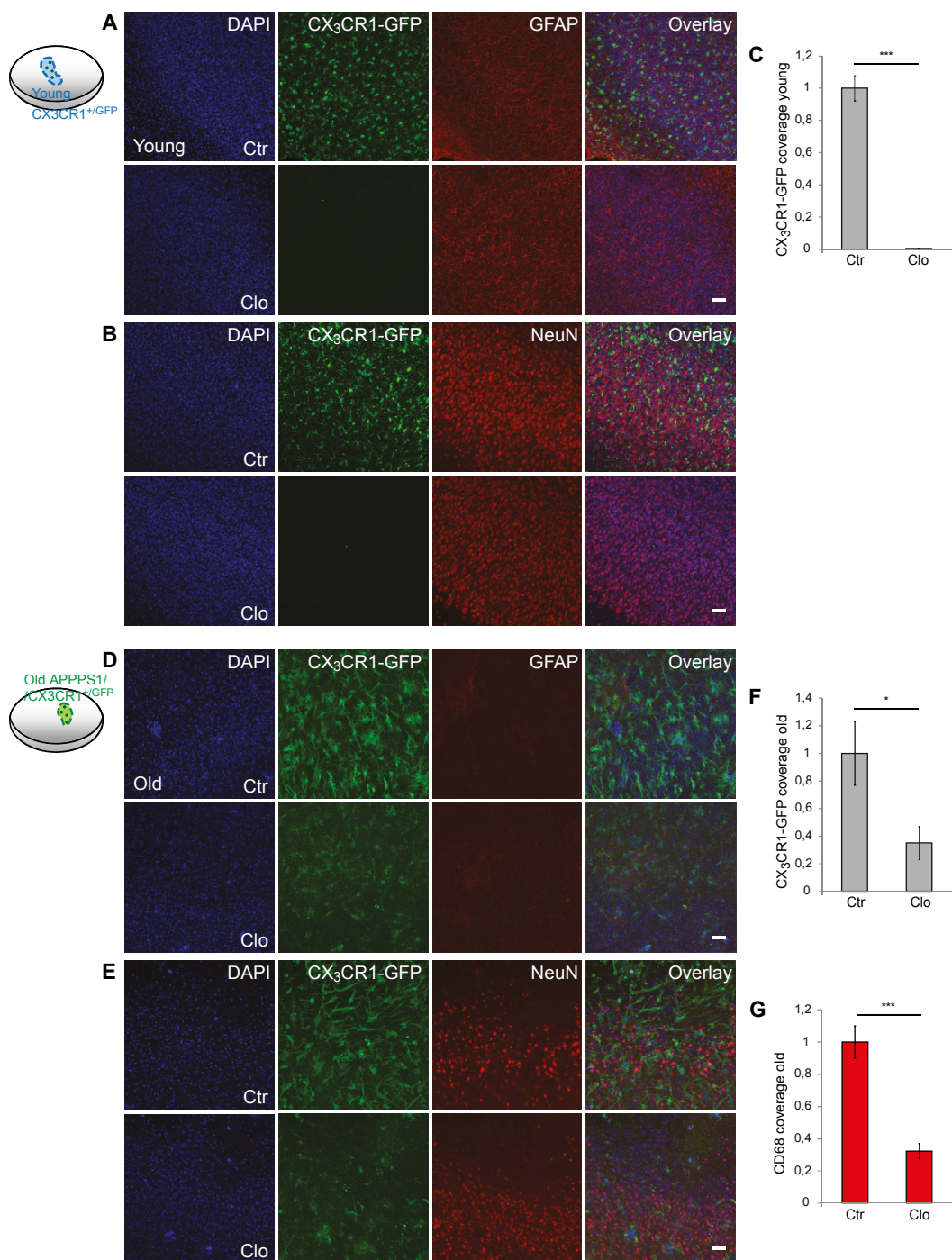
Figure 4.17. Clodronate treatment of young and old brain slices efficiently depletes microglial cells.
(A, B) Confocal images of the young CX$_3$CR1$^{+/GFP}$ brain slice treated with Clo and Ctr from 1 until 7 DIV and immunolabeled with GFP (green) and astrocytic-GFAP marker (red) in (A), and with GFP (green) and neuronal-NeuN marker (red) in (B). Nuclei were counterstained with DAPI (blue). Drawings on the left schematically illustrate conditions analyzed with GFP-expressing microglia depicted by green dots in the young slice. The signal of the GFP-expressing microglial cells was amplified using a GFP-specific antibody. Scale bars: 50 μm. **(C)** Area covered by CX$_3$CR1-GFP-positive cells in the young CX$_3$CR1$^{+/GFP}$ slice (CX$_3$CR1-GFP coverage young) treated with Clo and Ctr. CX$_3$CR1-GFP coverage indicates complete elimination of young microglial cells upon Clo treatment. Values are normalized to CX$_3$CR1-GFP coverage of the Ctr and are presented as mean ± SEM from three independent experiments, including total of six independent slice culture dishes. *P* values are derived from unpaired two-tailed Student's *t*-test. ***$P < 0.001$.
(D, E) Confocal images of the old APPPS1/CX$_3$CR1$^{+/GFP}$ brain slice treated with Clo and Ctr from 1 until 7 DIV and

76

immunolabeled with GFP (green) and astrocytic-GFAP marker (red) in (D), and with GFP (green) and neuronal-NeuN marker (red) in (E). Nuclei were counterstained with DAPI (blue). Drawings schematically illustrate conditions analyzed with GFP-expressing microglia depicted by green dots in the old slice. The signal of the GFP-expressing microglial cells was amplified using a GFP-specific antibody. Scale bars: 50 μm. **(F)** Area covered by CX_3CR1-GFP-positive cells in the old APPPS1/$CX3CR1^{+/GFP}$ slice (CX_3CR1-GFP coverage old) treated with Clo and Ctr. Reduced CX_3CR1-GFP coverage indicates removal of old microglial cells upon Clo treatment. Values are normalized to CX_3CR1-GFP coverage of the Ctr and are presented as mean ± SEM from three independent experiments, including total of six independent slice culture dishes. *P* values are derived from unpaired two-tailed Student's *t*-test. *P < 0.05. **(G)** Area covered by CD68-positive cells in the old APPPS1/$CX3CR1^{+/GFP}$ slice (CD68 coverage old) treated with Clo and Ctr and immunolabeled with CD68. Reduced CD68 coverage indicates also removal of old microglial cells upon Clo treatment, consistent with CX_3CR1-GFP coverage in (F). Values are normalized to CX_3CR1-GFP coverage of the Ctr and are presented as mean ± SEM from three independent experiments, including total of six independent slice culture dishes. *P* values are derived from unpaired two-tailed Student's *t*-test. ***P < 0.001.

In parallel, I analyzed clodronate treatment of brain slices from old APPPS1/$CX_3CR1^{+/GFP}$ mice and found that microglial removal was approximately 65 % efficient, as revealed by coverage analyses of old GFP-expressing microglial cells (Fig 4.17D-F). Consistent with this, tissue area covered by CD68 immunosignal was also reduced upon clodronate treatment of old slices (Fig 4.17G). As already described, I showed that old astrocytes and neurons survive poorly in the *ex vivo* model (Fig 4.5A, B, Fig 4.5D, E). In line with that, both control and clodronate treated old slices presented no GFAP immunopositivity and only sparse NeuN immunosignal (Fig 4.17D, E).

4.7.2 Both young and old microglia contribute to amyloid plaque clearance

Next, to discriminate a specific contribution of young or old microglia in the *ex vivo* co-culture model, young slices were pre-treated with clodronate from 1 until 7 DIV to remove microglia. Treatment was then stopped by exchanging media and subsequently old APPPS1 slices were added to restore the co-culture condition, as schematically indicated in Fig 4.19A. 14 days after, samples were fixed and the old APPPS1 tissue analyzed by immunofluorescence. Removal of young microglia caused a significant reduction in numbers of core-only plaques, reflecting a decreased amyloid plaque clearance and therefore supporting the involvement of young microglia in the Aβ clearing process (Fig 4.18B, C). In the parallel experiment, I pre-treated old slices with clodronate, stopped the treatment and subsequently added young WT slices (Fig 4.18D). The substantial depletion of old microglial cells, as showed by CD68 coverage analyses (Fig 4.18F), caused an even more pronounced reduction of amyloid plaque clearance with almost no core-only plaques detected (Fig 4.18E-G). Those additional quantitative analyses are in agreement with previous immunofluorescence analyses that identified microglial cells in the old APPPS1 tissue as cells that are responsible for amyloid clearance in the *ex vivo* co-culture model (see Fig 4.15 and Fig 4.16).

Altogether, the findings presented here indicate that both young and old microglia are required for amyloid plaque clearance, supporting a synergistic effect of both microglial populations.
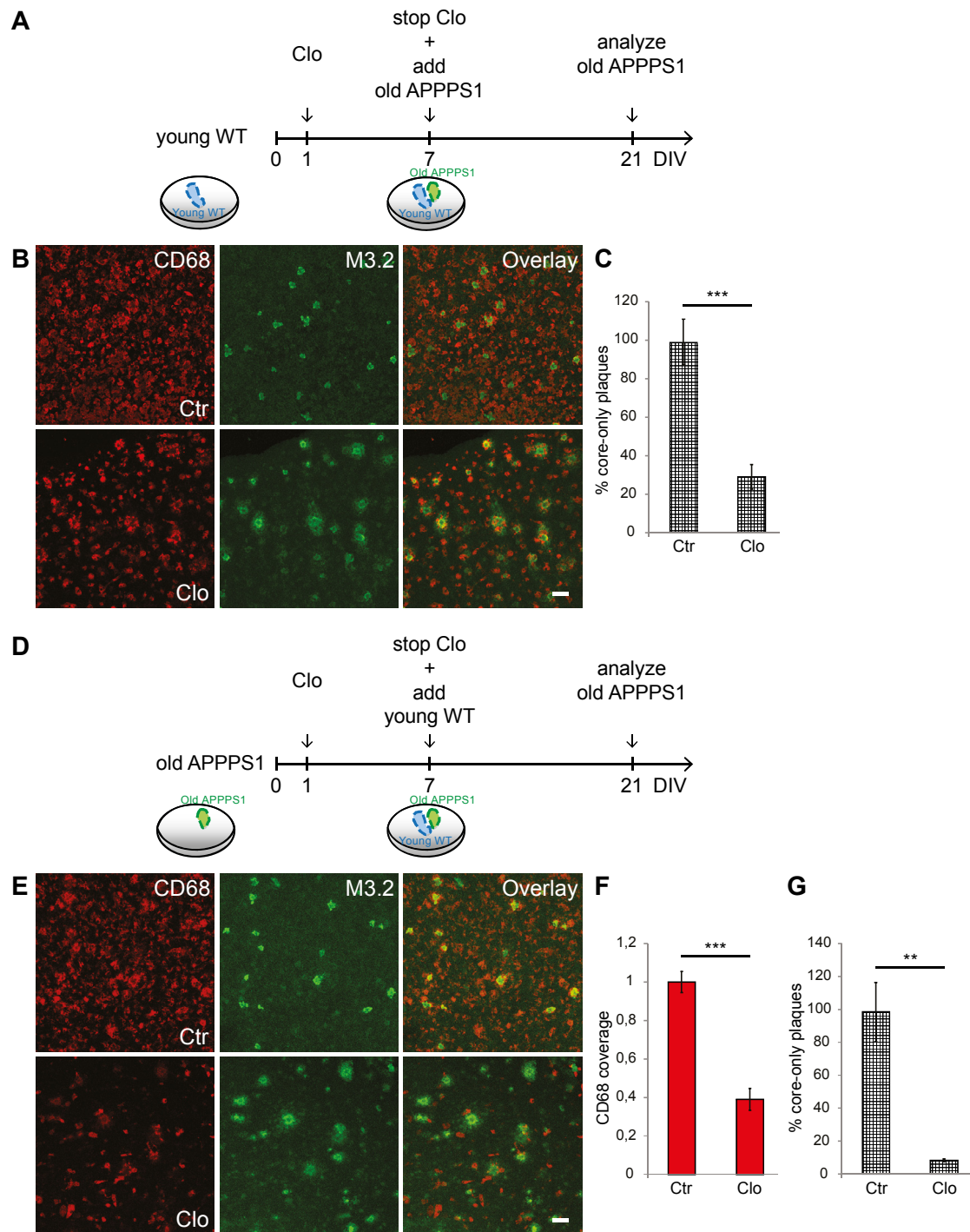
Figure 4.18. Amyloid plaque clearance depends on both young and old microglia.
(A) Schematic representation of the experimental procedure. **(B)** Confocal images of the old APPPS1 tissue co-cultured with the young WT tissue pre-treated with Clo and Ctr as presented in (A), and immunolabeled using CD68 (red) and M3.2 (green). Scale bar: 50 μm. **(C)** Quantifications of the % of core-only plaques from the total number of amyloid plaques in the old APPPS1 slice co-cultured with the young WT slice pre-treated with Clo and Ctr as presented in (A). Values show a reduced number of core-only plaques upon Clo treatment. Data are presented as mean ± SEM from three independent experiments, including total of six independent slice culture dishes. *P* values are derived from unpaired two-tailed Student's *t*-test. ***P* < 0.001. **(D)** Schematic representation of the experimental procedure. **(E)** Confocal images of the old APPPS1 tissue treated with Clo and Ctr and afterwards co-cultured with the young WT tissue as presented in (D), and immunolabeled using CD68 (red) and M3.2 (green). Scale bar: 50 μm. **(F)** Area covered by CD68-positive cells (CD68

78

coverage) in the old APPPS1 brain slice treated with Clo and Ctr and afterwards co-cultured with the young WT tissue as presented in (D). CD68 coverage is decreased upon Clo treatment. Values are normalized to CD68 coverage of the Ctr and are presented as mean ± SEM from three independent experiments, including total of six independent slice culture dishes. *P* values are derived from unpaired two-tailed Student's *t*-test. ***P < 0.001. **(G)** Quantifications of the % of core-only plaques from the total number of amyloid plaques in the old APPPS1 brain slice treated with Clo and Ctr and afterwards co-cultured with the young WT slice as presented in (D). Values show a reduced number of core-only plaques upon Clo treatment. Data are presented as mean ± SEM from three independent experiments, including total of six independent slice culture dishes. *P* values are derived from unpaired two-tailed Student's *t*-test. **P < 0.01.

4.8 Morphological characterization of microglia in the *ex vivo* model

Since it is known that microglial activation is accompanied by morphological transformation from a ramified morphology into cells with enlarged bodies and amoeboid morphology, I performed detailed morphological analyses. Brain slices were isolated from $CX_3CR1^{+/GFP}$ microglia/macrophage reporter mice, allowing better visualization of the whole microglial cell body and ramifications compared to CD68 used elsewhere. Microglial morphology was examined in young $CX_3CR1^{+/GFP}$ and old $APPPS1/CX_3CR1^{+/GFP}$ brain slices in the following conditions: freshly cut slices (0 DIV), young and old slices cultured alone at 10 DIV and co-cultures at 10 DIV (Fig 4.19A, B). Numbers of ramified *versus* amoeboid microglia were quantified using as a cut-off a cell body volume of 523 μm^3 (with radius equal to 5 μm) and expressed as percentages of amoeboid microglia from the total number of microglial cells analyzed. The results showed that immediately after cutting both young and old microglia appeared as ramified cells reflecting their *in vivo* morphology. After 10 DIV young microglia still exhibited mainly ramified morphology, whereas almost 70% of old microglial cells showed amoeboid morphology in the old APPPS1 slices cultured alone (Fig 4.19A, B). This might likely be attributed to the increased cell death occurring in cultured old slices (see Fig 4.4, Fig 4.5 and Fig 4.7). Importantly, numbers of old microglia with amoeboid shape were further augmented, to almost 90 %, upon co-culturing with the young slices (Fig 4.19A, B), well in accordance with the increased phagocytosis detected in co-cultures of old and young brain slices (see Fig 4.10 and Fig 4.11). Thus, morphological changes in old microglial cells *ex vivo* precisely reflect their activation state and phagocytic capacity.

Taken together, these results indicate that old APPPS1 microglia upon co-culturing present with amoeboid morphology, cluster around plaques, and become competent for the uptake of Aβ.
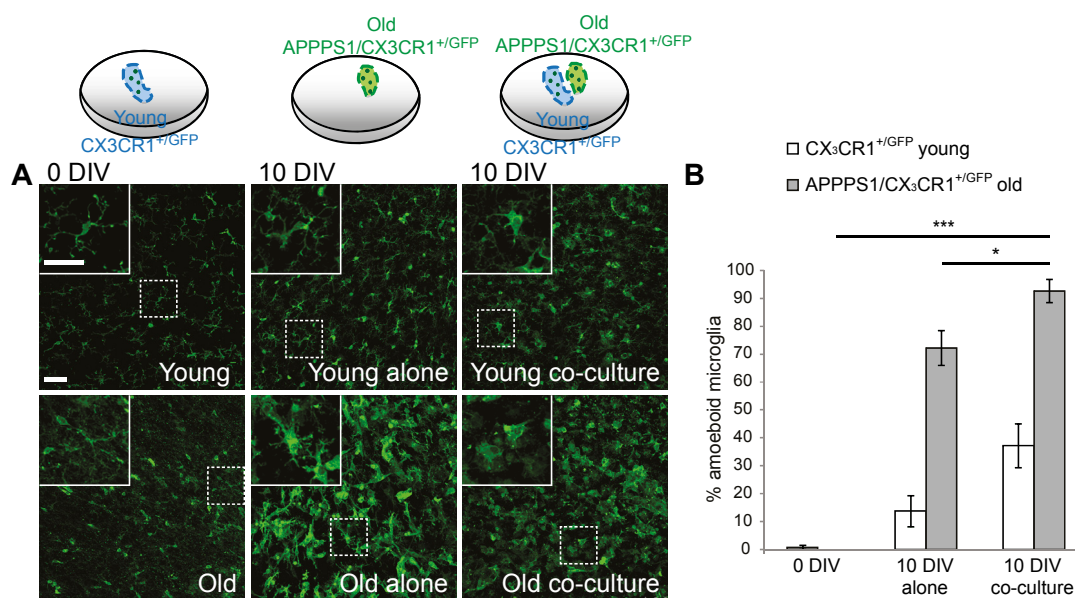
Figure 4.19. Morphological characterization of microglia in the *ex vivo* model.
(A) Confocal images of young CX₃CR1$^{+/GFP}$ and old APPPS1/CX₃CR1$^{+/GFP}$ brain slices immediately after the cut at 0 DIV, cultured alone or in co-culture at 10 DIV, and immunolabeled with GFP (green) to amplify the signal of the GFP-expressing microglial cells. Drawings schematically illustrate analyzed conditions with the GFP-expressing microglia depicted by dots in both young and old slices. Immunofluorescence analysis reveals altered microglial morphology of old cells upon culturing. Boxed regions are shown in enlargement in the upper left panels. Scale bars: 50 μm. **(B)** Quantifications of the numbers of amoeboid microglial cells in young CX₃CR1$^{+/GFP}$ (white bars) and old APPPS1/CX₃CR1$^{+/GFP}$ (grey bars) tissues immediately after the cut at 0 DIV, and cultured alone or in co-culture at 10 DIV. Values are reported as % of amoeboid microglia from the total number of microglial cells and are presented as mean ± SEM from three independent experiments, each experiment including at least 250 cells per condition. *P* values are derived from unpaired two-tailed Student's *t*-test. *$P < 0.05$, ***$P < 0.001$.

4.9 Soluble factors released by young microglia promote Aβ uptake of old microglia

The results described so far confirmed by using independent experimental approaches that both young and old microglia actively contribute to amyloid plaque clearance. In particular, old microglia are directly responsible for phagocytosing amyloid plaque halos, while young microglia may contribute by releasing soluble factor(s) that promote Aβ uptake of old microglia. To test this hypothesis, I first examined whether soluble factors produced by young slices contribute to amyloid clearance. For this purpose I incubated old APPPS1 tissue in conditioned media collected from young WT brain slices. Histological analyses showed that young conditioned media triggered clearance of Aβ halos, as reflected by increased numbers of core-only plaques compared to old tissue cultured in unconditioned slice culture media (Fig 4.20A). Remarkably, core-only plaque numbers raised to a very similar extent to that detected upon co-culturing of old and young brain slices at 7, 11, and 14 DIV (Fig 4.20A). As additional negative control, I included old APPPS1 brain slices cultured in conditioned media collected from old APPPS1 slices. As expected, numbers of core-only plaques were not significantly different compared to old tissue cultured in unconditioned culturing media (Fig 4.20A).

To determine the cellular population in the young tissue that is secreting phagocytosis-promoting factors, I first treated young WT brain slices with clodronate to induce microglial

depletion and subsequently started with the collection of the conditioned media. Upon incubation of old APPPS1 slices in conditioned media from microglia-depleted young slices I did not detect alteration in core-only plaque numbers. On the contrary, conditioned media collected from vehicle -treated young slices induced a progressive raise in core-only plaques at 7, 11 and 14 DIV, reproducing above presented results (Fig 4.20B). This suggests that young microglial cells in the young tissue secrete soluble factors that act in trans on old APPPS1 microglial cells and enables them to re-gain or at least enhance their phagocytic function.

To further corroborate whether the observed effect on plaque clearance was mediated by the young microglial cells, I collected conditioned media from young primary microglial cultures, which I used for culturing of the old APPPS1 brain slices. As expected, numbers of core-only plaques increased again significantly compared to old brain slices cultured in unconditioned media (Fig 4.20C), supporting the conclusion that soluble factors secreted by the young microglia are directly responsible for restoring Aβ phagocytic capacity of old microglia.
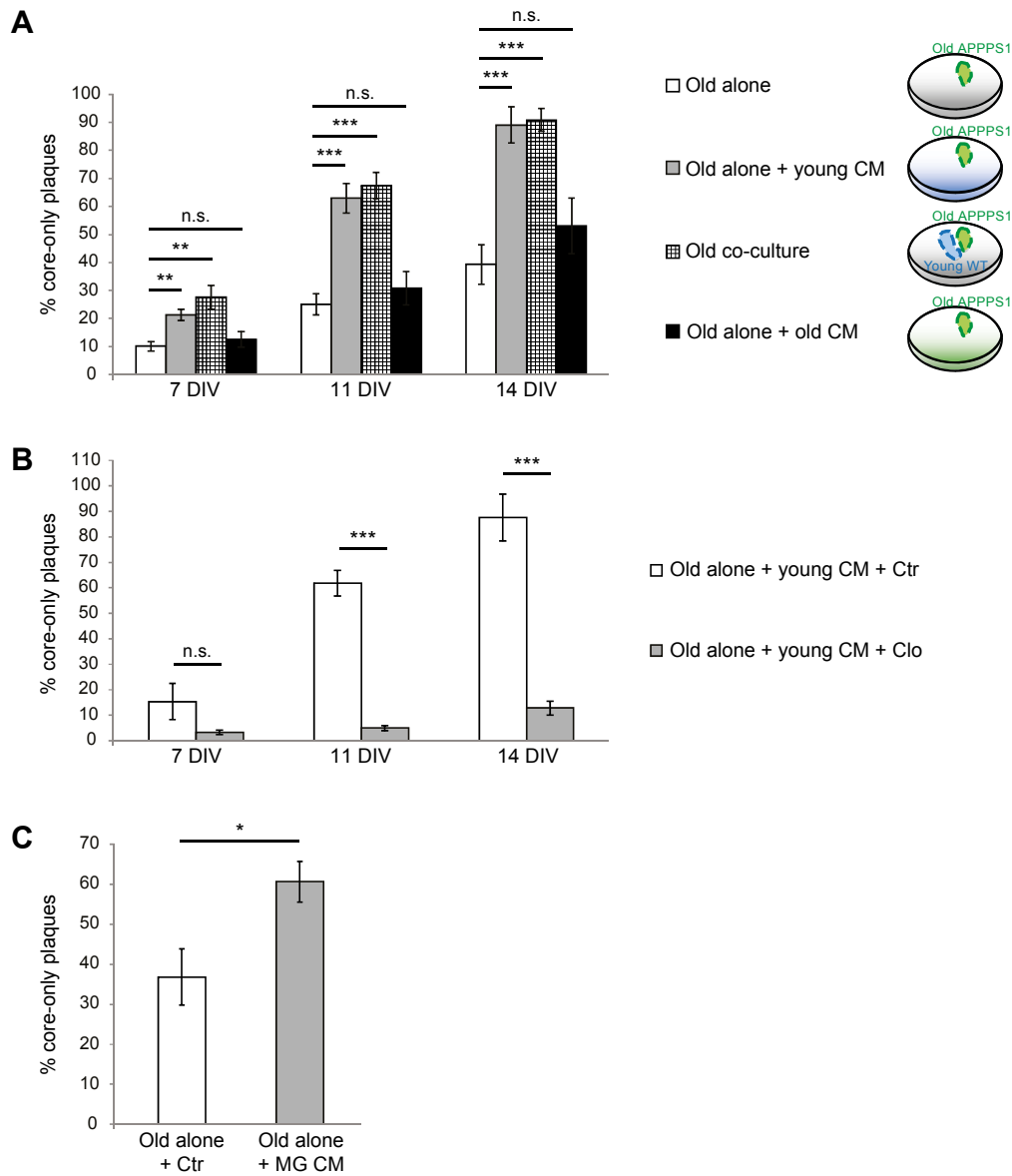
Figure 4.20. Factors secreted by young microglia promote amyloid plaque clearance.
(A) Old APPPS1 brain slices were cultured alone (old alone, white bars) or exposed to conditioned media (CM) derived from young WT tissue (old alone + young CM, grey bars). The analysis included co-culture of old APPPS1 and young WT brain slices (old co-culture, squared bars) as a positive control and old APPPS1 slices exposed to conditioned media derived from old APPPS1 tissue (old alone + old CM, black bars) as a negative control. Drawings schematically illustrate analyzed conditions. Quantifications of the % of core-only plaques from the total number of amyloid plaques in the old APPPS1 brain slices as described above at 7, 11, and 14 DIV. Data show higher numbers of core-only plaques upon addition of conditioned media collected from young WT tissue to the old APPPS1 slices, fully mimicking core-only plaque numbers detected upon co-culturing conditions. Values are presented as mean ± SEM from three independent experiments, each experiment including at least two independent slice culture dishes. P values are derived from unpaired two-tailed Student's t-test. n.s. = not significant, **$P < 0.01$, ***$P < 0.001$. **(B)** Old APPPS1 brain slices were exposed to conditioned media derived from young WT tissue pre-treated with clodronate (old alone + young CM + Clo, grey bars) and vehicle control (old alone + young CM + Ctr, white bars). Quantifications of the % of core-only plaques from the total number of amyloid plaques at 7, 11, and 14 DIV show reduced numbers of core-only plaques upon exposure of the old APPPS1 brain slices to the conditioned media derived from microglia-depleted young WT tissue. Values are presented as mean ± SEM from three independent experiments, each experiment including at least two independent slice culture dishes. P values are derived from unpaired two-tailed Student's t-test. n.s. = not significant, ***$P < 0.001$. **(C)** Old APPPS1 brain slices were exposed to conditioned media derived from cultured WT primary microglial cells (old alone + MG CM, grey bar) or to unconditioned slice culture media as a control (old alone + Ctr, white bar). Quantifications of the % of core-only plaques from the total number of

amyloid plaques at 14 DIV show increased numbers of core-only plaques upon exposure of the old APPPS1 slices to conditioned media derived from cultured WT primary microglia. Values are presented as mean ± SEM from three independent experiments, each experiment including two independent slice culture dishes. *P* values are derived from unpaired two-tailed Student's *t*-test. *P < 0.05.

4.10 GM-CSF stimulates Aβ uptake of old microglia

As the previous results pointed towards the involvement of secreted factors in inducing Aβ phagocytosis, I next aimed at identifying factors that enhance Aβ uptake and phagocytic capacity of old microglial cells. It has been described that several pro- and anti-inflammatory cytokines may impact microglial Aβ phagocytosis (Chakrabarty et al 2015, Guillot-Sestier et al 2015, Lai & McLaurin 2012, Wilcock 2012). Therefore, to directly evaluate stimulatory effects of soluble factors on Aβ phagocytosis in the *ex vivo* model, I started with testing several selected pro- and anti-inflammatory cytokines by adding them directly to the old APPPS1 tissue. I analyzed whether addition of a single factor was enough to increase Aβ uptake and thus would reproduce the effect observed upon co-culturing of old and young brain slices. As can be seen in Fig 4.21A-E, immunofluorescence analyses revealed that treatment with the anti-inflammatory cytokines interleukin-10 (IL-10) and transforming growth factor β (TGF-β), as well as the pro-inflammatory cytokines IL-6 and IL-12/p40 resulted in preservation of the M3.2-positive plaque halo surrounding the plaque core in the *ex vivo* model (Fig 4.21A-E). In contrast, treatment of old APPPS1 brain slices with granulocyte-macrophage colony-stimulating factor (GM-CSF) promoted clearance of the Aβ plaque halo by the old CD68-positive microglial cells as evident by the increased appearance of core-only plaques (Fig 4.21F and Fig 4.22A, C). This effect was as potent as co-cultures of old and young brain slices (see Fig 4.10).
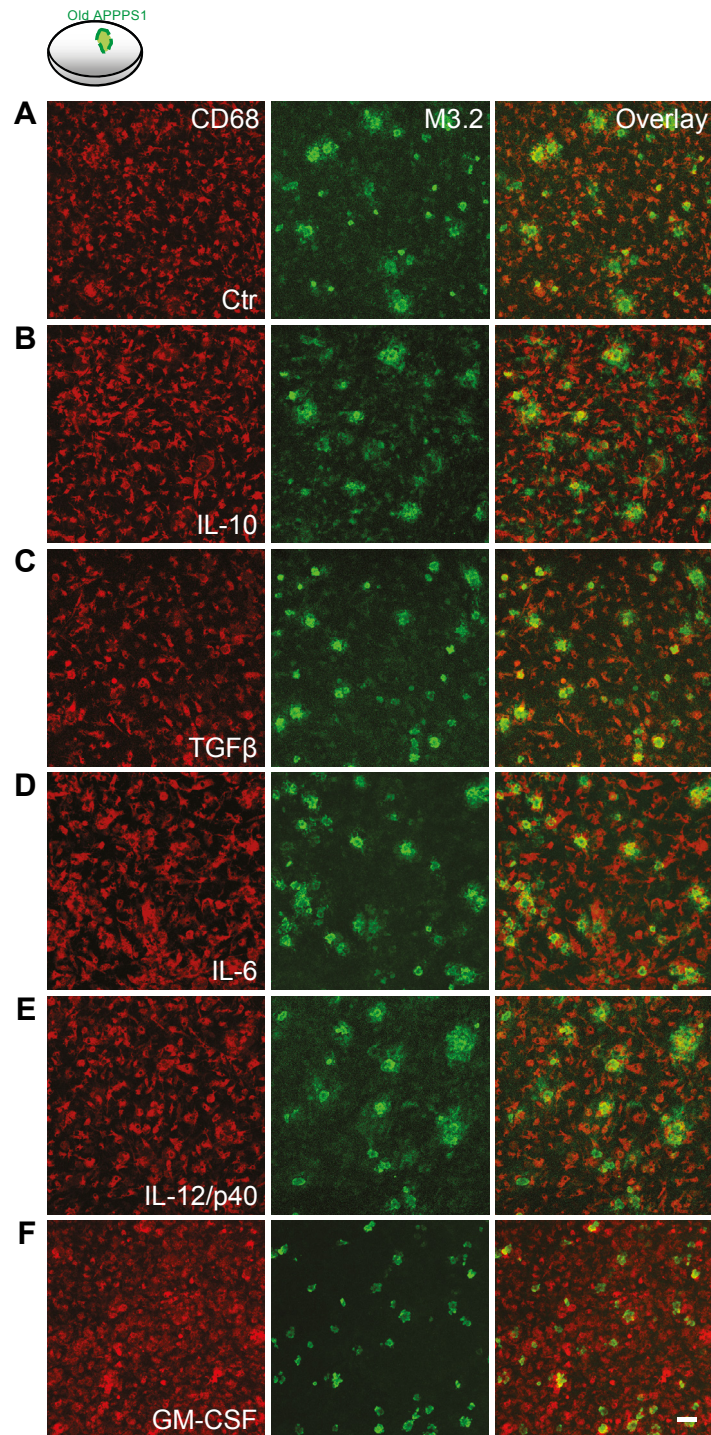
Figure 4.21. The pro-inflammatory factor GM-CSF promotes amyloid plaque clearance.
(A–F) Confocal images of the old APPPS1 tissue at 14 DIV treated with vehicle Ctr in (A), anti-inflammatory cytokines IL-10 and TGF-β in (B, C) and pro-inflammatory cytokines IL-6, IL-12/p40, and GM-CSF in (D, E, and F), respectively, and immunolabeled using CD68 (red) and M3.2 (green). Immunofluorescence analysis shows appearance of core-only plaques only upon GM-CSF treatment. Other factors tested did not stimulate amyloid clearance, as the typical amyloid plaque morphology with the M3.2-positive halos of Aβ surrounding amyloid cores was fully preserved. Scale bar: 50 μm.

Besides involvement in inflammation, cell differentiation, survival and phagocytosis, GM-CSF is also known for its mitogen capacity of inducing proliferation of microglial cells (Lee et al 1994, Suh et al 2005). Therefore, I performed quantitative analyses of GM-CSF effect on the CD68-positive coverage area based on immunofluorescence analyses. As already indicated in Fig 4.21F, these quantitative analyses revealed significantly increased CD68 coverage upon GM-CSF treatment of the old slices (Fig 4.22A, B). This was paralleled by significantly increased numbers of core-only plaques reflecting an enhanced phagocytosis of the plaque halo compared to vehicle-treated old brain slices (Fig 4.22A-C). Of note, upon GM-CSF treatment, numbers of core-only plaques increased to a very similar extent to what I measured upon co-culturing conditions (see Fig 4.10 and Fig 4.20A).

Since I previously observed an almost identical increase in core-only plaque numbers upon co-culturing and upon addition of conditioned media from young WT slices to the old APPPS1 slices, I additionally measured CD68 coverage area in the old APPPS1 brain slices incubated in young conditioned media. I found that young conditioned media was able to increase CD68-positive microglial density compared to unconditioned slice culture media, mimicking the observed effect of GM-CSF on the old APPPS1 brain slices (Fig 4.22D).
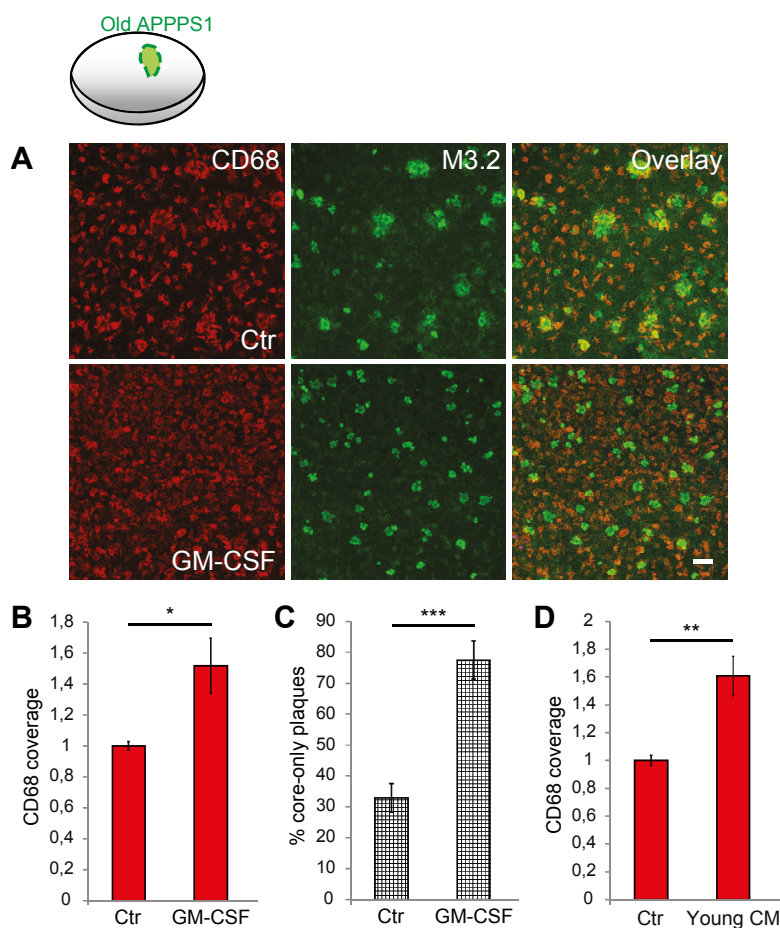
Figure 4.22. GM-CSF enhances amyloid plaque clearance and expands CD68-positive coverage.
(A) Confocal images of the old APPPS1 brain slice at 14 DIV treated with GM-CSF and vehicle Ctr and immunolabeled with CD68 (red) and M3.2 (green). Scale bar: 50 µm. **(B)** Area covered by CD68-positive cells (CD68 coverage) in the old APPPS1

brain slice at 14 DIV treated with GM-CSF and vehicle Ctr. CD68 coverage is enhanced upon GM-CSF treatment. Values are normalized to CD68 coverage of the Ctr and are presented as mean ± SEM from three independent experiments, each experiment including two independent slice culture dishes. *P* values are derived from unpaired two-tailed Student's *t*-test. *$P < 0.05$. **(C)** Quantifications of the % of core-only plaques from the total number of amyloid plaques in the old APPPS1 tissue at 14 DIV treated with GM-CSF and Ctr. Data show higher numbers of core-only plaques upon GM-CSF treatment. Values are presented as mean ± SEM from three independent experiments, each experiment including three independent slice culture dishes. *P* values are derived from unpaired two-tailed Student's *t*-test. ***$P < 0.001$. **(D)** Area covered by CD68-positive cells (CD68 coverage) in the old APPPS1 brain slice at 14 DIV exposed to conditioned media derived from young WT tissue (young CM) or to non-conditioned slice culture media (Ctr). CD68 coverage is enhanced upon exposure of the APPPS1 slice to the young CM. Values are normalized to CD68 coverage of the Ctr and are presented as mean ± SEM from three independent experiments, each experiment including two independent slice culture dishes. *P* values are derived from unpaired two-tailed Student's *t*-test. **$P < 0.01$.

Altogether observed similarities between GM-CSF and co-culturing suggest that GM-CSF might be one potential factor released by the young microglia and responsible for increasing Aβ uptake and clearance in the *ex vivo* co-culture model of young and old brain slices.

4.11 Amyloid clearance can be achieved upon co-culturing of young GM-CSF$^{-/-}$ and old APPPS1 brain slices

To investigate whether GM-CSF is the sole factor responsible for triggering proliferation of old microglial cells and Aβ phagocytosis in the *ex vivo* model, I analyzed amyloid plaque clearance in the absence of GM-CSF. For this purpose I prepared slice cultures from young GM-CSF knock-out (GM-CSF$^{-/-}$) mice and co-cultured together with old APPPS1 brain slices (Fig 4.23A). Surprisingly, lack of GM-CSF secretion by the young brain slices did not result in a reduction of Aβ clearance, but instead, similarly to WT brain slices, still allowed amyloid clearance (Fig 4.23A, B). In line with the induced occurrence of core-only plaques, also the density of CD68-positive cells was enhanced in the old APPPS1 slices co-cultured with the young GM-CSF$^{-/-}$ slices in contrast to the old slices cultured alone (Fig 4.23C).
Thus, these data indicate that GM-CSF is not the only factor mediating microglial proliferation and Aβ uptake in the *ex vivo* co-culture model.
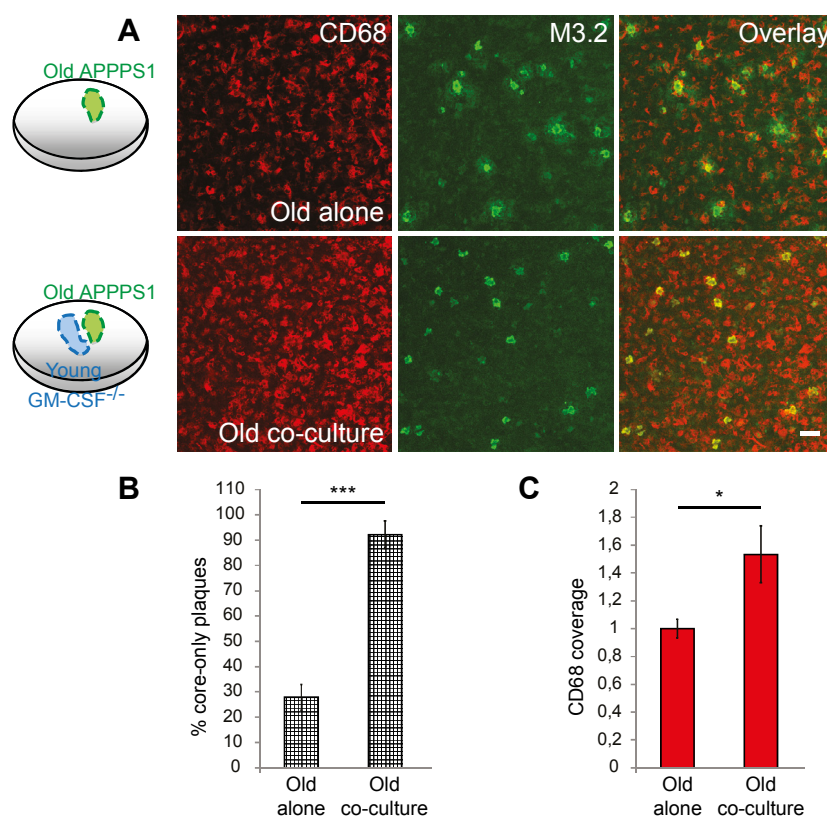
Figure 4.23. Amyloid plaque clearance is enhanced in the co-culture of old APPPS1 and young GM-CSF⁻/⁻ brain slices.
(A) Confocal images of the old APPPS1 brain slice alone in culture (old alone) or in co-culture with young GM-CSF⁻/⁻ brain slices (old co-culture) at 14 DIV and immunlabeled using CD68 (red) and M3.2 (green). Immunofluorescence analysis shows higher numbers of core-only plaques upon co-culturing with young GM-CSF⁻/⁻ slices. Scale bar: 50 µm. **(B)** Quantifications of the % of core-only plaques from the total number of amyloid plaques in the old APPPS1 tissue alone in culture or in co-culture with young GM-CSF⁻/⁻ slices at 14 DIV. Data show higher numbers of core-only plaques upon co-culturing of old APPPS1 brain slices together with young GM-CSF⁻/⁻ slices. Values are presented as mean ± SEM from three independent experiments, each experiment including three independent slice culture dishes. *P* values are derived from unpaired two-tailed Student's *t*-test. ****P* < 0.001. **(C)** Area covered by CD68-positive cells (CD68 coverage) in the old APPPS1 slice at 14 DIV alone in culture or in co-culture with young GM-CSF⁻/⁻ slices. CD68 coverage is enhanced upon co-culturing of old APPPS1 brain slices with young GM-CSF⁻/⁻ slices. Values are normalized to CD68 coverage of the old slice cultured alone and are presented as mean ± SEM from three independent experiments, each experiment including two independent slice culture dishes. *P* values are derived from unpaired two-tailed Student's *t*-test. **P* < 0.05.

4.12 Aggregated Aβ is reduced upon co-culturing and not upon GM-CSF application

To further characterize the effect of GM-CSF on amyloid plaque clearance and microglial numbers and compare it to the *ex vivo* co-culture model, I performed biochemical analyses of Aβ levels. Formic acid extracts of old APPPS1 brain slices cultured and treated with GM-CSF were prepared. Western blot analyses revealed no difference in aggregated Aβ levels in old APPPS1 slices upon GM-CSF treatment compared to vehicle-treated old slices (Fig 4.24A). Although I could detect increased protein levels of microglial CD68 upon GM-CSF, this effect was less pronounced compared to co-culture samples of young and old brain slices (Fig 4.24B and Fig 4.7), suggesting a more robust stimulation of amyloid clearance in the co-culture condition with

respect to GM-CSF. In contrast, as previously showed, I could detect a strong reduction of aggregated Aβ upon co-culturing of old and young brain slices compared to old tissue cultured alone (see Fig 4.11A, B), fully reflecting the increased Aβ phagocytosis observed in the co-culture model. In line with that, also CD68 levels were strongly elevated in the old tissue co-cultured with the young tissue (Fig 4.7 and Fig 4.24B).

Thus, these results confirm prior data obtained with GM-CSF^{-/-} mice (Fig 4.23A-C) and are consistent with the conclusion that GM-CSF is not the only factor necessary for modulating plaque phagocytosis in the *ex vivo* co-culture model.
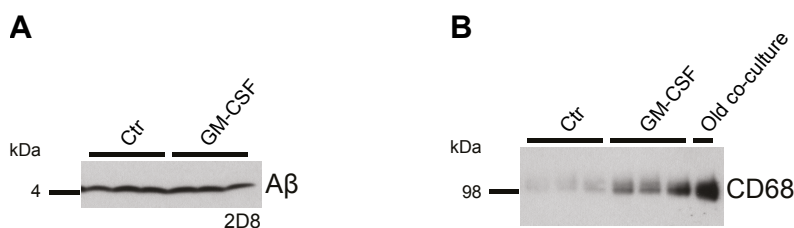
Figure 4.24. Analysis of fibrillar Aβ and CD68 levels in old APPPS1 tissue upon GM-CSF treatment.
(A, B) Immunoblot of Aβ using 2D8 antibody (A) and CD68 levels in (B) in the old APPPS1 tissue treated with GM-CSF and vehicle Ctr at 14 DIV. For both analyzed conditions samples were loaded in triplicates. In (B) old APPPS1 tissue co-cultured with the young WT at 14 DIV was included in the analysis for the comparison.

4.13 GM-CSF as well as co-culturing induces proliferation of old microglial cells

Based on above results and on the observation that the CD68 coverage in the old APPPS1 tissue was increased both upon GM-CSF treatment as well as upon incubation of the old brain slices in the young WT conditioned media (Fig 4.22B, D), I next analyzed microglial proliferation and investigated its potential link to amyloid clearance in the *ex vivo* model.

To evaluate numbers of proliferating cells, I utilized a cell proliferation marker Ki67, which detects proliferating cells in all active phases of the cell cycle (G1, S, G2, and mitosis) (Scholzen & Gerdes 2000). Quantitative analyses based on immunofluorescence data revealed higher numbers of Ki67-positive cells upon GM-CSF treatment of old APPPS1 slices compared to control-treated slices (Fig 4.25A). Specifically the number of CD68-positive microglia that were positive also for Ki67 was highly enhanced (Fig 4.25A, B), confirming the described mitogenic potential of GM-CSF on microglia (Lee et al 1994, Suh et al 2005).

Next, to investigate whether cell proliferation takes place also in co-cultures of young and old brain slices, I performed the same quantitative measurements on co-cultured samples. Similarly to GM-CSF effect, also upon co-culturing conditions I could detect increased numbers of proliferating microglial cells that were positive for both Ki67 and CD68 markers, compared to old tissue cultured alone (Fig 4.25C, D). Higher magnification images in Fig 4.26A and B demonstrate that nuclei positive for Ki67 are also positive for microglial marker CD68 and can be easily detected both upon GM-CSF application and in the co-culture model.

These results suggested the involvement of microglial proliferation in both GM-CSF as well as co-culture paradigm.
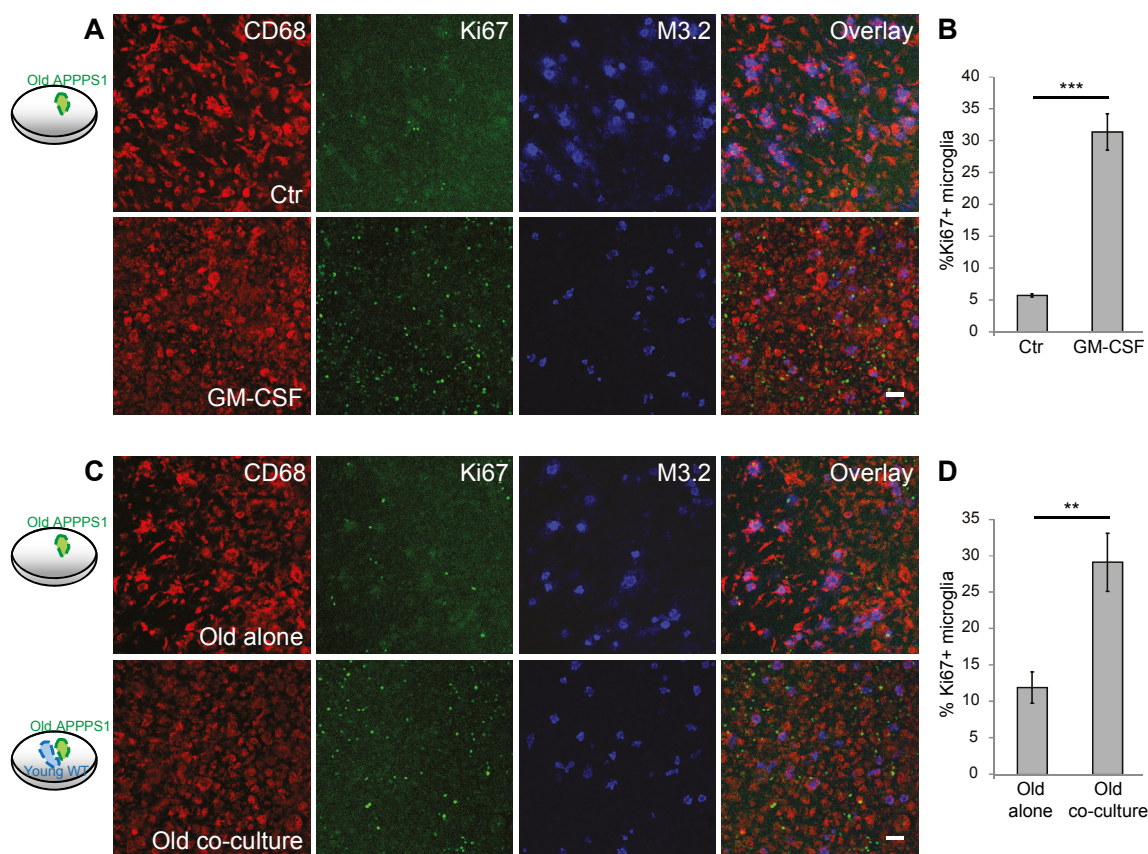
Figure 4.25. GM-CSF as well as co-culturing induces proliferation of old microglial cells.
(A) Confocal images of the old APPPS1 tissue at 14 DIV treated with GM-CSF and vehicle Ctr and immunolabeled using CD68 (red), cell proliferation marker Ki67 (green) and M3.2 (blue). Scale bar: 50 µm. **(B)** Quantifications of the % of Ki67 and CD68 double-positive microglial cells from the total number of CD68-positive cells in the old APPPS1 tissue at 14 DIV treated with GM-CSF and Ctr. Data show enhanced proliferation of microglia upon GM-CSF treatment. Values are presented as mean ± SEM from two independent experiments, each experiment including four independent slice culture dishes. *P* values are derived from unpaired two-tailed Student's *t*-test. ***$P < 0.001$. **(C)** Confocal images of the old APPPS1 slice alone in culture or in co-culture with the young WT tissue at 14 DIV and immunolabeled using CD68 (red), Ki67 (green) and M3.2 (blue) Scale bar: 50 µm. **(D)** Quantifications of the % of Ki67 and CD68 double-positive microglial cells from the total number of CD68-positive cells in the old APPPS1 tissue alone in culture or in co-culture with the young tissue at 14 DIV. Data show enhanced proliferation of microglia upon co-culturing of old and young brain slices. Values as presented as mean ± SEM from three independent experiments, each experiment including two independent slice culture dishes. *P* values are derived from unpaired two-tailed Student's *t*-test. **$P < 0.01$.
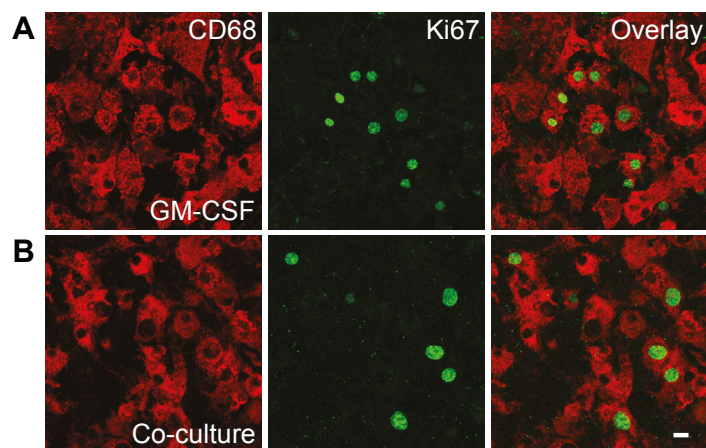
Figure 4.26. Proliferating microglial cells can easily be detected in the co-culture model and upon GM-CSF treatment.
(A, B) Confocal images of proliferating microglial cells in old APPPS1 brain slice treated with GM-CSF (A) or in co-culture with young WT brain slices (B) at 14 DIV and immunolabeled using CD68 (red) and cell proliferation marker Ki67 (green). Proliferating microglial cells are detectable upon both GM-CSF treatment and co-culturing and are clearly double-positive for CD68 and Ki67. Scale bar: 10 μm.

4.14 Proliferation of old microglial cells is required for amyloid clearance

As above results indicated that GM-CSF treatment as well as the addition of young WT conditioned media to old APPPS1 slices lead to increased CD68 coverage that is reflected by elevated numbers of proliferating microglial cells in the old APPPS1 tissue, I next investigated the potential connection between microglial proliferation and Aβ clearance in the *ex vivo* model. I cultured the old APPPS1 slices in young WT conditioned media with and without the addition of cytosine arabinose (AraC), a well-known inhibitor of cell proliferation (Doetsch et al 1999, Gomez-Nicola et al 2013). As can be seen in Fig 4.27A, immunofluorescence analyses revealed that microglial cells do not proliferate upon AraC treatment and at the same time amyloid plaque clearance is abolished (Fig 4.27A, B). Indeed, the number of core-only plaques measured in AraC-treated old slices was significantly reduced compared to vehicle-treated old slices (Fig 4.27A). This suggested that proliferation of old microglial cells is necessary for promoting amyloid uptake and clearance in the *ex vivo* model. Moreover, proliferative and phagocytic pathways might be interconnected.

Altogether, these results indicate that soluble factors released in the media by the young microglia can stimulate old microglial cells to proliferate, and this is required for increasing Aβ clearance in the *ex vivo* co-culture model. Such effect on old microglia is also very well recapitulated by GM-CSF treatment.
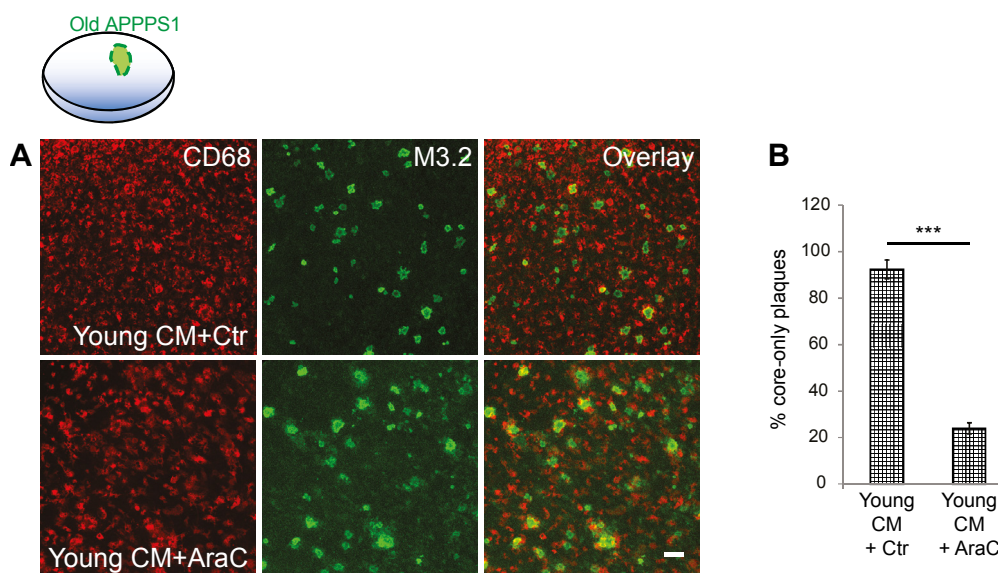
Figure 4.27. Microglial proliferation is required for amyloid plaque clearance.
Old APPPS1 brain slices were exposed to conditioned media derived from young WT tissue and simultaneously treated with AraC (young CM + AraC), which inhibits cell proliferation, or vehicle Ctr (young CM + Ctr). **(A)** Confocal images of the old APPPS1 tissue as described at 14 DIV immunolabeled with CD68 (red) and M3.2 (green). Scale bar: 50 μm. **(B)** Quantifications of the % of core-only plaques from the total number of amyloid plaques in the old APPPS1 slice exposed to conditioned media from young WT tissue and at the same time treated with AraC or Ctr at 14 DIV. Data show a reduced number of core-only plaques upon AraC treatment. Values are presented as mean ± SEM from three independent experiments, each including two independent slice culture dishes. *P* values are derived from unpaired two-tailed Student's *t*-test. ***$P < 0.001$.

5. Discussion

5.1 Studying amyloid plaque clearance of microglia

A characteristic feature of Alzheimer's disease is the pathological accumulation of Aβ in the form of amyloid plaques in the patients' brain. One of the main beliefs currently is that Aβ deposits originate from a disturbed balance between production and removal of Aβ peptides (Selkoe & Hardy 2016). Indeed, the beneficial effect of reduced Aβ peptide production is supported by mutations that, decreasing β-secretase cleavage of APP, lower Aβ peptide production and protect against AD (Jonsson et al 2012). On the other hand, decreased Aβ clearance was detected in sporadic AD patients, which comprise approximately 90% of all AD patients (Mawuenyega et al 2010). The brain's phagocytic effectors, microglial cells, are engaged in the removal of Aβ (Bolmont et al 2008, Rodriguez et al 2010). Microglia seem not to be capable of sustaining the increased amount of Aβ in the diseased brain, resulting in a progressive Aβ accumulation (Mawuenyega et al 2010, Wildsmith et al 2013). Therefore, it would be very important to better understand microglial-mediated mechanisms of Aβ clearance in the course of AD. Studies on microglial functions in the context of amyloid plaque phagocytosis have so far been restricted by the limitations of suitable model systems. Researchers often used *in vitro* cultures of microglial cells isolated from neonatal pups that are not suitable for investigations of age-related changes occurring in AD (Butovsky et al 2014). Moreover, it has been shown that microglia undergo changes during aging (Hickman et al 2008, Krabbe et al 2013, Orre et al 2014, Streit et al 2008). Thus, in my PhD work I decided to explore organotypic slice cultures from mouse brain to study the phagocytic capacity of microglial cells towards Aβ.

5.1.1 Organotypic brain slice culture as a model to study microglial phagocytosis of amyloid plaques (*ex vivo* model)

Among diverse applications, the organotypic brain slice culture model has been used so far as a model for studying Aβ toxicity. For example, it has been shown that treatment of rat hippocampal slices with oligomeric Aβ42 species induced cell toxicity, probably via activation of the ERK signaling pathway, which in turn activated caspase-3 and triggered apoptotic cell death (Chong et al 2006). In another study, using entorhinal-hippocampal organotypic slices, it has been found that oligomeric Aβ induced rise in intracellular Ca^{2+} and apoptotic cell death through a mechanism requiring NMDA and AMPA receptor activation (Alberdi et al 2010). Moreover, in organotypic hippocampal slice cultures it was shown that ganglioside GM1, a glycosphingolipid of the cellular plasma membrane, exhibited a neuroprotective activity upon Aβ-induced apoptosis (Kreutz et al 2011).

Brain slice cultures have also been explored in an attempt to mimic the Aβ plaque pathology in AD. However, it was shown that hippocampal slice cultures from AD mice unfortunately did not develop Aβ plaques even after long-term culturing (Novotny et al 2016). Absence of *de novo* plaque formation in APPPS1 brain slices was indeed confirmed in the laboratory of Sabina Tahirovic (unpublished data). It is likely that because of the required regular exchange of the

media (each 3-4 days), the threshold concentration of Aβ needed to nucleate the aggregation process could not be achieved. However, the *ex vivo* cellular environment seemed to help in producing better seeding material upon addition of brain homogenate from different aged AD mouse models together with continuous treatment with synthetic Aβ (Novotny et al 2016). Along this line, another study described that repeated applications of synthetic Aβ42 to WT mouse hippocampal slices failed to induce Aβ plaque formation. This can be explained by the fact that microglial cells were able to phagocytose Aβ. Indeed, only after microglial depletion, Aβ aggregates could be detected in WT hippocampal slices (Hellwig et al 2015).

Thus, despite some limitations, the slice culture approach represents a useful method to study the involvement of microglia in phagocytosis of amyloid exogenously added to cultured brain slices. However, what remains challenging is to study aged microglia and their capacity to clear amyloid *ex vivo*.

Therefore, within my PhD, I set up an *ex vivo* co-culture model of old APPPS1 and young WT brain slices to investigate microglial contribution to amyloid plaque clearance. This co-culture system enabled monitoring the behavior of microglial cells in the vicinity of amyloid plaques and their phagocytic activity over longer culturing times.

Remarkably, my work demonstrates that amyloid clearance dysfunction of AD microglia can be reversed in the *ex vivo* co-culture model, regardless of the massive neuronal and astrocytic loss, inevitably occurring in the old tissue in culture. According to PI analyses, I measured approximately 70% reduction in cell viability in the old APPPS1 brain slice already after 7 days in culture and more than 80% after 14 days. Such poor survival of neurons and astrocytes in cultured brain slices from aged mice has been reported also by others (Humpel 2015, Mewes et al 2012, Staal et al 2011). Actually, I believe that it is important to consider microglial response not only in an amyloid plaque-containing environment but also in presence of ongoing neuronal degeneration. Transgenic mouse models, like the APPPS1 model used in this thesis, recapitulate well the plaque pathology typical of AD, however they do not display evident neurodegeneration. On the other hand, it is very likely to expect that microglia in the human AD brain are influenced by the continuous neurodegeneration. Therefore, the *ex vivo* model may more closely reproduce the hostile environment of the human AD brain, even though the mechanisms of cell death may be different in an *ex vivo* model compared to human brain.

5.2 Role of microglia in Aβ clearance

In the AD brain microglia rapidly react to Aβ plaque formation by extending their processes and forming tight clusters around the plaques (Bolmont et al 2008, Meyer-Luehmann et al 2008). However, as recapitulated in mouse models of AD, despite recruitment of microglia to sites of Aβ deposition, Aβ levels continue to accumulate (Bittner et al 2012, Hefendehl et al 2011). It has been described that, along the progression of AD-like pathology, microglia become dysfunctional and lose their capacity to phagocytose and degrade Aβ (Hickman et al 2008, Krabbe et al 2013, Meyer-Luehmann et al 2008). This is in line with the human pathology, where reduced Aβ clearance rates have been observed in sporadic AD patients (Mawuenyega et al 2010), and an inefficient phagocytosis of myeloid cells from AD patients compared to non-AD control patients

has also been reported (Fiala et al 2005). Moreover, recent genome-wide association studies have identified several risk alleles for AD that belong to innate immune responses and are functionally linked to microglial phagocytosis (Karch et al 2014). So, specific variants that modify microglial efficiency of Aβ clearance might have detrimental effects in the brain.

Additionally, microglia in the AD brain have been reported to be similar to aged microglia and to present impairments in phagocytosis and motility, as well as altered morphology (Mosher & Wyss-Coray 2014). This may result in age-related defects of microglia in binding and digesting Aβ. For example, it has been found that microglia from 8 month old APPPS1 mice demonstrate significantly reduced expression of Aβ binding receptors as well as Aβ degrading enzymes compared to WT littermates, and levels decline even further by 14 months of age (Hickman et al 2008). Other transcriptional analyses have also reported that genes implicated in phagocytosis were downregulated in microglia from aged AD mice (Orre et al 2014). Moreover, *in vitro* studies using microglia cultured from adult animals have shown that aged microglia internalize less Aβ peptide than young microglial cells (Floden & Combs 2011, Njie et al 2012). In particular, while aging negatively affects microglial Aβ-phagocytosing function, it does not appear to limit their ability to interact with amyloid plaques or Aβ fibrils (Floden & Combs 2011). Likewise, young microglia from AD mice were able to clear exogenously added amyloid in organotypic slice cultures, whereas microglia from adult AD mice displayed a significant loss of their Aβ phagocytic function (Hellwig et al 2015).

In full agreement with above discussed studies, data presented in this thesis also reflect a defective ability of microglia from aged AD mice to phagocytose Aβ. This is illustrated by the fact that the majority of amyloid plaques I observed in the *ex vivo* cultures of brain slices from old APPPS1 mice displayed typical morphology of a fibrillar Aβ core surrounded by a halo of diffuse Aβ. Interestingly, I observed that amyloid plaques become drastically smaller in size upon co-culturing of APPPS1 brain slices carrying aged AD microglia together with brain slices from WT neonatal mice in the same culture dish, suggesting a potential for stimulation of old and diseased AD microglia. Remarkably, soluble factors released by the young microglia were sufficient to activate aged AD microglia and fully restore their Aβ phagocytic capacity of aged AD microglia.

Activated microglial cells accumulating in the vicinity of amyloid plaques and decreased amyloid plaque size in the *ex vivo* co-culture model described here, have indeed been described in amyloidosis mouse models as well as in AD patients following Aβ immunotherapy (Bard et al 2000, Boche & Nicoll 2008, Nicoll et al 2006, Schenk et al 1999, Wilcock et al 2004). The idea of using anti-Aβ antibodies as therapeutic agents to treat AD might be a useful approach, especially in light of the promising data obtained from an ongoing clinical trial with aducanumab (Sevigny et al 2016). A human recombinant monoclonal antibody developed by Biogen Inc., which selectively targets aggregated forms of Aβ, has been employed in this trial. Early data showed that intravenous infusions of aducanumab reduce Aβ plaque load in a dose- and time-dependent fashion. Aβ clearance is accompanied by enhanced recruitment of microglia, suggesting increased microglial-mediated plaque phagocytosis and clearance (Sevigny et al 2016). This also seems to correlate with cognitive improvement, although larger cohorts are necessary to verify this initial observation.

Even though the involved mechanisms are not completely clear yet, it is well accepted that anti-Aβ antibodies can stimulate microglia to actively clear amyloid plaques (Fu et al 2010, Moreth et al 2013, Wisniewski & Goni 2015). For example, upon treatment with anti-Aβ antibodies, Aβ has

been detected within microglia and found to co-localize with CD68, marker for microglial/macrophage lysosomes, which is indicative of phagocytically active microglia (Nicoll et al 2006, Xiang et al 2016, Zotova et al 2011). Similarly, I found that stimulation with factors secreted from young microglia can induce a strong CD68 immunoreactivity and Aβ uptake in aged microglial cells, reflecting that they also acquired a phagocytically active phenotype.

Moreover, core-only plaques that lack the halo of diffuse Aβ, as I have observed in the *ex vivo* model, have also been described in AD patients following Aβ immunization and are often referred to as "naked" dense core plaques (Boche & Nicoll 2008, Nicoll et al 2006, Nicoll et al 2003, Sevigny et al 2016). Indeed, removal of soluble forms of Aβ has been shown to occur more efficiently than that of compact fibrillar Aβ forming the plaque core, which is well in line with results of this thesis study (Mandrekar et al 2009, Nicoll et al 2006, Serrano-Pozo et al 2010). Of note, soluble oligomeric forms of Aβ are believed to be the toxic entity in AD (Umeda et al 2011). Specifically, soluble Aβ has been associated with spine loss, neuritic and synaptic degeneration in AD and therefore a reduction in soluble Aβ levels might positively influence memory and cognition (Koffie et al 2009, Selkoe 2008).

Taken together, data presented here and obtained in immunotherapeutic studies strongly suggest that stimulation of microglial functions to reduce amyloid burden might be a useful approach for treating AD (Fig 5.1).

5.3 Modulation of microglial activity as a tool to reduce Aβ load

It is very important to keep in mind that microglia directly control various pro- and anti-inflammatory signaling pathways, which are often affected in AD (Lucin & Wyss-Coray 2009, Weitz & Town 2012). Therefore, modulation of their activity requires caution. Microglia can acquire different phenotypes and their activation may have both beneficial and detrimental effects, which are strongly linked to the specific stage of the disease and brain area affected as well as to the level of exposure to Aβ, cytokines and other inflammatory mediators (Heneka et al 2015, Lucin & Wyss-Coray 2009, Weitz & Town 2012). Indeed, it has been shown that in the AD brain microglia can mount exaggerated immune responses and release molecular mediators that trigger pro-inflammatory reactions, eventually causing neuronal damage as well as contributing to microglial dysfunction (Heneka et al 2015, Weitz & Town 2012). Thus, it would be adequate to activate beneficial responses of microglia and at the same time to try avoiding the damage. Although this will be difficult, the more we know about pathways regulating microglial functions, the better we may be able to keep the microglial activation status under control. This PhD study indeed developed a suitable model system for studying microglial phagocytic functions in AD and shows that upon appropriate stimulation aged AD microglia acquire an activated state that make them capable of clearing Aβ.

One of the initial approaches targeting microglia in AD consisted in the inhibition of microglia using nonsteroidal anti-inflammatory drugs (NSAIDs). This idea was based on previous epidemiological findings reporting a lower incidence of AD in elderly patients with arthritis under NSAIDs compared to the general population, thus suggesting a beneficial effect of reduced inflammation (McGeer & Rogers 1992). Indeed, the chronic administration of oral ibuprofen in Tg2576 (APPswe) mice reduced Aβ plaque load and diminished IL-1β production in the brain of

treated mice (Lim et al 2000). Analysis of phosphotyrosin-labeled microglia showed lower recruitment of microglia to the Aβ plaques and reduced microglial cell activation in the ibuprofen-treated mice (Lim et al 2000). Similarly, another study in Tg2576 mice confirmed ibuprofen effects in reducing Aβ plaque burden, which was accompanied by decreased levels of the microglial activation markers CD45 and CD11b (Yan et al 2003). However, despite these evidences from animal models, a clinical trial that used NSAIDs as a therapeutic approach in AD patients failed to show a protective effect, and was even found to be detrimental (Martin et al 2008).

In contrast, and well consistent with results described in this thesis, boosting the inflammatory response of microglia has also resulted in beneficial outcome. It has been reported that a single intrahippocampal injection of LPS (TLR4 ligand) in the brain of APPswe/PS1 mice resulted in activated MHCII-positive microglia and reduced cerebral Aβ load (DiCarlo et al 2001). More recently, another study showed that the chronic systemic administration of a detoxified LPS-derivative, namely monophosphoryl lipid A (MPL), reduced soluble and insoluble Aβ load in the brain of APPswe/PS1 mice, by stimulating microglial Aβ phagocytic capacity and triggering rather moderate inflammatory reaction (Michaud et al 2013).

In line with that, it has been reported that genetic depletion of the inflammatory protein complement factor C3 protein, in aged AD mice lowered microgliosis and increased Aβ burden (Maier et al 2008). The reduced microgliosis was accompanied by increase in IL-4 and IL-10 levels, and decrease in CD68, F4/80, inducible nitric oxide synthase (iNOS), and TNF-α levels. Those results propose a beneficial role for C3 in Aβ clearance via modulation of the microglial phenotype. A more recent study focused on the scavenger receptor Scara-1, which is expressed on microglia and has been reported to be involved in internalization and phagocytosis of Aβ (Hickman et al 2008). In this study, they showed that Scara-1 depletion in APPswe/PS1 mice accelerated Aβ accumulation, while the pharmacologically induced overexpression of Scara-1 enhanced phagocytosis and clearance of Aβ (Frenkel et al 2013).

This evidence together with data in my thesis suggest the possibility that microglial activation in AD is not detrimental and that the spatiotemporal context in which microglia are targeted and other factors play a determinant role (Breitner et al 2011).

5.3.1 Pro- and anti-inflammatory modulation of microglia through cytokines

Modulating the pro- or anti-inflammatory potential of microglia is far from being simple. As an example, it was originally thought that suppressing the inflammation by enhancing the anti-inflammatory signaling of microglia might produce beneficial effects. However, results obtained over the past years do not support this hypothesis. For example, one study enhancing the anti-inflammatory signaling through IL-10 overexpression in brains of two different AD mouse models increased soluble and insoluble Aβ and this was accompanied by impaired Aβ phagocytosis by microglia (Chakrabarty et al 2015). Consistent with it, a parallel study reported that genetic depletion of IL-10 in APPswe/PS1 mice reduced soluble and insoluble Aβ load (Guillot-Sestier et al 2015). Moreover, IL-10 depletion increased microglial migration and recruitment at Aβ plaques, and increased the number of Aβ-immunoreactive microglia, implying

an enhanced phagocytic capacity (Guillot-Sestier et al 2015). Data obtained in these two studies are a good demonstration that we have to deal with larger complexity of immune system responses than previously anticipated.

However, what has clearly been confirmed by number of studies in the literature is that modulation of microglial functions through inflammatory cytokines does have an impact on amyloid plaque pathology and can improve cognition in mouse models of AD (Zheng et al 2016). Some pro-inflammatory cytokines like IL-6 and TNF-α have been shown to associate with a reduction in amyloid plaque load by inducing microglial phagocytosis (Chakrabarty et al 2011, Chakrabarty et al 2010b). As an example, overexpression of INF-γ in AD mouse brains suppressed Aβ accumulation by activating immune system components that enhanced Aβ phagocytosis and clearance by microglia (Chakrabarty et al 2010a). In parallel, anti-inflammatory cytokines like IL-4 and IL-10 have been found to not decrease Aβ deposition (Chakrabarty et al 2015, Chakrabarty et al 2012). However, for several cytokines, including IL-10 and INF-γ there are studies reporting controversial results, suggesting that the same cytokine may have multiple and even opposite roles that may vary, most likely depending on the specific spatial-temporal context (Zheng et al 2016).

5.3.2 The pro-inflammatory factor GM-CSF induces amyloid clearance and proliferation of microglia in the *ex vivo* model

The increased phagocytosis in the *ex vivo* model described here was recapitulated by the application of the pro-inflammatory cytokine GM-CSF to the old APPPS1 tissue. At the same time, microglial Aβ uptake did not increase in the *ex vivo* model system upon treatment with pro-inflammatory cytokines IL-6 and IL-12/p40 or the anti-inflammatory factors IL-10 and TGF-β. Notably, the increase in amyloid clearance observed upon GM-CSF treatment, was accompanied by augmented microglial proliferation, as shown by increased CD68 coverage levels. On the contrary, I did not detect any increase in microglial density upon addition of other tested cytokines (IL-6, IL-12/p40, IL-10 and TGF-β), which was in line with the observed absence of Aβ-clearance.
It is worth to mention that upon addition of TGF-β, the density of CD68-positive cells in old APPPS1 slices seemed to be even diminished compared to controls, which is consistent with other studies showing an inhibitory effect on cell proliferation mediated by TGF-β (Datto et al 1995, Grainger et al 1994). In contrast, the increased CD68 coverage that I detected upon GM-CSF confirms its mitogenic-inducing potential on microglial cells (Lee et al 1994, Suh et al 2005).

Taken together, the observed induction of microglial activation and proliferation, and consequent enhancement of amyloid clearance in the *ex vivo* model seemed to be more specific for GM-CSF compared to all the other tested cytokines (Fig 5.1). My results reveal mechanistic similarities between co-culturing condition and GM-CSF application as microglial proliferation and amyloid plaque clearance occurred in both experimental paradigms. However, the effect on Aβ degradation was more robust in co-cultures compared to GM-CSF application. Although my immunofluorescence data clearly showed that GM-CSF induced clearance of the plaque halo of diffuse Aβ, biochemical analyses revealed that co-culturing of young and old tissue resulted in

addition in a decrease of fibrillar Aβ. Thus, the co-culture condition appears to act as a more potent stimulus on Aβ clearance compared to the tested GM-CSF treatment paradigm.

In line with these observations, co-culturing of old APPPS1 slices together with young GM-CSF$^{-/-}$ slices was still able to increase plaque phagocytosis and, in line with that, also CD68 coverage. This indicates that, in the *ex vivo* co-culture model, microglial population can expand also in absence of endogenous GM-CSF secretion and that other factors with a mitogenic potential may contribute to this effect. In addition, there are also evidences reporting that the GM-CSF$^{-/-}$ mice overproduce M-CSF, another cytokine capable of inducing microglial proliferation and I cannot exclude this as a possible compensatory mechanism (Bonfield et al 2008, Shibata et al 2001). Possibly, in addition to GM-CSF, other factors released by the young microglia may mediate phagocytic clearance.

It would be very interesting to identify those secreted factor(s) and their mode of action on amyloid clearance. One possible approach would be to use mass spectrometry analysis and compare secreted proteins in conditioned media from young/old slices cultured alone *versus* young and old slices co-cultured together. However, we ascertained that this is technically challenging due to the high amount of serum contained in the slice culture medium. Ongoing cell death occurring in old slices in culture may be additional challenge to this approach.
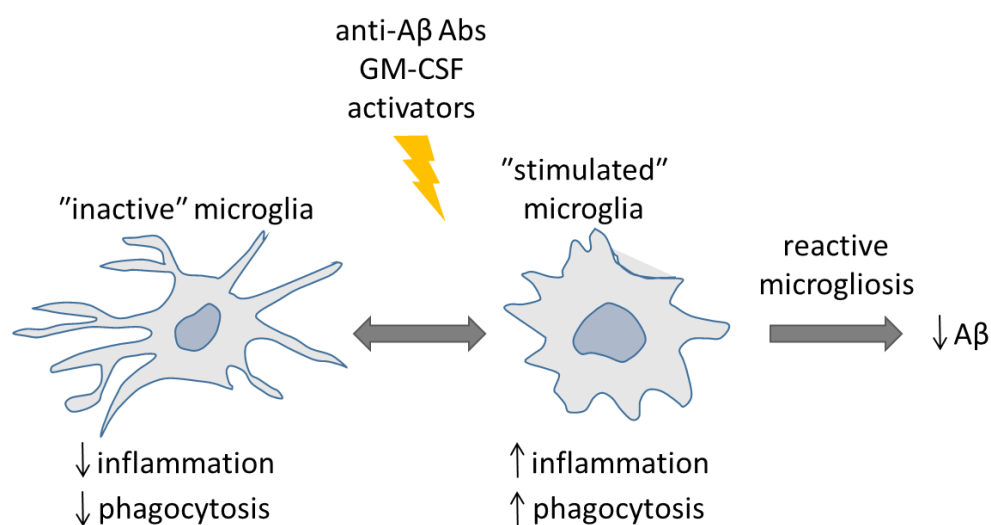
Figure 5.1. Model of effect of microglial immunomodulation on Aβ levels.
Schematic representation of the potential effect of microglial activation on Aβ levels. Aged AD microglia are less capable of orchestrating a controlled inflammatory response and have dysfunctional phagocytosis ("inactive" microglia). However, upon stimulation with anti-Aβ antibodies, as well as GM-CSF and other immune-modulators aged AD microglia can still acquire an activated state, which is also reflected by their amoeboid morphology ("stimulated" microglia). Reactive microglia may increase their inflammatory and phagocytic functions, leading to reduced Aβ accumulation.

5.4 Link between microglial proliferation and amyloid clearance

Data in this thesis propose that GM-CSF-mediated effects on amyloid clearance are linked to microglial proliferation. In agreement with that, other studies support a connection between proliferation of microglia and Aβ clearance. For example, it has been shown that deletion of the

microglial specific receptor CX3CR1 in a mouse model of AD resulted in higher proliferation rates of microglia and decreased plaque deposition, which was well associated with the increased microglial uptake and phagocytic ability and reflected by the high LAMP1-positive phagolysosomal Aβ content (Liu et al 2010). Moreover, another more recent study also pointed out the connection between proliferative and phagocytic processes and showed that TNF-α-induced proliferation of microglia stimulates phagocytosis of beads and increased phagocytosis of neurons *in vitro* (Neniskyte et al 2014). In line with these findings, it was reported that in an AD mouse heterozygous for the AD-associated microglial specific receptor TREM2 (*Trem2+/-*), proliferation of microglia in response to Aβ was impaired, suggesting that deficient phagocytosis might be linked with impaired microglial proliferation (Ulrich et al 2014).

On the contrary, recent findings reported increased microglial proliferation in AD that was correlating with disease severity. In this study, inhibition of microglial proliferation in a mouse model of AD, by specifically targeting microglial CSF1R, prevented disease progression with positive outcome on behavioral and memory tasks (Olmos-Alonso et al 2016). However, Aβ deposition remained unaffected even in the absence of proliferating microglia (Olmos-Alonso et al 2016). Similarly, a complete or partial blockage of microglial CSF1R lead to improved cognition in AD mice with no detectable changes in Aβ levels and plaque load (Dagher et al 2015).

Although microglial proliferation in the *ex vivo* co-culture model seems to be required to induce amyloid reduction, it is reasonable to think that the increase in phagocytosis might not simply be the consequence of augmented microglial numbers. Indeed, often microglial activation is associated with enhanced proliferation, but also with augmented phagocytic activity of the microglial cells (Giulian & Ingeman 1988). This suggests that both proliferation and phagocytosis may be interconnected processes possibly governed by the same signaling pathways. At the same time, also microglial morphology is presumed to relate with microglial function and a morphological transformation from ramified into amoeboid microglia denote them as activated microglial cells. Data in this thesis, indeed, show that microglia in the old APPPS1 slice exhibit mainly amoeboid morphology especially upon co-culture with the young slice, reflecting their highly active phagocytic phenotype in presence of young secreted factors as well as of GM-CSF (Fig 5.1).

As discussed above, similar to GM-CSF, also the cytokine M-CSF has been found to stimulate proliferation and phagocytosis of microglia (Mitrasinovic & Murphy 2002, Mitrasinovic et al 2003, Smith et al 2013). In particular, it has been reported that M-CSF can increase the acidity and hydrolytic activity of microglial lysosomes, resulting in a more efficient degradation of Aβ (Majumdar et al 2007). M-CSF injection in an AD mouse increased number of microglial cells, with the high proportion of microglia internalizing Aβ and displaying Aβ-containing lysosomes. This correlated well with the reduction in amyloid plaque load and improved cognitive impairment (Boissonneault et al 2009). Moreover, previous studies have reported that microglia might be incapable of efficiently eliminating internalized Aβ (Chung et al 1999, Frackowiak et al 1992, Paresce et al 1997), whereas, in a later study, increased Aβ degradation was induced after exogenous targeting of lysosomal enzymes (Majumdar et al 2008). This suggests that low lysosomal activity may account for a limited ability of microglia to degrade Aβ, and therefore, increasing the lysosomal degradation may be a way to promote amyloid clearance. In the *ex vivo* co-culture model presented here, I detected increased levels of the lysosomal marker CD68 in

AD microglia, which is indicative of enhanced lysosomal activity. It would be of relevance to study this aspect more closely and examine whether increased acidity and hydrolytic activity accompany the enhanced amyloid clearance effect observed in our model.

In light of these considerations, further analyses are required to better understand mechanisms of action of specific cytokines and their potential influence on microglial phagocytosis and amyloid removal.

5.4.1 Therapeutic potential of GM-CSF and other rejuvenating factors

Data presented here showed that administration of GM-CSF is sufficient to enhance amyloid clearance in the *ex vivo* model of AD, supporting a potential role for GM-CSF as a therapeutic molecule. In this regard, it has been reported that GM-CSF injection into an AD mouse model resulted in increased microglial density, reduced amyloid load of about 50%, and almost completely reversed cognitive impairment compared to saline-treated mice (Boyd et al 2010). These data strongly support that using the *ex vivo* model I was indeed able to identify a phagocytosis enhancing molecule that has the same properties when tested *in vivo*. Moreover, it is important to mention that GM-CSF already succeed in short-term Phase I clinical trials for assessing safety of a manufactured version of it (Sargramostim or Leukine®) and it is currently tested in Phase II clinical trials for long-term treatment of patients with AD [(www.alzforum.org/therapeutics/sargramostim)](www.alzforum.org/therapeutics/sargramostim) (Lai & McLaurin 2012). Nevertheless, there are also opposite reports showing that neutralization of GM-CSF may be beneficial for AD. In this study it has been reported that anti-GM-CSF antibody-injected AD mice exhibited decreased amyloid burden, while levels of activated microglia were reduced (Manczak et al 2009). However, they argue for a potential interference of the GM-CSF antibody with Aβ production, to explain reduced Aβ deposits, without taking into consideration eventual effects on Aβ phagocytosis.

Besides GM-CSF effect described here, other approaches showed a potential in reverting Aβ phagocytic dysfunction of microglia. It has been reported that microglia in the AD brain become dysfunctional and incapable of efficiently phagocytosing Aβ while undergoing age/disease-related changes, acquiring a so-called senescent phenotype (Streit et al 2008). In this regard, efforts to rejuvenate old microglia in order to rescue their young beneficial functions have been made. These may help us to gain some knowledge about the heterogeneity of microglial functions in AD as well as their pathological changes and may offer an intriguing way of reversing microglial disease-associated alterations. So far several studies focused on rejuvenating the brain as idea to reverse age-related deficits and reestablish brain functions. For example, heterochronic parabiosis studies, where aged and young animals share the circulatory system, showed increased neurogenesis and improved cognitive functions in the aged mice after being exposed to young blood (Baruch et al 2014, Smith et al 2015, Villeda et al 2014). Similarly, plasma transfer from younger mice into the aged mice replicated the same findings, implying the involvement of blood-derived soluble factors, and not only blood cells (Villeda et al 2011). Also, caloric restriction and aerobic exercise have been found to promote similar healthy effects (Willette et al 2012, Witte et al 2009) (Barrientos et al 2011). In a recent preclinical study, aged AD mice (16-20 months old) were heterochronically connected with a young WT mouse (2-3

months old) or repeatedly injected with plasma from young mice. That was sufficient to restore synaptic protein levels and cognitive deficits observed in AD mice, demonstrating therapeutic properties of young plasma, however without reducing Aβ burden, at least at the time of their analysis (Middeldorp et al 2016). Of note, clinical trials involving plasma protein transfer from young individuals are currently ongoing for treating patients with AD, such as the Plasma for Alzheimer SymptoM Amelioration (PLASMA) study (clinicaltrials.gov; NCT02256306) (Niraula et al 2016).

The *ex vivo* model could be of great help in identifying and verifying potential key factors capable of inducing Aβ clearance and lowering Aβ accumulation.

5.5 Diseased microglia display specific gene expression alterations

The fact that microglial cells in the old APPPS1 tissue - when co-cultured with the young WT tissue or supplemented by GM-CSF - acquired an activated state, illustrated by amoeboid cell morphology, increased proliferation and enhanced Aβ clearance, may suggest changes in the gene expression profile of those cells. This indicates that a specific condition/factor can act as trigger and induce a phenotypic switch of aged AD microglia from their inactive state into an active one. In this regard, recent studies invested big effort in characterizing gene signature alterations of microglia in disease. Notably, one study using single-cell gene expression profiling to better define subsets of immune cells in brains of 5XFAD mice identified a subpopulation of microglial cells, named as disease-associated microglia (DAM), characterized by a distinct profile of gene expression (Keren-Shaul et al 2017). During AD progression homeostatic microglia activate the "DAM program" and begin to express genes implicated in phagocytosis and lipid metabolism, like *Trem2*, lipoprotein lipase (*Lpl*) and *ApoE*. DAM microglia have been found to localize in proximity of amyloid plaques in both mouse and human AD brains and to contain Aβ material, and are considered to be the cells enrolled against AD pathology (Keren-Shaul et al 2017). Very similarly, additional transcriptomic analyses, identified a disease-associated molecular signature in a subset of microglia (MGnD, microglial neurodegenerative phenotype), which was found to be present in several neurodegenerative models, including the APPPS1 model as well as in plaque-associated microglia in brains of AD patients (Krasemann et al 2017). Specifically, they reported that the molecular mechanism leading to MGnD phenotype was triggered by upregulation of the phagocytosis regulating gene *Trem2*, resulting in the activation of APOE signaling, while microglial homeostatic genes, such as *P2ry12*, *Tmem119*, *Csf1r*, *Cx3cr1*, *Tgfb1* among others, were downregulated (Krasemann et al 2017). Indeed, when *Trem2* was knocked out in APPPS1 mice, inflammatory genes (e.g. *Trem2* and *ApoE*) were suppressed and homeostatic genes were restored (Krasemann et al 2017), indicating that presence of Trem2 can reverse homeostatic signature of microglia towards a diseased-associated signature. Moreover, in a previous study, TREM2 deficiency has been proposed to lock microglia in a homeostatic state, therefore preventing them from getting activated (Mazaheri et al 2017). Altogether, it seems we are starting to understand molecular changes microglia undergo in neurodegenerative disease conditions, which are responsible for their dysfunctions. This may give space for potential new strategies aimed at restoring fully functional microglia to fight neurodegenerative conditions like AD.

102

Along these lines, it would be highly interesting to decipher alterations in the microglial transcriptome in the *ex vivo* model when switching from an old and dysfunctional state of AD microglia into a phagocytically active state.

In addition, transcriptomic analyses could also help to explain the observed similarities as well as possible differences in the phagocytic state of microglia in the old APPPS1 tissue upon GM-CSF treatment and co-culturing paradigm. Knowing the mitogenic potential of GM-CSF, it may be likely to expect that RNA signature would reflect stronger proliferative capacity, whereas in the co-culture model the combined stimulation of several factors may reflect even stronger phagocytic response by microglia. However, this is very speculative and further investigations are needed to better understand this point.

Altogether, results of my PhD thesis support the view that modulating microglial activity may be beneficial for AD. Upon an appropriate stimulus AD microglia appear still capable of turning into an active state and exerting their innate capacity of phagocytosis and proliferation. Therefore, further investigations are definitely required to better understand microglial functional potential. It is very crucial to elucidate how this great potential is changing in the disease context in order to explore the possibility to restore those innate, young and protective functions that characterize microglia in a healthy context. Determining the transcriptome profile might be a potential initial step in that direction. However, we need to understand microglial changes not only on the molecular level with transcriptomic analyses but we would need also to combine with proteomic studies to validate those gene expression changes in microglia on a protein level. Once learned how to define those gene expression switches more precisely, we may be in a better position to specifically target and modulate microglial activity.

5.6 Conclusion

In this thesis work, I established an *ex vivo* model to study microglial phagocytosis of amyloid plaques. The findings described here suggest that phagocytic functions of old microglial cells that become dysfunctional and ineffective during the course of AD can be restored to lower the amyloid plaque load. These data support the view that enhancing microglial ability to clear Aβ may be a potential therapeutic strategy to fight AD. Therefore, it is of great importance to investigate further microglial phagocytic potential and expand ways of action to restore microglial function. The *ex vivo* model provides a valuable tissue culture system for identifying factors as well as testing molecules/compounds aiming at strengthening microglial phagocytosis and thus may help to identify novel and therapeutically relevant targets.

6. References

Ahmed M, Davis J, Aucoin D, Sato T, Ahuja S, et al. 2010. Structural conversion of neurotoxic amyloid-beta(1-42) oligomers to fibrils. *Nature structural & molecular biology* 17: 561-7

Alberdi E, Sanchez-Gomez MV, Cavaliere F, Perez-Samartin A, Zugaza JL, et al. 2010. Amyloid beta oligomers induce Ca2+ dysregulation and neuronal death through activation of ionotropic glutamate receptors. *Cell calcium* 47: 264-72

Alison Goate M-CC-H, Mike Mullan, Jeremy Brown, Fiona Crawford, Liana Fidani, Luis Giuffra, Andrew Haynes, Nick Irving, Louise James, Rebecca Mant, Phillippa Newton, Karen Rooke, Penelope Roques, Chris Talbot, Margaret Pericak-Vance, Alien Roses, Robert Williamson, Martin Rossor, Mike Owen & John Hardy. 1991. Segregation of a missense mutation in the amyloid precursor protein gene with familial Alzheimer's disease. *Nature* 349: 704-06

Alzheimer A. 1907. Über eine eigenartige Erkrankung der Hirnrinde. *Allgemeine Zeitschrift fur Psychiatrie und Psychisch-gerichtliche Medizin* 64: 146-8

Alzheimer A. 1911. Über eigenartige Krankheitsfälle des späteren Alters. *Zeitschrift für die gesamte Neurologie und Psychiatrie* Originalen vol. 4 356–85

Andrieu S, Coley N, Lovestone S, Aisen PS, Vellas B. 2015. Prevention of sporadic Alzheimer's disease: lessons learned from clinical trials and future directions. *Lancet Neurol* 14: 926-44

Bard F, Cannon C, Barbour R, Burke RL, Games D, et al. 2000. Peripherally administered antibodies against amyloid beta-peptide enter the central nervous system and reduce pathology in a mouse model of Alzheimer disease. *Nat Med* 6: 916-9

Barrientos RM, Frank MG, Crysdale NY, Chapman TR, Ahrendsen JT, et al. 2011. Little exercise, big effects: Reversing aging and infection-induced memory deficits, and underlying processes. *The Journal of neuroscience : the official journal of the Society for Neuroscience* 31: 11578-86

Baruch K, Deczkowska A, David E, Castellano JM, Miller O, et al. 2014. Aging. Aging-induced type I interferon signaling at the choroid plexus negatively affects brain function. *Science (New York, N.Y.)* 346: 89-93

Bayer TA, Cappai R, Masters CL, Beyreuther K, Multhaup G. 1999. It all sticks together--the APP-related family of proteins and Alzheimer's disease. *Mol Psychiatry* 4: 524-8

Beins E, Ulas T, Ternes S, Neumann H, Schultze JL, Zimmer A. 2016. Characterization of inflammatory markers and transcriptome profiles of differentially activated embryonic stem cell-derived microglia. *Glia* 64: 1007-20

Bennett DA, Schneider JA, Arvanitakis Z, Kelly JF, Aggarwal NT, et al. 2006. Neuropathology of older persons without cognitive impairment from two community-based studies. *Neurology* 66: 1837-44

References

Biffi A, Greenberg SM. 2011. Cerebral amyloid angiopathy: a systematic review. *Journal of clinical neurology (Seoul, Korea)* 7: 1-9

Bird TD. 2008. Genetic aspects of Alzheimer disease. *Genetics in medicine : official journal of the American College of Medical Genetics* 10: 231-9

Bittner T, Burgold S, Dorostkar MM, Fuhrmann M, Wegenast-Braun BM, et al. 2012. Amyloid plaque formation precedes dendritic spine loss. *Acta neuropathologica* 124: 797-807

Boche D, Nicoll JA. 2008. The role of the immune system in clearance of Abeta from the brain. *Brain Pathol* 18: 267-78

Boche D, Perry VH, Nicoll JA. 2013. Review: activation patterns of microglia and their identification in the human brain. *Neuropathology and applied neurobiology* 39: 3-18

Boissonneault V, Filali M, Lessard M, Relton J, Wong G, Rivest S. 2009. Powerful beneficial effects of macrophage colony-stimulating factor on beta-amyloid deposition and cognitive impairment in Alzheimer's disease. *Brain* 132: 1078-92

Bolmont T, Haiss F, Eicke D, Radde R, Mathis CA, et al. 2008. Dynamics of the microglial/amyloid interaction indicate a role in plaque maintenance. *J Neurosci* 28: 4283-92

Bonfield TL, Thomassen MJ, Farver CF, Abraham S, Koloze MT, et al. 2008. Peroxisome proliferator-activated receptor-gamma regulates the expression of alveolar macrophage macrophage colony-stimulating factor. *J Immunol* 181: 235-42

Boyd-Kimball D, Sultana R, Mohmmad-Abdul H, Butterfield DA. 2004. Rodent Aβ(1–42) exhibits oxidative stress properties similar to those of human Aβ(1–42): Implications for proposed mechanisms of toxicity. *Journal of Alzheimer's Disease* 6: 515-25

Boyd TD, Bennett SP, Mori T, Governatori N, Runfeldt M, et al. 2010. GM-CSF upregulated in rheumatoid arthritis reverses cognitive impairment and amyloidosis in Alzheimer mice. *J Alzheimers Dis* 21: 507-18

Breitner JC, Baker LD, Montine TJ, Meinert CL, Lyketsos CG, et al. 2011. Extended results of the Alzheimer's disease anti-inflammatory prevention trial. *Alzheimer's & dementia : the journal of the Alzheimer's Association* 7: 402-11

Brookmeyer R, Evans DA, Hebert L, Langa KM, Heeringa SG, et al. 2011. National estimates of the prevalence of Alzheimer's disease in the United States. *Alzheimer's & dementia : the journal of the Alzheimer's Association* 7: 61-73

Butovsky O, Jedrychowski MP, Moore CS, Cialic R, Lanser AJ, et al. 2014. Identification of a unique TGF-beta-dependent molecular and functional signature in microglia. *Nature neuroscience* 17: 131-43

Calhoun ME, Burgermeister P, Phinney AL, Stalder M, Tolnay M, et al. 1999. Neuronal overexpression of mutant amyloid precursor protein results in prominent deposition of cerebrovascular amyloid. *Proc Natl Acad Sci U S A* 96: 14088-93

Cameron B, Landreth GE. 2010. Inflammation, microglia, and Alzheimer's disease. *Neurobiol Dis* 37: 503-9

Cao X, Sudhof TC. 2001. A transcriptionally [correction of transcriptively] active complex of APP with Fe65 and histone acetyltransferase Tip60. *Science* 293: 115-20

Carare RO, Bernardes-Silva M, Newman TA, Page AM, Nicoll JAR, et al. 2008. Solutes, but not cells, drain from the brain parenchyma along basement membranes of capillaries and arteries: significance for cerebral amyloid angiopathy and neuroimmunology. *Neuropathology and applied neurobiology* 34: 131-44

Carson MJ, Crane J, Xie AX. 2008. Modeling CNS microglia: the quest to identify predictive models. *Drug Discov Today Dis Models* 5: 19-25

Castano EM, Prelli F, Wisniewski T, Golabek A, Kumar RA, et al. 1995. Fibrillogenesis in Alzheimer's disease of amyloid β peptides and apolipoprotein E. *Biochemical Journal* 306: 599-604

Chakrabarty P, Ceballos-Diaz C, Beccard A, Janus C, Dickson D, et al. 2010a. IFN-gamma promotes complement expression and attenuates amyloid plaque deposition in amyloid beta precursor protein transgenic mice. *J Immunol* 184: 5333-43

Chakrabarty P, Herring A, Ceballos-Diaz C, Das P, Golde TE. 2011. Hippocampal expression of murine TNFalpha results in attenuation of amyloid deposition in vivo. *Molecular neurodegeneration* 6: 16

Chakrabarty P, Jansen-West K, Beccard A, Ceballos-Diaz C, Levites Y, et al. 2010b. Massive gliosis induced by interleukin-6 suppresses Abeta deposition in vivo: evidence against inflammation as a driving force for amyloid deposition. *Faseb j* 24: 548-59

Chakrabarty P, Li A, Ceballos-Diaz C, Eddy James A, Funk Cory C, et al. 2015. IL-10 Alters Immunoproteostasis in APP Mice, Increasing Plaque Burden and Worsening Cognitive Behavior. *Neuron* 85: 519-33

Chakrabarty P, Tianbai L, Herring A, Ceballos-Diaz C, Das P, Golde TE. 2012. Hippocampal expression of murine IL-4 results in exacerbation of amyloid deposition. *Mol Neurodegener* 7: 36

Chavez-Gutierrez L, Bammens L, Benilova I, Vandersteen A, Benurwar M, et al. 2012. The mechanism of gamma-Secretase dysfunction in familial Alzheimer disease. *Embo j* 31: 2261-74

Chishti MA, Yang DS, Janus C, Phinney AL, Horne P, et al. 2001. Early-onset amyloid deposition and cognitive deficits in transgenic mice expressing a double mutant form of amyloid precursor protein 695. *J Biol Chem* 276: 21562-70

Cholerton B, Baker LD, Craft S. 2013. Insulin, cognition, and dementia. *European journal of pharmacology* 719: 170-9

Chong YH, Shin YJ, Lee EO, Kayed R, Glabe CG, Tenner AJ. 2006. ERK1/2 activation mediates Abeta oligomer-induced neurotoxicity via caspase-3 activation and tau cleavage in rat organotypic hippocampal slice cultures. *J Biol Chem* 281: 20315-25

Chow HM, Herrup K. 2015. Genomic integrity and the ageing brain. *Nat Rev Neurosci* 16: 672-84

Chung H, Brazil MI, Soe TT, Maxfield FR. 1999. Uptake, degradation, and release of fibrillar and soluble forms of Alzheimer's amyloid beta-peptide by microglial cells. *J Biol Chem* 274: 32301-8

Crehan H, Hardy J, Pocock J. 2013. Blockage of CR1 prevents activation of rodent microglia. *Neurobiol Dis* 54: 139-49

Crotti A, Ransohoff RM. 2016. Microglial Physiology and Pathophysiology: Insights from Genome-wide Transcriptional Profiling. *Immunity* 44: 505-15

Cummings BJ, Satou T, Head E, Milgram NW, Cole GM, et al. 1996. Diffuse plaques contain C-terminal A beta 42 and not A beta 40: evidence from cats and dogs. *Neurobiol Aging* 17: 653-9

D'Andrea MR, Cole GM, Ard MD. 2004. The microglial phagocytic role with specific plaque types in the Alzheimer disease brain. *Neurobiology of aging* 25: 675-83

Dagher NN, Najafi AR, Kayala KMN, Elmore MRP, White TE, et al. 2015. Colony-stimulating factor 1 receptor inhibition prevents microglial plaque association and improves cognition in 3xTg-AD mice. *Journal of Neuroinflammation* 12: 139

Datto MB, Li Y, Panus JF, Howe DJ, Xiong Y, Wang XF. 1995. Transforming growth factor beta induces the cyclin-dependent kinase inhibitor p21 through a p53-independent mechanism. *Proceedings of the National Academy of Sciences of the United States of America* 92: 5545-49

Dawkins E, Small DH. 2014. Insights into the physiological function of the β-amyloid precursor protein: beyond Alzheimer's disease. *Journal of neurochemistry* 129: 756-69

De Strooper B, Umans L, Van Leuven F, Van Den Berghe H. 1993. Study of the synthesis and secretion of normal and artificial mutants of murine amyloid precursor protein (APP): cleavage of APP occurs in a late compartment of the default secretion pathway. *The Journal of cell biology* 121: 295-304

Deane R, Du Yan S, Submamaryan RK, LaRue B, Jovanovic S, et al. 2003. RAGE mediates amyloid-[beta] peptide transport across the blood-brain barrier and accumulation in brain. *Nat Med* 9: 907-13

DiCarlo G, Wilcock D, Henderson D, Gordon M, Morgan D. 2001. Intrahippocampal LPS injections reduce Abeta load in APP+PS1 transgenic mice. *Neurobiology of aging* 22: 1007-12

Doetsch F, Garcia-Verdugo JM, Alvarez-Buylla A. 1999. Regeneration of a germinal layer in the adult mammalian brain. *Proc Natl Acad Sci U S A* 96: 11619-24

Doody RS, Raman R, Farlow M, Iwatsubo T, Vellas B, et al. 2013. A phase 3 trial of semagacestat for treatment of Alzheimer's disease. *N Engl J Med* 369: 341-50

Doody RS, Thomas RG, Farlow M, Iwatsubo T, Vellas B, et al. 2014. Phase 3 trials of solanezumab for mild-to-moderate Alzheimer's disease. *N Engl J Med* 370: 311-21

Dranoff G, Crawford AD, Sadelain M, Ream B, Rashid A, et al. 1994. Involvement of granulocyte-macrophage colony-stimulating factor in pulmonary homeostasis. *Science* 264: 713-6

Drechsel DN, Hyman AA, Cobb MH, Kirschner MW. 1992. Modulation of the dynamic instability of tubulin assembly by the microtubule-associated protein tau. *Mol Biol Cell* 3: 1141-54

Eckman EA, Watson M, Marlow L, Sambamurti K, Eckman CB. 2003. Alzheimer's Disease β-Amyloid Peptide Is Increased in Mice Deficient in Endothelin-converting Enzyme. *Journal of Biological Chemistry* 278: 2081-84

Edbauer D, Winkler E, Regula JT, Pesold B, Steiner H, Haass C. 2003. Reconstitution of gamma-secretase activity. *Nat Cell Biol* 5: 486-8

Elder GA, Gama Sosa MA, De Gasperi R. 2010. Transgenic mouse models of Alzheimer's disease. *The Mount Sinai journal of medicine, New York* 77: 69-81

Farris W, Mansourian S, Chang Y, Lindsley L, Eckman EA, et al. 2003. Insulin-degrading enzyme regulates the levels of insulin, amyloid beta-protein, and the beta-amyloid precursor protein intracellular domain in vivo. *Proc Natl Acad Sci U S A* 100: 4162-7

Farris W, Schutz SG, Cirrito JR, Shankar GM, Sun X, et al. 2007. Loss of neprilysin function promotes amyloid plaque formation and causes cerebral amyloid angiopathy. *Am J Pathol* 171: 241-51

Ferreira ST, Clarke JR, Bomfim TR, De Felice FG. 2014. Inflammation, defective insulin signaling, and neuronal dysfunction in Alzheimer's disease. *Alzheimer's & dementia : the journal of the Alzheimer's Association* 10: S76-83

Fiala M, Lin J, Ringman J, Kermani-Arab V, Tsao G, et al. 2005. Ineffective phagocytosis of amyloid-beta by macrophages of Alzheimer's disease patients. *J Alzheimers Dis* 7: 221-32; discussion 55-62

Floden AM, Combs CK. 2006. Beta-amyloid stimulates murine postnatal and adult microglia cultures in a unique manner. *J Neurosci* 26: 4644-8

Floden AM, Combs CK. 2011. Microglia Demonstrate Age-Dependent Interaction with Beta-amyloid Fibrils. *Journal of Alzheimer's Disease* 25: 279-93

Frackowiak J, Wisniewski HM, Wegiel J, Merz GS, Iqbal K, Wang KC. 1992. Ultrastructure of the microglia that phagocytose amyloid and the microglia that produce beta-amyloid fibrils. *Acta Neuropathol* 84: 225-33

Francisco-Cruz A, Aguilar-Santelises M, Ramos-Espinosa O, Mata-Espinosa D, Marquina-Castillo B, et al. 2013. Granulocyte–macrophage colony-stimulating factor: not just another haematopoietic growth factor. *Medical Oncology* 31: 774

Frautschy SA, Yang F, Irrizarry M, Hyman B, Saido TC, et al. 1998. Microglial response to amyloid plaques in APPsw transgenic mice. *The American journal of pathology* 152: 307-17

Frenkel D, Wilkinson K, Zhao L, Hickman SE, Means TK, et al. 2013. Scara1 deficiency impairs clearance of soluble amyloid-beta by mononuclear phagocytes and accelerates Alzheimer's-like disease progression. *Nature communications* 4: 2030

Frisoni GB, Boccardi M, Barkhof F, Blennow K, Cappa S, et al. 2017. Strategic roadmap for an early diagnosis of Alzheimer's disease based on biomarkers. *Lancet Neurol* 16: 661-76

References

Fu H, Liu B, Frost JL, Hong S, Jin M, et al. 2012. Complement component C3 and complement receptor type 3 contribute to the phagocytosis and clearance of fibrillar Abeta by microglia. *Glia* 60: 993-1003

Fu HJ, Liu B, Frost JL, Lemere CA. 2010. Amyloid-β Immunotherapy for Alzheimer's Disease. *CNS & neurological disorders drug targets* 9: 197-206

Games D, Adams D, Alessandrini R, Barbour R, Berthelette P, et al. 1995. Alzheimer-type neuropathology in transgenic mice overexpressing V717F beta-amyloid precursor protein. *Nature* 373: 523-7

Garwood CJ, Pooler AM, Atherton J, Hanger DP, Noble W. 2011. Astrocytes are important mediators of Abeta-induced neurotoxicity and tau phosphorylation in primary culture. *Cell death & disease* 2: e167

Ginhoux F, Greter M, Leboeuf M, Nandi S, See P, et al. 2010. Fate mapping analysis reveals that adult microglia derive from primitive macrophages. *Science* 330: 841-5

Giulian D, Ingeman JE. 1988. Colony-stimulating factors as promoters of ameboid microglia. *J Neurosci* 8: 4707-17

Gomez-Nicola D, Fransen NL, Suzzi S, Perry VH. 2013. Regulation of microglial proliferation during chronic neurodegeneration. *J Neurosci* 33: 2481-93

Gosselin D, Skola D, Coufal NG, Holtman IR, Schlachetzki JCM, et al. 2017. An environment-dependent transcriptional network specifies human microglia identity. *Science* 356

Graham WV, Bonito-Oliva A, Sakmar TP. 2017. Update on Alzheimer's Disease Therapy and Prevention Strategies. *Annual review of medicine* 68: 413-30

Grainger DJ, Kemp PR, Witchell CM, Weissberg PL, Metcalfe JC. 1994. Transforming growth factor beta decreases the rate of proliferation of rat vascular smooth muscle cells by extending the G2 phase of the cell cycle and delays the rise in cyclic AMP before entry into M phase. *Biochem J* 299 (Pt 1): 227-35

Grathwohl SA, Kalin RE, Bolmont T, Prokop S, Winkelmann G, et al. 2009. Formation and maintenance of Alzheimer's disease beta-amyloid plaques in the absence of microglia. *Nat Neurosci* 12: 1361-3

Griciuc A, Serrano-Pozo A, Parrado AR, Lesinski AN, Asselin CN, et al. 2013. Alzheimer's disease risk gene CD33 inhibits microglial uptake of amyloid beta. *Neuron* 78: 631-43

Grundke-Iqbal I, Iqbal K, Tung YC, Quinlan M, Wisniewski HM, Binder LI. 1986. Abnormal phosphorylation of the microtubule-associated protein tau (tau) in Alzheimer cytoskeletal pathology. *Proc Natl Acad Sci U S A* 83: 4913-7

Guillot-Sestier M-V, Doty Kevin R, Gate D, Rodriguez Jr J, Leung Brian P, et al. 2015. Il10 Deficiency Rebalances Innate Immunity to Mitigate Alzheimer-Like Pathology. *Neuron* 85: 534-48

Haass C. 2004. Take five—BACE and the γ-secretase quartet conduct Alzheimer's amyloid β-peptide generation. *The EMBO Journal* 23: 483-88

Haass C, Hung AY, Schlossmacher MG, Teplow DB, Selkoe DJ. 1993. beta-Amyloid peptide and a 3-kDa fragment are derived by distinct cellular mechanisms. *Journal of Biological Chemistry* 268: 3021-24

Haass C, Lemere CA, Capell A, Citron M, Seubert P, et al. 1995. The Swedish mutation causes early-onset Alzheimer's disease by beta-secretase cleavage within the secretory pathway. *Nat Med* 1: 1291-6

Haass C, Selkoe DJ. 1993. Cellular processing of β-amyloid precursor protein and the genesis of amyloid β-peptide. *Cell* 75: 1039-42

Haass C, Selkoe DJ. 2007. Soluble protein oligomers in neurodegeneration: lessons from the Alzheimer's amyloid beta-peptide. *Nat Rev Mol Cell Biol* 8: 101-12

Hardy JA, Higgins GA. 1992. Alzheimer's disease: the amyloid cascade hypothesis. *Science* 256: 184

Harrison JK, Jiang Y, Chen S, Xia Y, Maciejewski D, et al. 1998. Role for neuronally derived fractalkine in mediating interactions between neurons and CX3CR1-expressing microglia. *Proc Natl Acad Sci U S A* 95: 10896-901

Hefendehl JK, Wegenast-Braun BM, Liebig C, Eicke D, Milford D, et al. 2011. Long-Term In Vivo Imaging of β-Amyloid Plaque Appearance and Growth in a Mouse Model of Cerebral β-Amyloidosis. *The Journal of Neuroscience* 31: 624-29

Hellwig S, Masuch A, Nestel S, Katzmarski N, Meyer-Luehmann M, Biber K. 2015. Forebrain microglia from wild-type but not adult 5xFAD mice prevent amyloid-β plaque formation in organotypic hippocampal slice cultures. *Scientific Reports* 5: 14624

Heneka MT, Carson MJ, El Khoury J, Landreth GE, Brosseron F, et al. 2015. Neuroinflammation in Alzheimer's disease. *Lancet Neurol* 14: 388-405

Heneka MT, Kummer MP, Stutz A, Delekate A, Schwartz S, et al. 2013. NLRP3 is activated in Alzheimer's disease and contributes to pathology in APP/PS1 mice. *Nature* 493: 674-8

Henn A, Lund S, Hedtjarn M, Schrattenholz A, Porzgen P, Leist M. 2009. The suitability of BV2 cells as alternative model system for primary microglia cultures or for animal experiments examining brain inflammation. *Altex* 26: 83-94

Heuer E, Rosen RF, Cintron A, Walker LC. 2012. Nonhuman primate models of Alzheimer-like cerebral proteopathy. *Curr Pharm Des* 18: 1159-69

Hickman SE, Allison EK, El Khoury J. 2008. Microglial dysfunction and defective beta-amyloid clearance pathways in aging Alzheimer's disease mice. *The Journal of neuroscience : the official journal of the Society for Neuroscience* 28: 8354-60

Hickman SE, Kingery ND, Ohsumi TK, Borowsky ML, Wang LC, et al. 2013. The microglial sensome revealed by direct RNA sequencing. *Nat Neurosci* 16: 1896-905

Holcomb L, Gordon MN, McGowan E, Yu X, Benkovic S, et al. 1998. Accelerated Alzheimer-type phenotype in transgenic mice carrying both mutant amyloid precursor protein and presenilin 1 transgenes. *Nature medicine* 4: 97-100

Holtzman DM, Morris JC, Goate AM. 2011. Alzheimer's disease: the challenge of the second century. *Sci Transl Med* 3: 77sr1

Hsiao K, Chapman P, Nilsen S, Eckman C, Harigaya Y, et al. 1996. Correlative memory deficits, Abeta elevation, and amyloid plaques in transgenic mice. *Science* 274: 99-102

Humpel C. 2015a. Organotypic brain slice cultures: A review. *Neuroscience* 305: 86-98

Humpel C. 2015b. Organotypic vibrosections from whole brain adult Alzheimer mice (overexpressing amyloid-precursor-protein with the Swedish-Dutch-Iowa mutations) as a model to study clearance of beta-amyloid plaques. *Front Aging Neurosci* 7: 47

Iqbal K, Alonso Adel C, Chen S, Chohan MO, El-Akkad E, et al. 2005. Tau pathology in Alzheimer disease and other tauopathies. *Biochim Biophys Acta* 1739: 198-210

Iwatsubo T, Odaka A, Suzuki N, Mizusawa H, Nukina N, Ihara Y. 1994. Visualization of Aβ42(43) and Aβ40 in senile plaques with end-specific Aβ monoclonals: Evidence that an initially deposited species is Aβ42(43). *Neuron* 13: 45-53

Ji K, Akgul G, Wollmuth LP, Tsirka SE. 2013. Microglia Actively Regulate the Number of Functional Synapses. *PLoS ONE* 8: e56293

Jin M, Shepardson N, Yang T, Chen G, Walsh D, Selkoe DJ. 2011. Soluble amyloid beta-protein dimers isolated from Alzheimer cortex directly induce Tau hyperphosphorylation and neuritic degeneration. *Proc Natl Acad Sci U S A* 108: 5819-24

Jones RS, Minogue AM, Connor TJ, Lynch MA. 2013. Amyloid-β-Induced Astrocytic Phagocytosis is Mediated by CD36, CD47 and RAGE. *Journal of Neuroimmune Pharmacology* 8: 301-11

Jonsson T, Atwal JK, Steinberg S, Snaedal J, Jonsson PV, et al. 2012. A mutation in APP protects against Alzheimer's disease and age-related cognitive decline. *Nature* 488: 96-9

Jonsson T, Stefansson H, Steinberg S, Jonsdottir I, Jonsson PV, et al. 2013. Variant of TREM2 associated with the risk of Alzheimer's disease. *N Engl J Med* 368: 107-16

Jung S, Aliberti J, Graemmel P, Sunshine MJ, Kreutzberg GW, et al. 2000. Analysis of fractalkine receptor CX(3)CR1 function by targeted deletion and green fluorescent protein reporter gene insertion. *Mol Cell Biol* 20: 4106-14

Karch CM, Cruchaga C, Goate AM. 2014. Alzheimer's disease genetics: from the bench to the clinic. *Neuron* 83: 11-26

Karran E, De Strooper B. 2016. The amyloid cascade hypothesis: are we poised for success or failure? *J Neurochem* 139 Suppl 2: 237-52

Karran E, Hardy J. 2014. A critique of the drug discovery and phase 3 clinical programs targeting the amyloid hypothesis for Alzheimer disease. *Ann Neurol* 76: 185-205

Keren-Shaul H, Spinrad A, Weiner A, Matcovitch-Natan O, Dvir-Szternfeld R, et al. 2017. A Unique Microglia Type Associated with Restricting Development of Alzheimer's Disease. *Cell* 169: 1276-90.e17

Kettenmann H, Hanisch UK, Noda M, Verkhratsky A. 2011. Physiology of microglia. *Physiol Rev* 91: 461-553

Kim WS, Li H, Ruberu K, Chan S, Elliott DA, et al. 2013. Deletion of Abca7 increases cerebral amyloid-beta accumulation in the J20 mouse model of Alzheimer's disease. *J Neurosci* 33: 4387-94

Kimberly WT, LaVoie MJ, Ostaszewski BL, Ye W, Wolfe MS, Selkoe DJ. 2003. Gamma-secretase is a membrane protein complex comprised of presenilin, nicastrin, Aph-1, and Pen-2. *Proc Natl Acad Sci U S A* 100: 6382-7

Kimelberg HK, Nedergaard M. 2010. Functions of astrocytes and their potential as therapeutic targets. *Neurotherapeutics* 7: 338-53

Kleinberger G, Yamanishi Y, Suarez-Calvet M, Czirr E, Lohmann E, et al. 2014. TREM2 mutations implicated in neurodegeneration impair cell surface transport and phagocytosis. *Sci Transl Med* 6: 243ra86

Knopman DS, Parisi JE, Salviati A, Floriach-Robert M, Boeve BF, et al. 2003. Neuropathology of cognitively normal elderly. *J Neuropathol Exp Neurol* 62: 1087-95

Koffie RM, Meyer-Luehmann M, Hashimoto T, Adams KW, Mielke ML, et al. 2009. Oligomeric amyloid beta associates with postsynaptic densities and correlates with excitatory synapse loss near senile plaques. *Proceedings of the National Academy of Sciences of the United States of America* 106: 4012-7

Kohl A, Dehghani F, Korf HW, Hailer NP. 2003. The bisphosphonate clodronate depletes microglial cells in excitotoxically injured organotypic hippocampal slice cultures. *Experimental neurology* 181: 1-11

Korzhevskii DE, Kirik OV. 2016. Brain Microglia and Microglial Markers. *Neuroscience and Behavioral Physiology* 46: 284-90

Krabbe G, Halle A, Matyash V, Rinnenthal JL, Eom GD, et al. 2013. Functional impairment of microglia coincides with Beta-amyloid deposition in mice with Alzheimer-like pathology. *PloS one* 8: e60921

Krasemann S, Madore C, Cialic R, Baufeld C, Calcagno N, et al. 2017. The TREM2-APOE Pathway Drives the Transcriptional Phenotype of Dysfunctional Microglia in Neurodegenerative Diseases. *Immunity* 47: 566-81.e9

Kretner B, Trambauer J, Fukumori A, Mielke J, Kuhn PH, et al. 2016. Generation and deposition of Aβ43 by the virtually inactive presenilin-1 L435F mutant contradicts the presenilin loss-of-function hypothesis of Alzheimer's disease. *EMBO Molecular Medicine* 8: 458-65

Kreutz F, Frozza RL, Breier AC, de Oliveira VA, Horn AP, et al. 2011. Amyloid-beta induced toxicity involves ganglioside expression and is sensitive to GM1 neuroprotective action. *Neurochem Int* 59: 648-55

Kreutz S, Koch M, Bottger C, Ghadban C, Korf HW, Dehghani F. 2009. 2-Arachidonoylglycerol elicits neuroprotective effects on excitotoxically lesioned dentate gyrus granule cells via abnormal-cannabidiol-sensitive receptors on microglial cells. *Glia* 57: 286-94

Kruman, II, Wersto RP, Cardozo-Pelaez F, Smilenov L, Chan SL, et al. 2004. Cell cycle activation linked to neuronal cell death initiated by DNA damage. *Neuron* 41: 549-61

Kuhn PH, Wang H, Dislich B, Colombo A, Zeitschel U, et al. 2010. ADAM10 is the physiologically relevant, constitutive alpha-secretase of the amyloid precursor protein in primary neurons. *Embo j* 29: 3020-32

Lai AY, McLaurin J. 2012. Clearance of amyloid-β peptides by microglia and macrophages: the issue of what, when and where. *Future neurology* 7: 165-76

Lambert JC, Ibrahim-Verbaas CA, Harold D, Naj AC, Sims R, et al. 2013. Meta-analysis of 74,046 individuals identifies 11 new susceptibility loci for Alzheimer's disease. *Nat Genet* 45: 1452-8

Lampron A, Elali A, Rivest S. 2013. Innate immunity in the CNS: redefining the relationship between the CNS and Its environment. *Neuron* 78: 214-32

Lawson LJ, Perry VH, Dri P, Gordon S. 1990. Heterogeneity in the distribution and morphology of microglia in the normal adult mouse brain. *Neuroscience* 39: 151-70

Lee S, Varvel NH, Konerth ME, Xu G, Cardona AE, et al. 2010. CX3CR1 deficiency alters microglial activation and reduces beta-amyloid deposition in two Alzheimer's disease mouse models. *The American journal of pathology* 177: 2549-62

Lee SC, Liu W, Brosnan CF, Dickson DW. 1994. GM-CSF promotes proliferation of human fetal and adult microglia in primary cultures. *Glia* 12: 309-18

Leissring MA, Farris W, Chang AY, Walsh DM, Wu X, et al. 2003. Enhanced proteolysis of beta-amyloid in APP transgenic mice prevents plaque formation, secondary pathology, and premature death. *Neuron* 40: 1087-93

Li N, Liu K, Qiu Y, Ren Z, Dai R, et al. 2016. Effect of Presenilin Mutations on APP Cleavage; Insights into the Pathogenesis of FAD. *Front Aging Neurosci* 8: 51

Lian H, Yang L, Cole A, Sun L, Chiang AC, et al. 2015. NFkappaB-activated astroglial release of complement C3 compromises neuronal morphology and function associated with Alzheimer's disease. *Neuron* 85: 101-15

Lim GP, Yang F, Chu T, Chen P, Beech W, et al. 2000. Ibuprofen suppresses plaque pathology and inflammation in a mouse model for Alzheimer's disease. *J Neurosci* 20: 5709-14

Liu Y, Walter S, Stagi M, Cherny D, Letiembre M, et al. 2005. LPS receptor (CD14): a receptor for phagocytosis of Alzheimer's amyloid peptide. *Brain : a journal of neurology* 128: 1778-89

Liu Z, Condello C, Schain A, Harb R, Grutzendler J. 2010. CX3CR1 in microglia regulates brain amyloid deposition through selective protofibrillar amyloid-beta phagocytosis. *J Neurosci* 30: 17091-101

Lu T, Pan Y, Kao SY, Li C, Kohane I, et al. 2004. Gene regulation and DNA damage in the ageing human brain. *Nature* 429: 883-91

Lucin KM, Wyss-Coray T. 2009. Immune activation in brain aging and neurodegeneration: too much or too little? *Neuron* 64: 110-22

Lue LF, Walker DG, Brachova L, Beach TG, Rogers J, et al. 2001. Involvement of microglial receptor for advanced glycation endproducts (RAGE) in Alzheimer's disease: identification of a cellular activation mechanism. *Exp Neurol* 171: 29-45

Maier M, Peng Y, Jiang L, Seabrook TJ, Carroll MC, Lemere CA. 2008. Complement C3 deficiency leads to accelerated amyloid beta plaque deposition and neurodegeneration and modulation of the microglia/macrophage phenotype in amyloid precursor protein transgenic mice. *The Journal of neuroscience : the official journal of the Society for Neuroscience* 28: 6333-41

Majumdar A, Chung H, Dolios G, Wang R, Asamoah N, et al. 2008. Degradation of fibrillar forms of Alzheimer's amyloid β-peptide by macrophages. *Neurobiology of aging* 29: 707-15

Majumdar A, Cruz D, Asamoah N, Buxbaum A, Sohar I, et al. 2007. Activation of microglia acidifies lysosomes and leads to degradation of Alzheimer amyloid fibrils. *Mol Biol Cell* 18: 1490-6

Malm T, Magga J, Koistinaho J. 2012. Animal Models of Alzheimer's Disease: Utilization of Transgenic Alzheimer's Disease Models in Studies of Amyloid Beta Clearance. *Current Translational Geriatrics and Experimental Gerontology Reports* 1: 11-20

Manczak M, Mao P, Nakamura K, Bebbington C, Park B, Reddy PH. 2009. Neutralization of granulocyte macrophage colony-stimulating factor decreases amyloid beta 1-42 and suppresses microglial activity in a transgenic mouse model of Alzheimer's disease. *Hum Mol Genet* 18: 3876-93

Mandrekar S, Jiang Q, Lee CY, Koenigsknecht-Talboo J, Holtzman DM, Landreth GE. 2009. Microglia mediate the clearance of soluble Abeta through fluid phase macropinocytosis. *The Journal of neuroscience : the official journal of the Society for Neuroscience* 29: 4252-62

Martin BK, Szekely C, Brandt J, Piantadosi S, Breitner JC, et al. 2008. Cognitive function over time in the Alzheimer's Disease Anti-inflammatory Prevention Trial (ADAPT): results of a randomized, controlled trial of naproxen and celecoxib. *Arch Neurol* 65: 896-905

Masters CL, Simms G, Weinman NA, Multhaup G, McDonald BL, Beyreuther K. 1985. Amyloid plaque core protein in Alzheimer disease and Down syndrome. *Proceedings of the National Academy of Sciences of the United States of America* 82: 4245-9

Mawuenyega KG, Sigurdson W, Ovod V, Munsell L, Kasten T, et al. 2010. Decreased clearance of CNS beta-amyloid in Alzheimer's disease. *Science* 330: 1774

Mazaheri F, Snaidero N, Kleinberger G, Madore C, Daria A, et al. 2017. TREM2 deficiency impairs chemotaxis and microglial responses to neuronal injury. *EMBO Rep* 18: 1186-98

McGeer PL, Rogers J. 1992. Anti-inflammatory agents as a therapeutic approach to Alzheimer's disease. *Neurology* 42: 447-9

Meda L, Cassatella MA, Szendrei GI, Otvos L, Jr., Baron P, et al. 1995. Activation of microglial cells by beta-amyloid protein and interferon-gamma. *Nature* 374: 647-50

Mewes A, Franke H, Singer D. 2012. Organotypic brain slice cultures of adult transgenic P301S mice--a model for tauopathy studies. *PLoS One* 7: e45017

Meyer-Luehmann M, Spires-Jones TL, Prada C, Garcia-Alloza M, de Calignon A, et al. 2008. Rapid appearance and local toxicity of amyloid-[bgr] plaques in a mouse model of Alzheimer/'s disease. *Nature* 451: 720-24

Michaud JP, Halle M, Lampron A, Theriault P, Prefontaine P, et al. 2013. Toll-like receptor 4 stimulation with the detoxified ligand monophosphoryl lipid A improves Alzheimer's disease-related pathology. *Proc Natl Acad Sci U S A* 110: 1941-6

Middeldorp J, Lehallier B, Villeda SA, Miedema SSM, Evans E, et al. 2016. Preclinical Assessment of Young Blood Plasma for Alzheimer Disease. *JAMA neurology* 73: 1325-33

Migheli A, Butler M, Brown K, Shelanski M. 1988. Light and electron microscope localization of the microtubule- associated tau protein in rat brain. *The Journal of Neuroscience* 8: 1846-51

Mitrasinovic OM, Murphy GM. 2002. Accelerated Phagocytosis of Amyloid-β by Mouse and Human Microglia Overexpressing the Macrophage Colony-stimulating Factor Receptor. *Journal of Biological Chemistry* 277: 29889-96

Mitrasinovic OM, Vincent VAM, Simsek D, Murphy Jr GM. 2003. Macrophage colony stimulating factor promotes phagocytosis by murine microglia. *Neuroscience Letters* 344: 185-88

Moehlmann T, Winkler E, Xia X, Edbauer D, Murrell J, et al. 2002. Presenilin-1 mutations of leucine 166 equally affect the generation of the Notch and APP intracellular domains independent of their effect on Abeta 42 production. *Proc Natl Acad Sci U S A* 99: 8025-30

Moreth J, Mavoungou C, Schindowski K. 2013. Passive anti-amyloid immunotherapy in Alzheimer's disease: What are the most promising targets? *Immunity & Ageing : I & A* 10: 18-18

Mori T, Koyama N, Arendash GW, Horikoshi-Sakuraba Y, Tan J, Town T. 2010. Overexpression of human S100B exacerbates cerebral amyloidosis and gliosis in the Tg2576 mouse model of Alzheimer's disease. *Glia* 58: 300-14

Morris JC, Aisen PS, Bateman RJ, Benzinger TL, Cairns NJ, et al. 2012. Developing an international network for Alzheimer research: The Dominantly Inherited Alzheimer Network. *Clinical investigation* 2: 975-84

Mosher KI, Wyss-Coray T. 2014. Microglial dysfunction in brain aging and Alzheimer's disease. *Biochemical pharmacology* 88: 594-604

Mosley K, Cuzner ML. 1996. Receptor-mediated phagocytosis of myelin by macrophages and microglia: effect of opsonization and receptor blocking agents. *Neurochem Res* 21: 481-7

Moussaud S, Draheim HJ. 2010. A new method to isolate microglia from adult mice and culture them for an extended period of time. *J Neurosci Methods* 187: 243-53

Mullan Mike CF, Axelman Karin, Houlden Henry, Lilius Lena, Winbland Bengt & Lannfelt Lars. 1992. A pathogenic mutation for probable Alzheimer's disease in the APP gene at the N−terminus of bold beta−amyloid. *Nature Genetics* 1: 345-47

Muller UC, Deller T, Korte M. 2017. Not just amyloid: physiological functions of the amyloid precursor protein family. *Nat Rev Neurosci* 18: 281-98

Naj AC, Schellenberg GD, for the Alzheimer's Disease Genetics C. 2017. Genomic variants, genes, and pathways of Alzheimer's disease: An overview. *American Journal of Medical Genetics Part B: Neuropsychiatric Genetics* 174: 5-26

Neniskyte U, Vilalta A, Brown GC. 2014. Tumour necrosis factor alpha-induced neuronal loss is mediated by microglial phagocytosis. *FEBS Lett* 588: 2952-6

Nicoll JA, Barton E, Boche D, Neal JW, Ferrer I, et al. 2006. Abeta species removal after abeta42 immunization. *J Neuropathol Exp Neurol* 65: 1040-8

Nicoll JA, Wilkinson D, Holmes C, Steart P, Markham H, Weller RO. 2003. Neuropathology of human Alzheimer disease after immunization with amyloid-beta peptide: a case report. *Nat Med* 9: 448-52

Nimmerjahn A, Kirchhoff F, Helmchen F. 2005. Resting Microglial Cells Are Highly Dynamic Surveillants of Brain Parenchyma in Vivo. *Science* 308: 1314-18

Niraula A, Sheridan JF, Godbout JP. 2016. Microglia Priming with Aging and Stress. *Neuropsychopharmacology* 42: 318

Njie eG, Boelen E, Stassen FR, Steinbusch HWM, Borchelt DR, Streit WJ. 2012. Ex vivo cultures of microglia from young and aged rodent brain reveal age-related changes in microglial function. *Neurobiology of aging* 33: 195.e1-95.e12

Novotny R, Langer F, Mahler J, Skodras A, Vlachos A, et al. 2016. Conversion of Synthetic Abeta to In Vivo Active Seeds and Amyloid Plaque Formation in a Hippocampal Slice Culture Model. *J Neurosci* 36: 5084-93

Oakley H, Cole SL, Logan S, Maus E, Shao P, et al. 2006. Intraneuronal beta-amyloid aggregates, neurodegeneration, and neuron loss in transgenic mice with five familial Alzheimer's disease mutations: potential factors in amyloid plaque formation. *J Neurosci* 26: 10129-40

Oddo S, Caccamo A, Shepherd JD, Murphy MP, Golde TE, et al. 2003. Triple-transgenic model of Alzheimer's disease with plaques and tangles: intracellular Abeta and synaptic dysfunction. *Neuron* 39: 409-21

Okun E, Mattson MP, Arumugam TV. 2010. Involvement of Fc Receptors in Disorders of the Central Nervous System. *NeuroMolecular Medicine* 12: 164-78

Olmos-Alonso A, Schetters ST, Sri S, Askew K, Mancuso R, et al. 2016. Pharmacological targeting of CSF1R inhibits microglial proliferation and prevents the progression of Alzheimer's-like pathology. *Brain* 139: 891-907

Orre M, Kamphuis W, Osborn LM, Jansen AH, Kooijman L, et al. 2014. Isolation of glia from Alzheimer's mice reveals inflammation and dysfunction. *Neurobiology of aging* 35: 2746-60

Pan X-d, Zhu Y-g, Lin N, Zhang J, Ye Q-y, et al. 2011. Microglial phagocytosis induced by fibrillar β-amyloid is attenuated by oligomeric β-amyloid: implications for Alzheimer's disease. *Molecular neurodegeneration* 6: 45-45

Parajuli B, Sonobe Y, Horiuchi H, Takeuchi H, Mizuno T, Suzumura A. 2013. Oligomeric amyloid beta induces IL-1beta processing via production of ROS: implication in Alzheimer's disease. *Cell death & disease* 4: e975

Paresce DM, Chung H, Maxfield FR. 1997. Slow degradation of aggregates of the Alzheimer's disease amyloid beta-protein by microglial cells. *J Biol Chem* 272: 29390-7

Parkhurst CN, Yang G, Ninan I, Savas JN, Yates JR, 3rd, et al. 2013. Microglia promote learning-dependent synapse formation through brain-derived neurotrophic factor. *Cell* 155: 1596-609

Perlmutter LS, Barron E, Chui HC. 1990. Morphologic association between microglia and senile plaque amyloid in Alzheimer's disease. *Neurosci Lett* 119: 32-6

Perrin RJ, Fagan AM, Holtzman DM. 2009. Multimodal techniques for diagnosis and prognosis of Alzheimer's disease. *Nature* 461: 916-22

Prokop S, Miller KR, Drost N, Handrick S, Mathur V, et al. 2015. Impact of peripheral myeloid cells on amyloid-beta pathology in Alzheimer's disease-like mice. *J Exp Med* 212: 1811-8

Radde R, Bolmont T, Kaeser SA, Coomaraswamy J, Lindau D, et al. 2006. Abeta42-driven cerebral amyloidosis in transgenic mice reveals early and robust pathology. *EMBO reports* 7: 940-6

Reed-Geaghan EG, Savage JC, Hise AG, Landreth GE. 2009. CD14 and toll-like receptors 2 and 4 are required for fibrillar A{beta}-stimulated microglial activation. *J Neurosci* 29: 11982-92

Reiman EM, Langbaum JB, Fleisher AS, Caselli RJ, Chen K, et al. 2011. Alzheimer's Prevention Initiative: a plan to accelerate the evaluation of presymptomatic treatments. *J Alzheimers Dis* 26 Suppl 3: 321-9

Richard KL, Filali M, Prefontaine P, Rivest S. 2008. Toll-like receptor 2 acts as a natural innate immune receptor to clear amyloid beta 1-42 and delay the cognitive decline in a mouse model of Alzheimer's disease. *The Journal of neuroscience : the official journal of the Society for Neuroscience* 28: 5784-93

Rodriguez JJ, Witton J, Olabarria M, Noristani HN, Verkhratsky A. 2010. Increase in the density of resting microglia precedes neuritic plaque formation and microglial activation in a transgenic model of Alzheimer's disease. *Cell death & disease* 1: e1

Rovelet-Lecrux A, Hannequin D, Raux G, Le Meur N, Laquerriere A, et al. 2006. APP locus duplication causes autosomal dominant early-onset Alzheimer disease with cerebral amyloid angiopathy. *Nat Genet* 38: 24-6

Saito T, Matsuba Y, Mihira N, Takano J, Nilsson P, et al. 2014. Single App knock-in mouse models of Alzheimer's disease. *Nat Neurosci* 17: 661-3

Saito T, Suemoto T, Brouwers N, Sleegers K, Funamoto S, et al. 2011. Potent amyloidogenicity and pathogenicity of Abeta43. *Nat Neurosci* 14: 1023-32

Sasaki Y, Ohsawa K, Kanazawa H, Kohsaka S, Imai Y. 2001. Iba1 Is an Actin-Cross-Linking Protein in Macrophages/Microglia. *Biochemical and biophysical research communications* 286: 292-97

Schafer DP, Stevens B. 2015. Microglia Function in Central Nervous System Development and Plasticity. *Cold Spring Harbor perspectives in biology* 7: a020545

Schenk D, Barbour R, Dunn W, Gordon G, Grajeda H, et al. 1999. Immunization with amyloid-beta attenuates Alzheimer-disease-like pathology in the PDAPP mouse. *Nature* 400: 173-7

Scheuner D, Eckman C, Jensen M, Song X, Citron M, et al. 1996. Secreted amyloid [beta]-protein similar to that in the senile plaques of Alzheimer's disease is increased in vivo by the presenilin 1 and 2 and APP mutations linked to familial Alzheimer's disease. *Nat Med* 2: 864-70

Schliwa M. 1982. Action of cytochalasin D on cytoskeletal networks. *The Journal of cell biology* 92: 79-91

Scholzen T, Gerdes J. 2000. The Ki-67 protein: from the known and the unknown. *J Cell Physiol* 182: 311-22

Selkoe DJ. 2001. Alzheimer's disease: genes, proteins, and therapy. *Physiol Rev* 81: 741-66

Selkoe DJ. 2008. Soluble Oligomers of the Amyloid β-Protein Impair Synaptic Plasticity and Behavior. *Behavioural brain research* 192: 106-13

Selkoe DJ, Hardy J. 2016. The amyloid hypothesis of Alzheimer's disease at 25 years. *EMBO Molecular Medicine* 8: 595-608

Serrano-Pozo A, Muzikansky A, Gomez-Isla T, Growdon JH, Betensky RA, et al. 2013. Differential relationships of reactive astrocytes and microglia to fibrillar amyloid deposits in Alzheimer disease. *J Neuropathol Exp Neurol* 72: 462-71

Serrano-Pozo A, William CM, Ferrer I, Uro-Coste E, Delisle MB, et al. 2010. Beneficial effect of human anti-amyloid-beta active immunization on neurite morphology and tau pathology. *Brain* 133: 1312-27

Sevigny J, Chiao P, Bussiere T, Weinreb PH, Williams L, et al. 2016. The antibody aducanumab reduces Abeta plaques in Alzheimer's disease. *Nature* 537: 50-6

Shankar GM, Li S, Mehta TH, Garcia-Munoz A, Shepardson NE, et al. 2008. Amyloid-beta protein dimers isolated directly from Alzheimer's brains impair synaptic plasticity and memory. *Nature medicine* 14: 837-42

Shibata M, Yamada S, Kumar SR, Calero M, Bading J, et al. 2000. Clearance of Alzheimer's amyloid-β1-40 peptide from brain by LDL receptor–related protein-1 at the blood-brain barrier. *The Journal of clinical investigation* 106: 1489-99

Shibata Y, Berclaz PY, Chroneos ZC, Yoshida M, Whitsett JA, Trapnell BC. 2001. GM-CSF regulates alveolar macrophage differentiation and innate immunity in the lung through PU.1. *Immunity* 15: 557-67

Shirotani K, Tomioka M, Kremmer E, Haass C, Steiner H. 2007. Pathological activity of familial Alzheimer's disease-associated mutant presenilin can be executed by six different gamma-secretase complexes. *Neurobiol Dis* 27: 102-7

Shoji M, Golde TE, Ghiso J, Cheung TT, Estus S, et al. 1992. Production of the Alzheimer amyloid beta protein by normal proteolytic processing. *Science* 258: 126

Sierra A, Encinas JM, Deudero JJP, Chancey JH, Enikolopov G, et al. 2010. Microglia shape adult hippocampal neurogenesis through apoptosis-coupled phagocytosis. *Cell stem cell* 7: 483-95

Sims R, van der Lee SJ, Naj AC, Bellenguez C, Badarinarayan N, et al. 2017. Rare coding variants in PLCG2, ABI3, and TREM2 implicate microglial-mediated innate immunity in Alzheimer's disease. *Nat Genet* 49: 1373-84

Sisodia SS. 1992. Beta-amyloid precursor protein cleavage by a membrane-bound protease. *Proceedings of the National Academy of Sciences of the United States of America* 89: 6075-79

Slooter AJ, Cruts M, Kalmijn S, Hofman A, Breteler MM, et al. 1998. Risk estimates of dementia by apolipoprotein E genotypes from a population-based incidence study: the Rotterdam Study. *Arch Neurol* 55: 964-8

Smith AM, Gibbons HM, Oldfield RL, Bergin PM, Mee EW, et al. 2013. M-CSF increases proliferation and phagocytosis while modulating receptor and transcription factor expression in adult human microglia. *J Neuroinflammation* 10: 85

Smith EE, Greenberg SM. 2009. Beta-amyloid, blood vessels, and brain function. *Stroke* 40: 2601-6

Smith LK, He Y, Park JS, Bieri G, Snethlage CE, et al. 2015. beta2-microglobulin is a systemic pro-aging factor that impairs cognitive function and neurogenesis. *Nat Med* 21: 932-7

Sonnen JA, Breitner JC, Lovell MA, Markesbery WR, Quinn JF, Montine TJ. 2008. Free radical-mediated damage to brain in Alzheimer's disease and its transgenic mouse models. *Free radical biology & medicine* 45: 219-30

Sousa C, Biber K, Michelucci A. 2017. Cellular and Molecular Characterization of Microglia: A Unique Immune Cell Population. *Frontiers in immunology* 8: 198

Staal JA, Alexander SR, Liu Y, Dickson TD, Vickers JC. 2011. Characterization of cortical neuronal and glial alterations during culture of organotypic whole brain slices from neonatal and mature mice. *PLoS One* 6: e22040

Steen E, Terry BM, Rivera EJ, Cannon JL, Neely TR, et al. 2005. Impaired insulin and insulin-like growth factor expression and signaling mechanisms in Alzheimer's disease--is this type 3 diabetes? *J Alzheimers Dis* 7: 63-80

Steinberg S, Stefansson H, Jonsson T, Johannsdottir H, Ingason A, et al. 2015. Loss-of-function variants in ABCA7 confer risk of Alzheimer's disease. *Nat Genet* 47: 445-7

Stoppini L, Buchs PA, Muller D. 1991. A simple method for organotypic cultures of nervous tissue. *J Neurosci Methods* 37: 173-82

Streit WJ, Miller KR, Lopes KO, Njie E. 2008. Microglial degeneration in the aging brain--bad news for neurons? *Front Biosci* 13: 3423-38

Suarez-Calvet M, Araque Caballero MA, Kleinberger G, Bateman RJ, Fagan AM, et al. 2016a. Early changes in CSF sTREM2 in dominantly inherited Alzheimer's disease occur after amyloid deposition and neuronal injury. *Sci Transl Med* 8: 369ra178

Suarez-Calvet M, Kleinberger G, Araque Caballero MA, Brendel M, Rominger A, et al. 2016b. sTREM2 cerebrospinal fluid levels are a potential biomarker for microglia activity in early-stage Alzheimer's disease and associate with neuronal injury markers. *EMBO Mol Med* 8: 466-76

Suh H-S, Kim M-O, Lee SC. 2005. Inhibition of Granulocyte-Macrophage Colony-Stimulating Factor Signaling and Microglial Proliferation by Anti-CD45RO: Role of Hck Tyrosine Kinase and Phosphatidylinositol 3-Kinase/Akt. *The Journal of Immunology* 174: 2712-19

Swerdlow RH, Khan SM. 2004. A "mitochondrial cascade hypothesis" for sporadic Alzheimer's disease. *Med Hypotheses* 63: 8-20

Takami M, Nagashima Y, Sano Y, Ishihara S, Morishima-Kawashima M, et al. 2009. γ-Secretase: Successive Tripeptide and Tetrapeptide Release from the Transmembrane Domain of β-Carboxyl Terminal Fragment. *The Journal of Neuroscience* 29: 13042

Tan J, Town T, Crawford F, Mori T, DelleDonne A, et al. 2002. Role of CD40 ligand in amyloidosis in transgenic Alzheimer's mice. *Nat Neurosci* 5: 1288-93

Tan J, Town T, Paris D, Mori T, Suo Z, et al. 1999. Microglial activation resulting from CD40-CD40L interaction after beta-amyloid stimulation. *Science* 286: 2352-5

Tanzi RE, McClatchey AI, Lamperti ED, Villa-Komaroff L, Gusella JF, Neve RL. 1988. Protease inhibitor domain encoded by an amyloid protein precursor mRNA associated with Alzheimer's disease. *Nature* 331: 528

Togo T, Akiyama H, Kondo H, Ikeda K, Kato M, et al. 2000. Expression of CD40 in the brain of Alzheimer's disease and other neurological diseases. *Brain Res* 885: 117-21

Tokuda T, Fukushima T, Ikeda S-I, Sekijima Y, Shoji SI, et al. 1997. Plasma Levels of amyloid β proteins Aβ1–40 and Aβ1–42(43) are elevated in Down's syndrome. *Annals of Neurology* 41: 271-73

Tosto G, Reitz C. 2016. Genomics of Alzheimer's disease: Value of high-throughput genomic technologies to dissect its etiology. *Molecular and cellular probes* 30: 397-403

References

Ueno M, Fujita Y, Tanaka T, Nakamura Y, Kikuta J, et al. 2013. Layer V cortical neurons require microglial support for survival during postnatal development. *Nat Neurosci* 16: 543-51

Ulrich JD, Finn MB, Wang Y, Shen A, Mahan TE, et al. 2014. Altered microglial response to Abeta plaques in APPPS1-21 mice heterozygous for TREM2. *Mol Neurodegener* 9: 20

Umeda T, Tomiyama T, Sakama N, Tanaka S, Lambert MP, et al. 2011. Intraneuronal amyloid β oligomers cause cell death via endoplasmic reticulum stress, endosomal/lysosomal leakage, and mitochondrial dysfunction in vivo. *Journal of Neuroscience Research* 89: 1031-42

Utter S, Tamboli IY, Walter J, Upadhaya AR, Birkenmeier G, et al. 2008. Cerebral Small Vessel Disease-Induced Apolipoprotein E Leakage Is Associated With Alzheimer Disease and the Accumulation of Amyloid β-Protein in Perivascular Astrocytes. *Journal of Neuropathology & Experimental Neurology* 67: 842-56

Van Cauwenberghe C, Van Broeckhoven C, Sleegers K. 2016. The genetic landscape of Alzheimer disease: clinical implications and perspectives. *Genetics in medicine : official journal of the American College of Medical Genetics* 18: 421-30

van Groen T, Kiliaan AJ, Kadish I. 2006. Deposition of mouse amyloid β in human APP/PS1 double and single AD model transgenic mice. *Neurobiology of Disease* 23: 653-62

Vandersteen A, Hubin E, Sarroukh R, De Baets G, Schymkowitz J, et al. 2012. A comparative analysis of the aggregation behavior of amyloid-β peptide variants. *FEBS letters* 586: 4088-93

Vassar R, Bennett BD, Babu-Khan S, Kahn S, Mendiaz EA, et al. 1999. Beta-secretase cleavage of Alzheimer's amyloid precursor protein by the transmembrane aspartic protease BACE. *Science* 286: 735-41

Vassar R, Kuhn P-H, Haass C, Kennedy ME, Rajendran L, et al. 2014. Function, therapeutic potential and cell biology of BACE proteases: current status and future prospects. *Journal of neurochemistry* 130: 4-28

Verghese PB, Castellano JM, Garai K, Wang Y, Jiang H, et al. 2013. ApoE influences amyloid-beta (Abeta) clearance despite minimal apoE/Abeta association in physiological conditions. *Proc Natl Acad Sci U S A* 110: E1807-16

Villeda SA, Luo J, Mosher KI, Zou B, Britschgi M, et al. 2011. The ageing systemic milieu negatively regulates neurogenesis and cognitive function. *Nature* 477: 90-4

Villeda SA, Plambeck KE, Middeldorp J, Castellano JM, Mosher KI, et al. 2014. Young blood reverses age-related impairments in cognitive function and synaptic plasticity in mice. *Nature medicine* 20: 659-63

Villegas-Llerena C, Phillips A, Garcia-Reitboeck P, Hardy J, Pocock JM. 2016. Microglial genes regulating neuroinflammation in the progression of Alzheimer's disease. *Curr Opin Neurobiol* 36: 74-81

Vinet J, Weering HR, Heinrich A, Kalin RE, Wegner A, et al. 2012. Neuroprotective function for ramified microglia in hippocampal excitotoxicity. *J Neuroinflammation* 9: 27

Von Bernhardi R, Eugenin-von Bernhardi L, Eugenin J. 2015. Microglial cell dysregulation in Brain Aging and Neurodegeneration. *Frontiers in Aging Neuroscience* 7

Wake H, Moorhouse AJ, Jinno S, Kohsaka S, Nabekura J. 2009. Resting microglia directly monitor the functional state of synapses in vivo and determine the fate of ischemic terminals. *J Neurosci* 29: 3974-80

Walker DG, Lue LF. 2005. Investigations with cultured human microglia on pathogenic mechanisms of Alzheimer's disease and other neurodegenerative diseases. *J Neurosci Res* 81: 412-25

Walsh DM, Hartley DM, Kusumoto Y, Fezoui Y, Condron MM, et al. 1999. Amyloid beta-protein fibrillogenesis. Structure and biological activity of protofibrillar intermediates. *J Biol Chem* 274: 25945-52

Wang Y, Cella M, Mallinson K, Ulrich JD, Young KL, et al. 2015. TREM2 lipid sensing sustains the microglial response in an Alzheimer's disease model. *Cell* 160: 1061-71

Weitz TM, Town T. 2012. Microglia in Alzheimer's Disease: It's All About Context. *Int J Alzheimers Dis* 2012: 314185

Weller RO, Massey A, Newman TA, Hutchings M, Kuo Y-M, Roher AE. 1998. Cerebral Amyloid Angiopathy. *The American journal of pathology* 153: 725-33

Wes PD, Holtman IR, Boddeke EW, Moller T, Eggen BJ. 2016. Next generation transcriptomics and genomics elucidate biological complexity of microglia in health and disease. *Glia* 64: 197-213

White JA, Manelli AM, Holmberg KH, Van Eldik LJ, Ladu MJ. 2005. Differential effects of oligomeric and fibrillar amyloid-beta 1-42 on astrocyte-mediated inflammation. *Neurobiol Dis* 18: 459-65

Wilcock DM. 2012. A Changing Perspective on the Role of Neuroinflammation in Alzheimer's Disease. *International Journal of Alzheimer's Disease* 2012: 7

Wilcock DM, Rojiani A, Rosenthal A, Levkowitz G, Subbarao S, et al. 2004. Passive amyloid immunotherapy clears amyloid and transiently activates microglia in a transgenic mouse model of amyloid deposition. *J Neurosci* 24: 6144-51

Wildsmith KR, Holley M, Savage JC, Skerrett R, Landreth GE. 2013. Evidence for impaired amyloid beta clearance in Alzheimer's disease. *Alzheimers Res Ther* 5: 33

Willem M, Tahirovic S, Busche MA, Ovsepian SV, Chafai M, et al. 2015. eta-Secretase processing of APP inhibits neuronal activity in the hippocampus. *Nature* 526: 443-7

Willette AA, Coe CL, Colman RJ, Bendlin BB, Kastman EK, et al. 2012. Calorie restriction reduces psychological stress reactivity and its association with brain volume and microstructure in aged rhesus monkeys. *Psychoneuroendocrinology* 37: 903-16

Wisniewski T, Goni F. 2015. Immunotherapeutic approaches for Alzheimer's disease. *Neuron* 85: 1162-76

Witte AV, Fobker M, Gellner R, Knecht S, Flöel A. 2009. Caloric restriction improves memory in elderly humans. *Proceedings of the National Academy of Sciences of the United States of America* 106: 1255-60

Wyss-Coray T. 2006. Inflammation in Alzheimer disease: driving force, bystander or beneficial response? *Nature medicine* 12: 1005-15

Wyss-Coray T, Loike JD, Brionne TC, Lu E, Anankov R, et al. 2003. Adult mouse astrocytes degrade amyloid-beta in vitro and in situ. *Nat Med* 9: 453-7

Xiang X, Werner G, Bohrmann B, Liesz A, Mazaheri F, et al. 2016. TREM2 deficiency reduces the efficacy of immunotherapeutic amyloid clearance. *EMBO Mol Med* 8: 992-1004

Yan P, Bero AW, Cirrito JR, Xiao Q, Hu X, et al. 2009. Characterizing the appearance and growth of amyloid plaques in APP/PS1 mice. *J Neurosci* 29: 10706-14

Yan Q, Zhang J, Liu H, Babu-Khan S, Vassar R, et al. 2003. Anti-inflammatory drug therapy alters beta-amyloid processing and deposition in an animal model of Alzheimer's disease. *J Neurosci* 23: 7504-9

Yan R, Vassar R. 2014. Targeting the β secretase BACE1 for Alzheimer's disease therapy. *Lancet neurology* 13: 319-29

Zhang F, Jiang L. 2015. Neuroinflammation in Alzheimer's disease. *Neuropsychiatric Disease and Treatment* 11: 243-56

Zhang Y, Chen K, Sloan SA, Bennett ML, Scholze AR, et al. 2014. An RNA-sequencing transcriptome and splicing database of glia, neurons, and vascular cells of the cerebral cortex. *J Neurosci* 34: 11929-47

Zheng C, Zhou X-W, Wang J-Z. 2016. The dual roles of cytokines in Alzheimer's disease: update on interleukins, TNF-α, TGF-β and IFN-γ. *Translational Neurodegeneration* 5: 7

Zigman WB, Devenny DA, Krinsky-McHale SJ, Jenkins EC, Urv TK, et al. 2008. Alzheimer's Disease in Adults with Down Syndrome. *International review of research in mental retardation* 36: 103-45

Zotova E, Holmes C, Johnston D, Neal JW, Nicoll JAR, Boche D. 2011. Microglial alterations in human Alzheimer's disease following Aβ42 immunization. *Neuropathology and applied neurobiology* 37: 513-24

Acknowledgements

Curriculum vitae

Personal details

Name	Anna Daria
Home Town	Santo Stefano di Cadore (BL) Italy
Citizenship	Italian

Education

07/2017 – 07/2018	Internship in the department of Neuroscience Discovery at Roche pRED "Pharmaceutical and Early Development" of F. Hoffman La Roche Innovation Center Basel (Basel, CH)
11/2012 – 06/2017	PhD thesis in the "Ex vivo model" laboratory of Dr. Sabina Tahirovic in the department of Prof. Dr. Dr. Christian Haass at BMC "Biomedical Center" of LMU "Ludwigs-Maximilians-Universität München" & DZNE "German Center for neurodegenerative diseases" (Munich, D)
03/2011 – 03/2012	Master thesis in the laboratory of Prof. Emanuele Buratti at ICGEB "International Center for Genetic Engineering and Biotechnology" (Area Science Park, Trieste, IT)
09/2009 – 03/2012	Master Degree (Laurea Magistrale) in Medical Biotechnology (Curriculum: Molecular medicine) at University of Trieste/Faculty of Medicine (Trieste, IT)
09/2008 – 04/2009	Bachelor thesis in the laboratory of Prof. Francesco Curcio at DPMSC "Dipartimento di Patologia e Medicina Sperimentale e Clinica" (Department of Pathology and Experimental and Clinical Medicine) (Udine, IT)
09/2005 – 04/2009	Bachelor Degree (Laurea Triennale) in Medical Biotechnology at University of Udine/Faculty of Medicine (Udine, IT)
09/2000 – 07/2005	High School Certificate (Maturità Classica) at "Liceo Classico Tiziano" Institute (Belluno, IT)

Scientific publications

Daria A, Colombo A, Llovera G, Willem M, Liesz A, Haass C, Tahirovic S. Young microglia restores amyloid plaque clearance of aged microglia (2016). **EMBO J** 36: 583-603

Willem M, Tahirovic S, Busche MA, Ovsepian SV, Chafai M, Kootar S, Hornburg D, Evans LD, Moore S, **Daria A**, Hampel H, Müller V, Giudici C, Nuscher B, Wenninger-Weinzierl A, Kremmer E, Heneka MT, Thal DR, Giedraitis V, Lannfelt L, Müller U, Livesey FJ, Meissner F, Herms J, Konnerth A, Marie H, Haass C. eta-Secretase processing of APP inhibits neuronal activity in the hippocampus (2015). **Nature** 526: 443-7

Mazaheri F, Snaidero N, Kleinberger G, Madore C, **Daria A**, Werner G, Krasemann S, Capell A, Trümbach D, Wurst W, Brunner B, Bultmann S, Tahirovic S, Kerschensteiner M, Misgeld T, Butovsky O, Haass C. TREM2 deficiency impairs chemotaxis and microglial responses to neuronal injury (2017). **EMBO Rep** 18: 1186-98